An introduction to Radio-Loud AGN

Paola Grandi (INAF-IASF Bologna)

&

Eleonora Torresi (DIFA & INAF-IASF Bologna)

Laboratorio X

03.10.2017

INAF - IASF BOLOGNA
ISTITUTO DI ASTROFISICA SPAZIALE E FISICA COSMICA - BOLOGNA

Outline

- RADIO-LOUD AGN IN GENERAL
  1) AGN classification
  2) Spectral energy distribution
  3) The FR dichotomy

- RADIATIVE PROCESSES
  1) Thermal emission
     - Accretion
  2) Non-thermal emission
     - Jets, Hot spots, Lobes

Almost every galaxy hosts a black hole from millions to billions of solar masses

(Magorrian et al. 1998, Tremaine et al. 2002, McConnell et al. 2011, Ghisellini 2011)

Almost every galaxy hosts a black hole from millions to billions of solar masses

(Magorrian et al. 1998, Tremaine et al. 2002, McConnell et al. 2011, Ghisellini 2011)

but...

1% active 99% silent

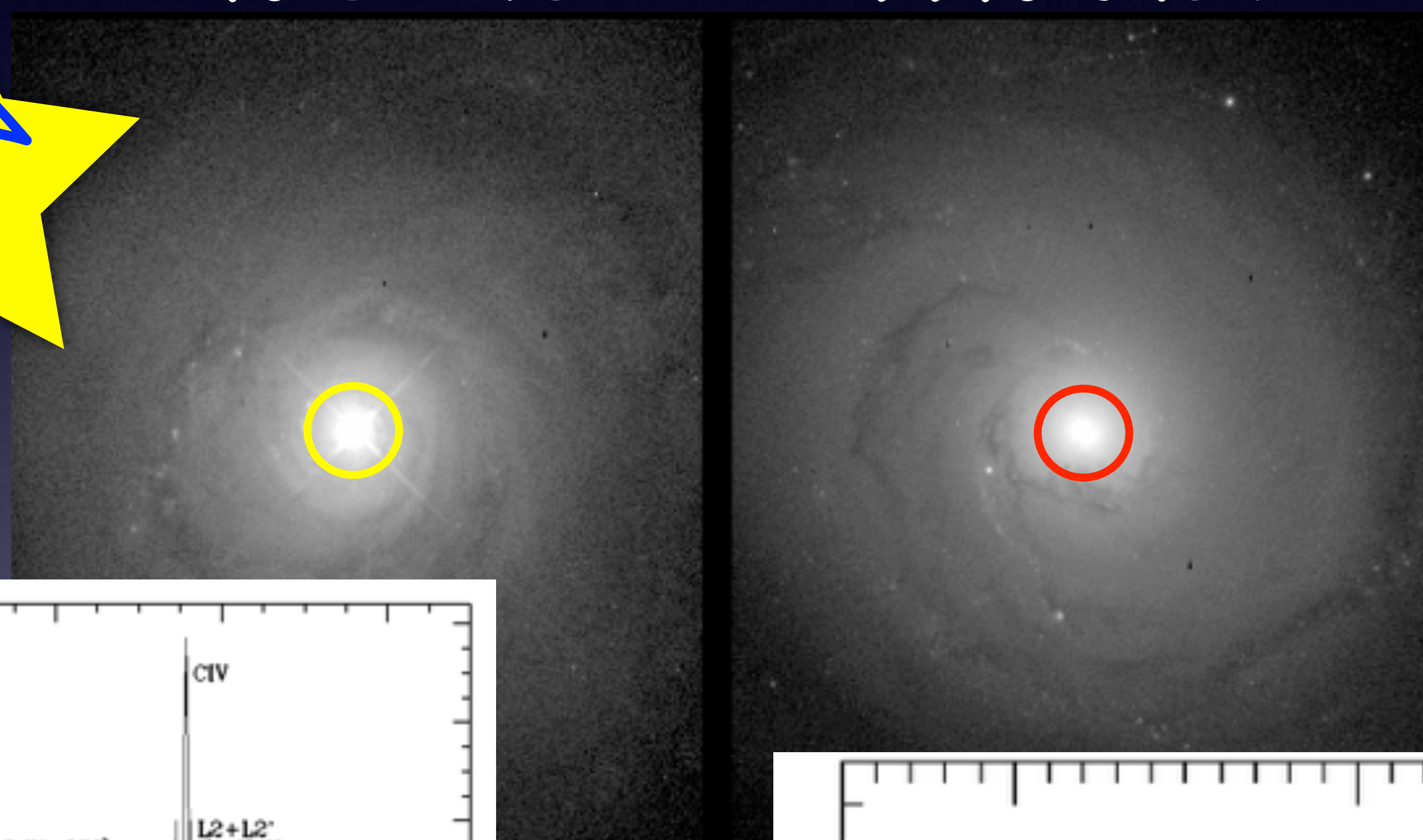

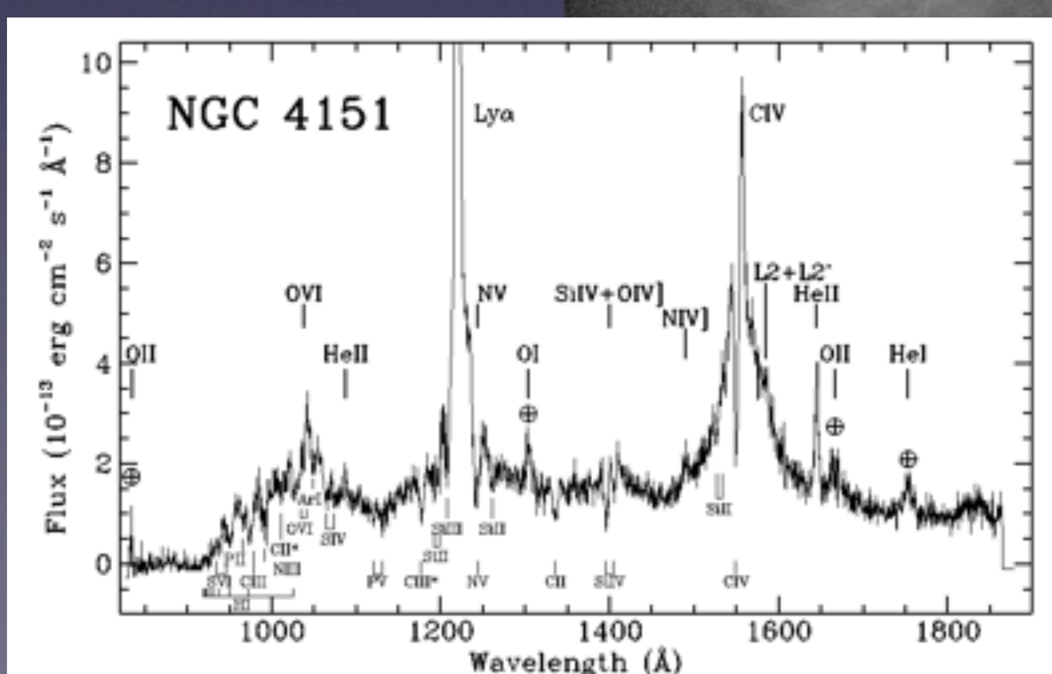

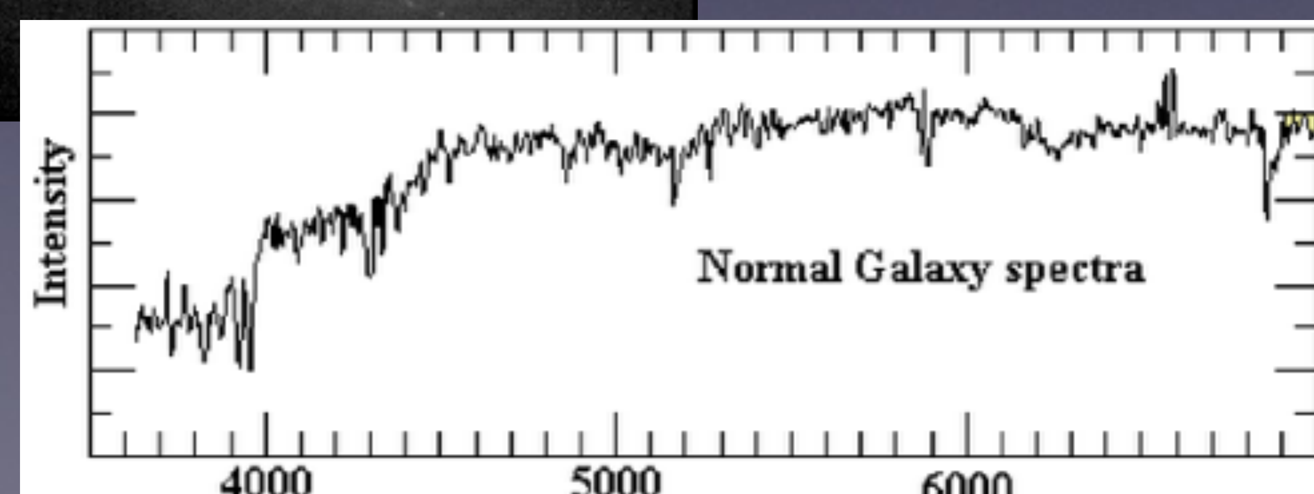

About 10% of AGNs are Radio-Loud,
i.e. these systems are able to launch relativistic jets

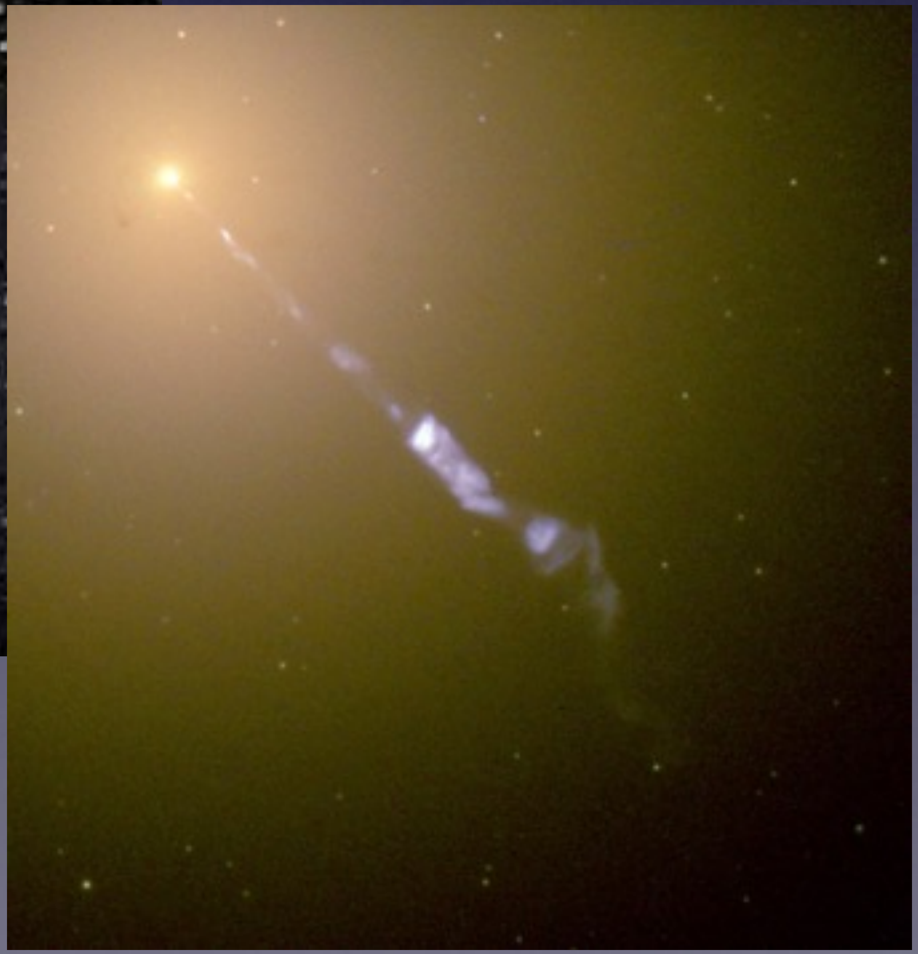

RL AGN lie in ellipticals
RQ AGN lie in spirals and ellipticals

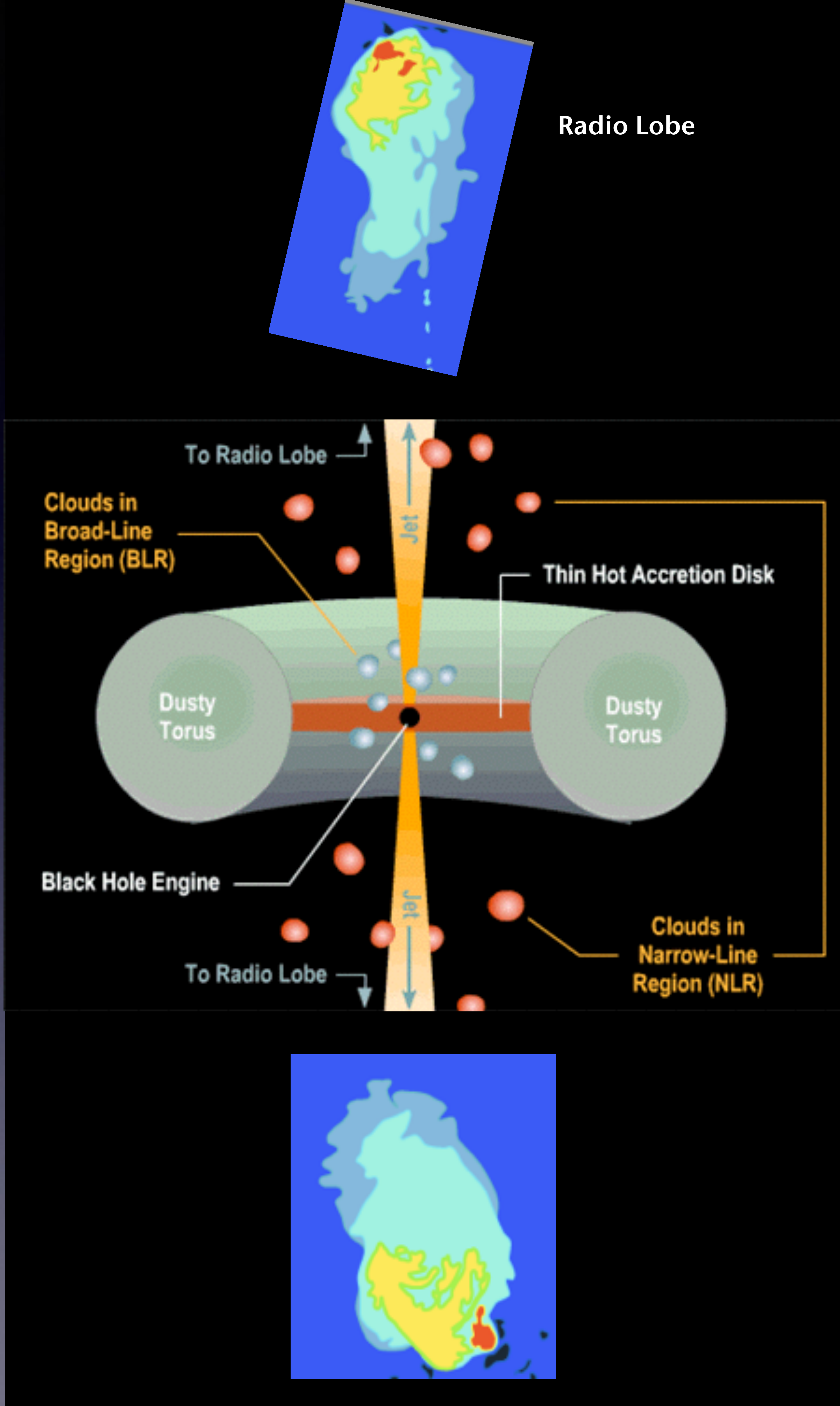

Some numbers for a typical AGN

BH Mass $\sim 10^8 M\odot$

Luminosity $\sim 10^{44}\ erg\ s^{-1}$

BH radius $\sim 3 \times 10^{13}\ cm$

BLR radius $\sim 2 - 20 \times 10^{16}\ cm$

NLR radius $\sim 10^{18} - 10^{20}\ cm$

In RL AGNs

Jets end at kpc distances forming radio lobes

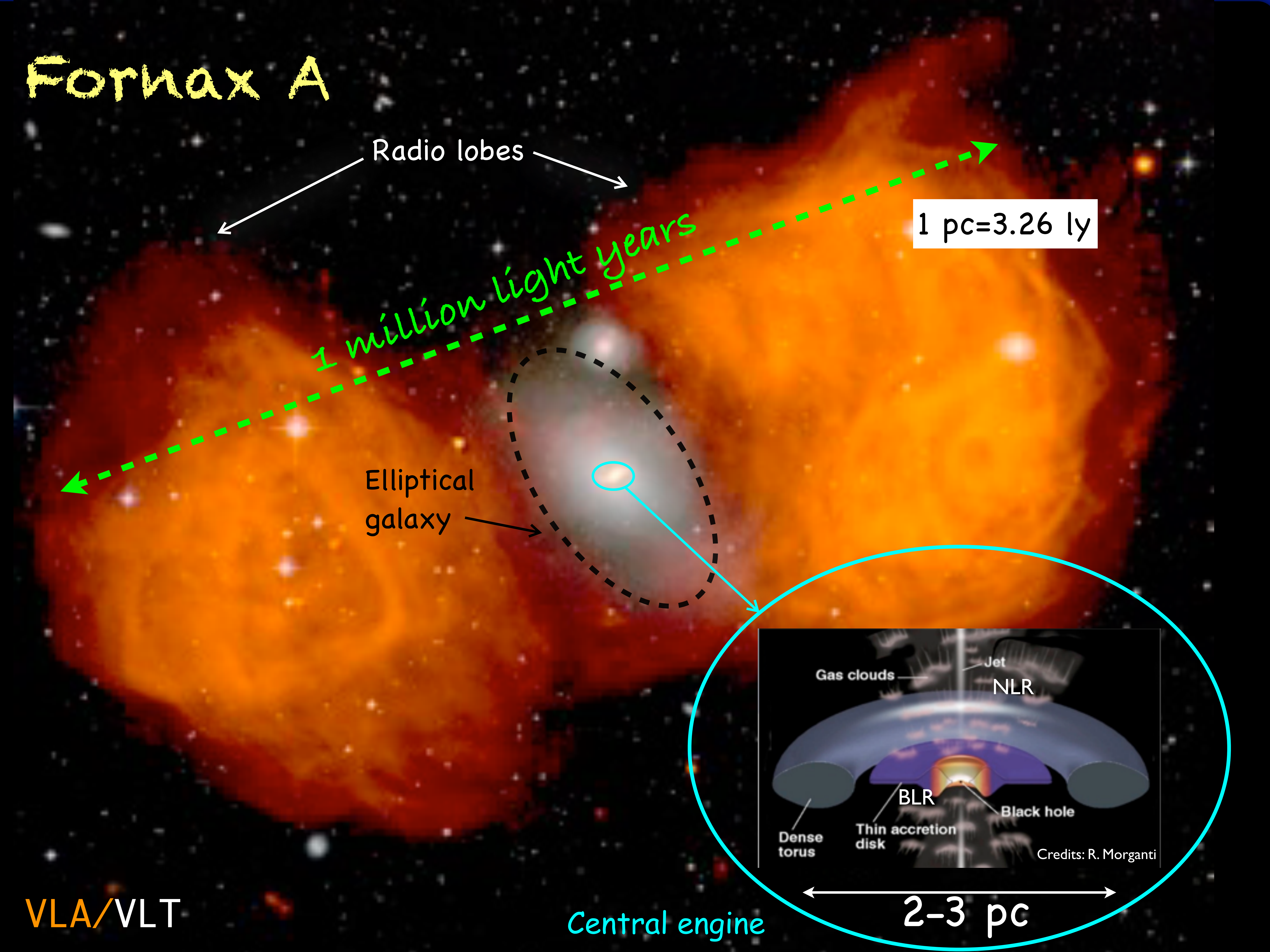

Fornax A
Radio lobes
1 million light years
1 pc=3.26 ly
Elliptical galaxy
Gas clouds
Jet
NLR
BLR
Black hole
Thin accretion disk
Dense torus
Credits: R. Morganti
2–3 pc
Central engine
VLA/VLT

RADIO LOUDNESS PARAMETER ($\mathcal{R}$)

$$\mathcal{R} = \frac{F_{5GHz}}{F_B} \geq 10$$

Kellermann et al. 1989

$$\log\ \mathrm{R}_X = \frac{\nu \mathrm{L}_\nu (5\mathrm{GHz})}{L_X} \ <= -4.5$$

Terashima & Wilson 2003

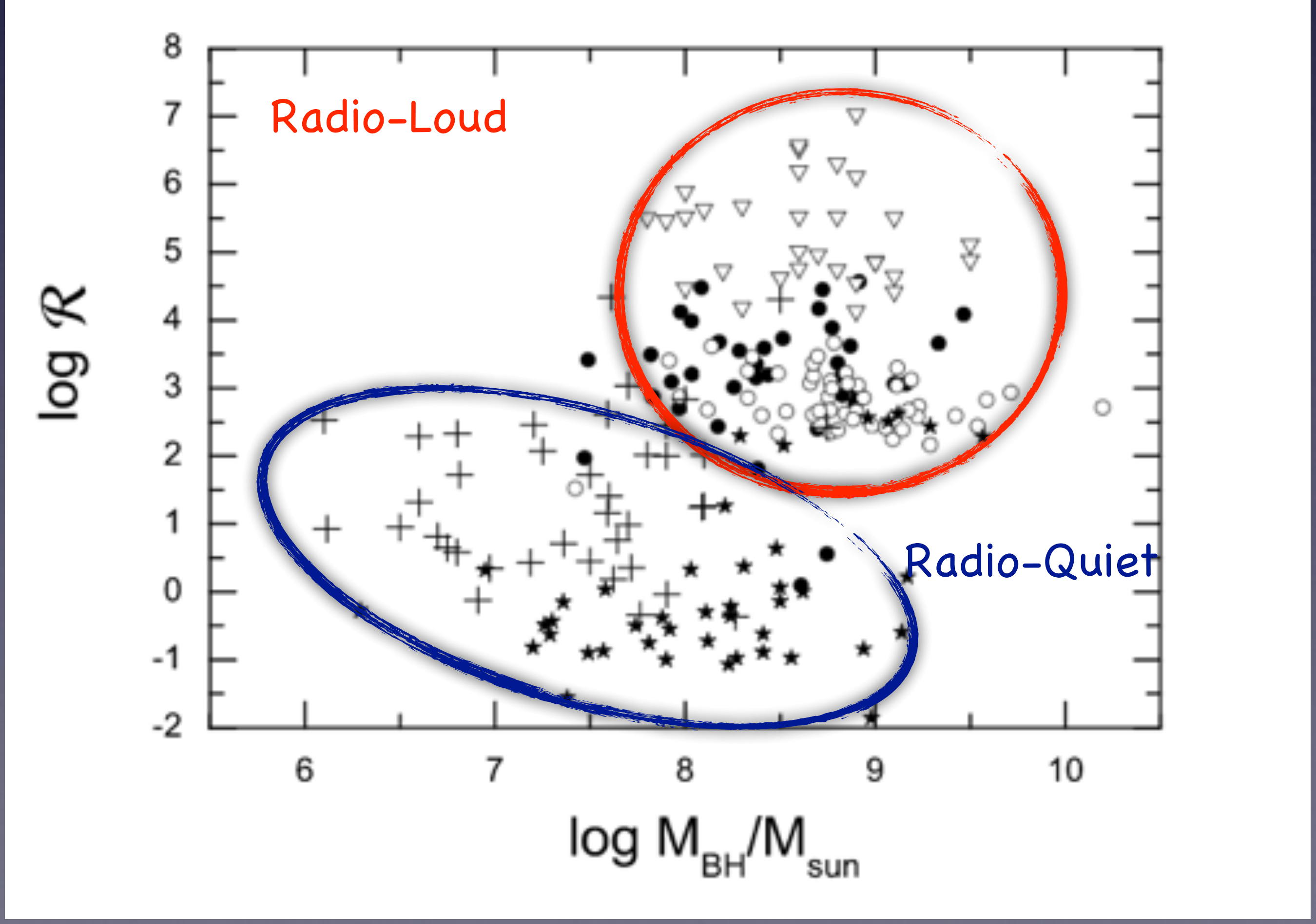

Sikora et al. 2007

Black hole-galaxy feedback

★ The mass of SMBH strongly correlates with the **stellar mass** or the **velocity dispersion** of the surrounding galaxy bulge (Best & Heckman 2012 and references therein)

★ Therefore there should be an intimate link between SMBH and their hosts

★ AGN activity plays an important role in the evolution of galaxies (Silk & Rees 1998, Fabian 1999, Cattaneo et al. 2009) by regulating the amount of gas available for the star formation

$$\log(M_{BH}/M_{\odot})=8.29+5.29\log[\sigma/(200\ \mathrm{km\ s^{-1}})]$$

The masses of SMBH correlate almost perfectly with the velocity dispersions of their host bulges.
The tightness of the M(BH)-sigma relation implies a strong link between black hole formation and the properties of the stellar bulge.

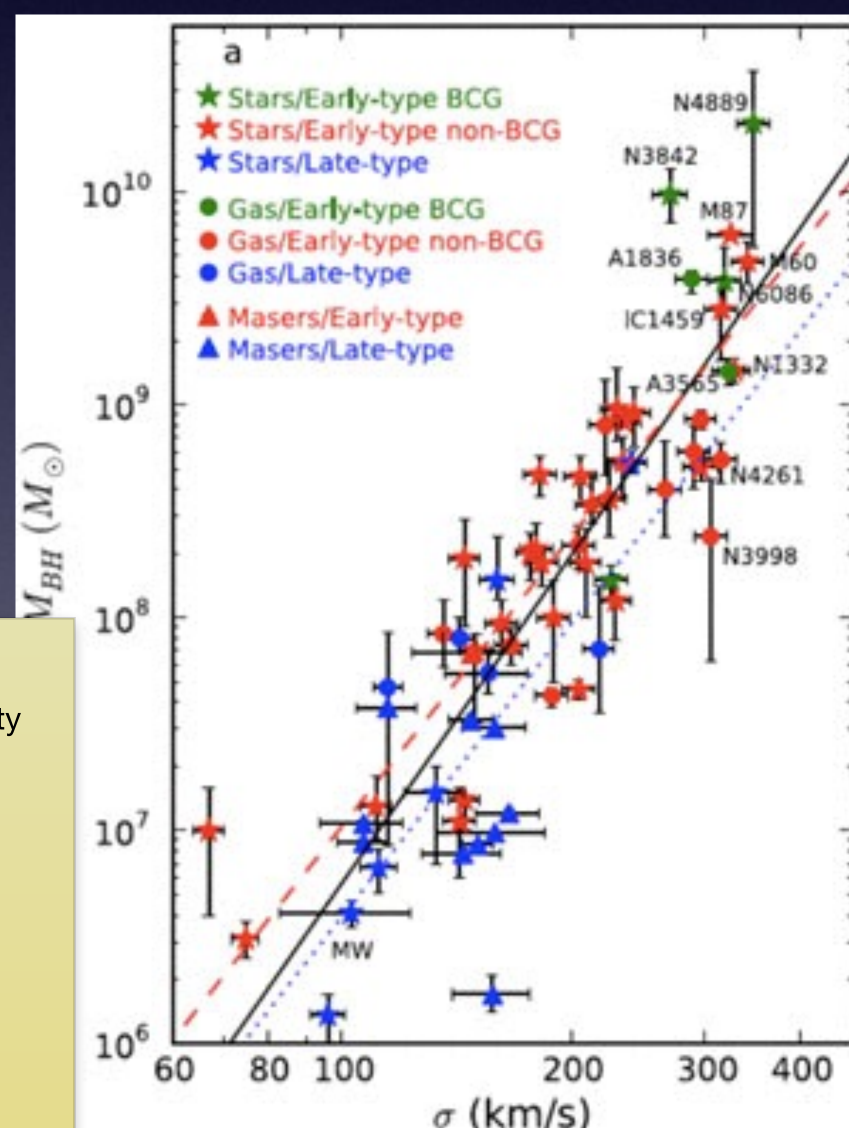

McConnell et al. 2011

There are two types of (negative) AGN feedback

QUASAR-MODE: large amounts of gas flow inwards feeding the black hole through a radiatively efficient Shakura & Sunyaev (1973) disk. This mode may have a role in reducing star formation at high-z setting up the observed M_{BH}-M_{bulge} relation.

RADIO-MODE: material is accreted on to the black hole in radiatively inefficient mode (e.g. ADAF). This kind of accretion leads to little radiated energy while the bulk of the emitted energy is in kinetic form through radio jets.
Jets can represent a very efficient feedback mechanism (e.g. bubbles and cavities). Radio-mode AGN are used as a mechanism to switch off star formation in the most massive galaxies (Best & Heckman 2012).

Positive feedback —> the AGN can trigger star formation (observational evidences in Feain et al. 2007, Zinn et al. 2013)

1. AGN classification

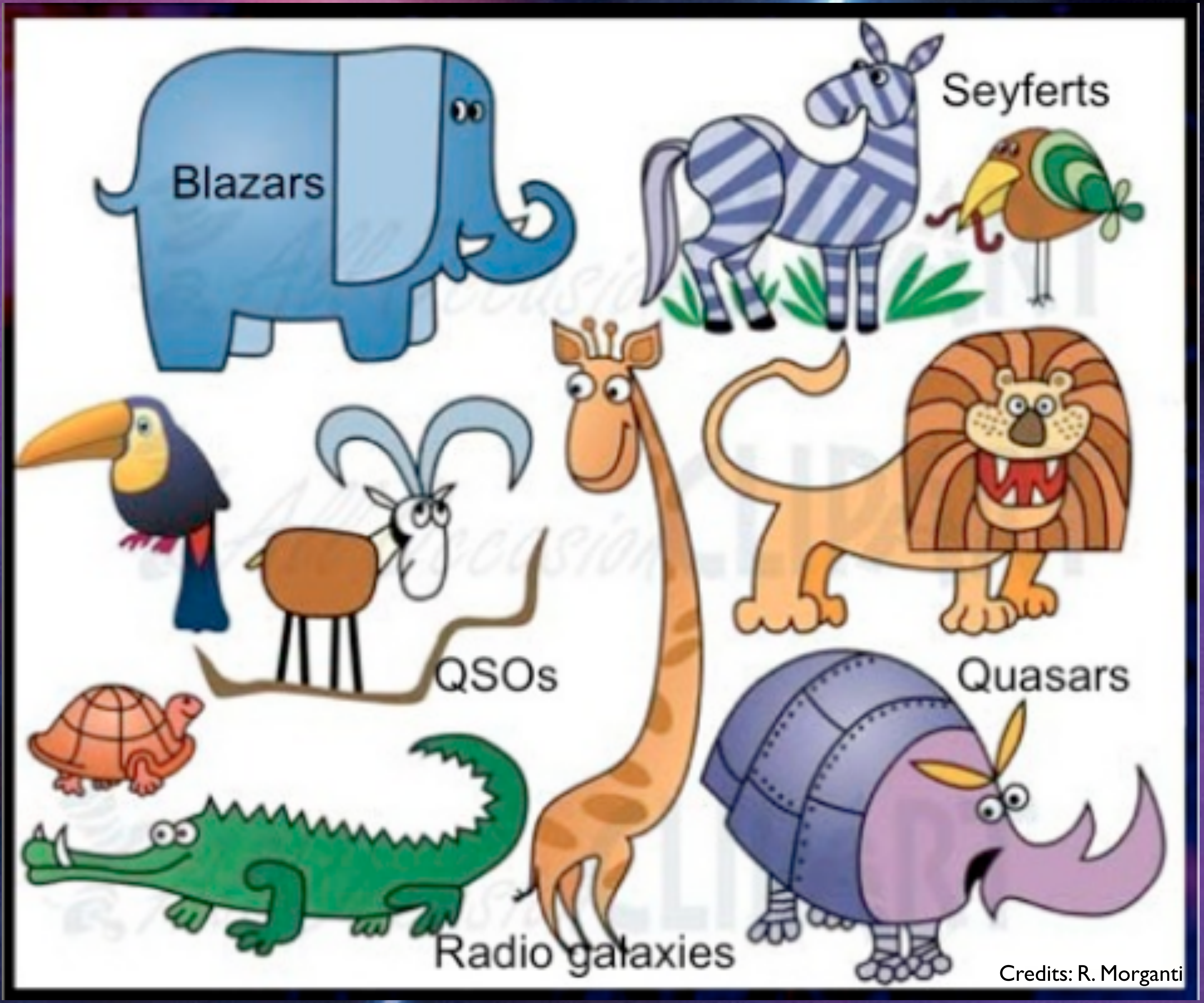

OPTICAL classification

Type I	bright continuum and BROAD emission lines from hot high velocity gas (FWHM~10^{3-4} km s^{-1})
Type II	weak continuum and only NARROW emission lines (FWHM~10^{2} km s^{-1})

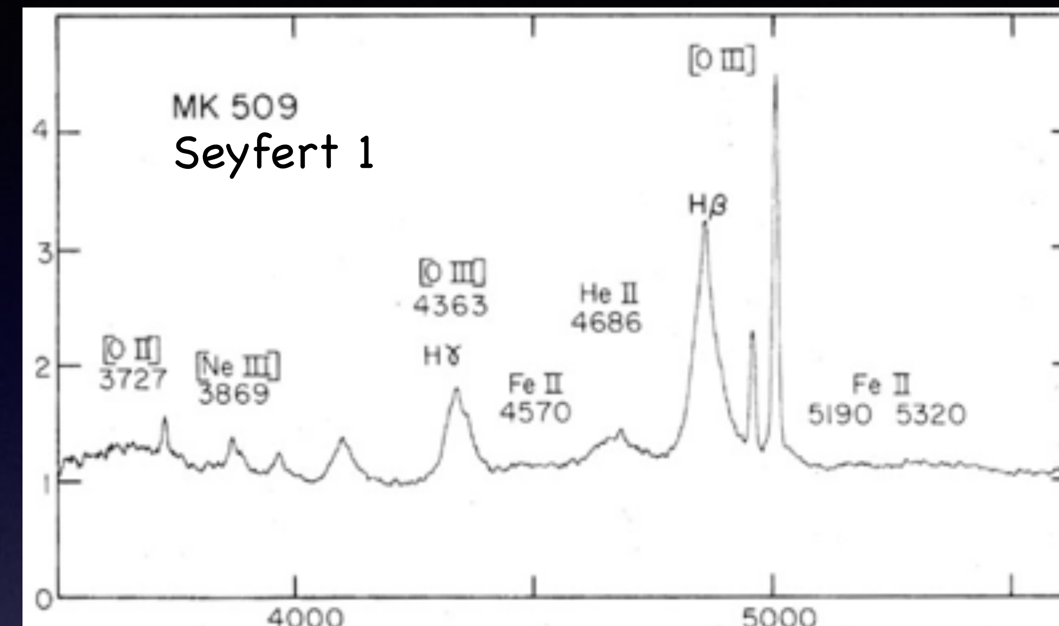

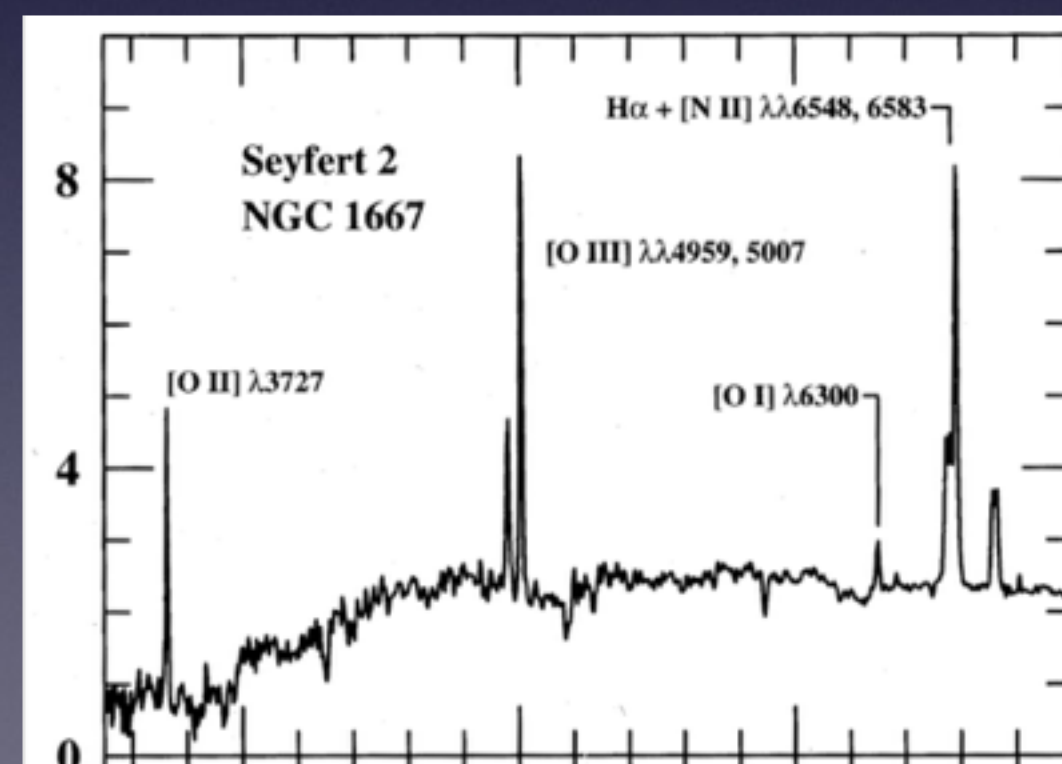

RADIO-LOUD AGN

Type 2
(Narrow Line Radio Galaxy)

Type 1
(Broad Line Radio Galaxy)

Blazar
(BL Lacs, Flat Spectrum Radio Quasars)

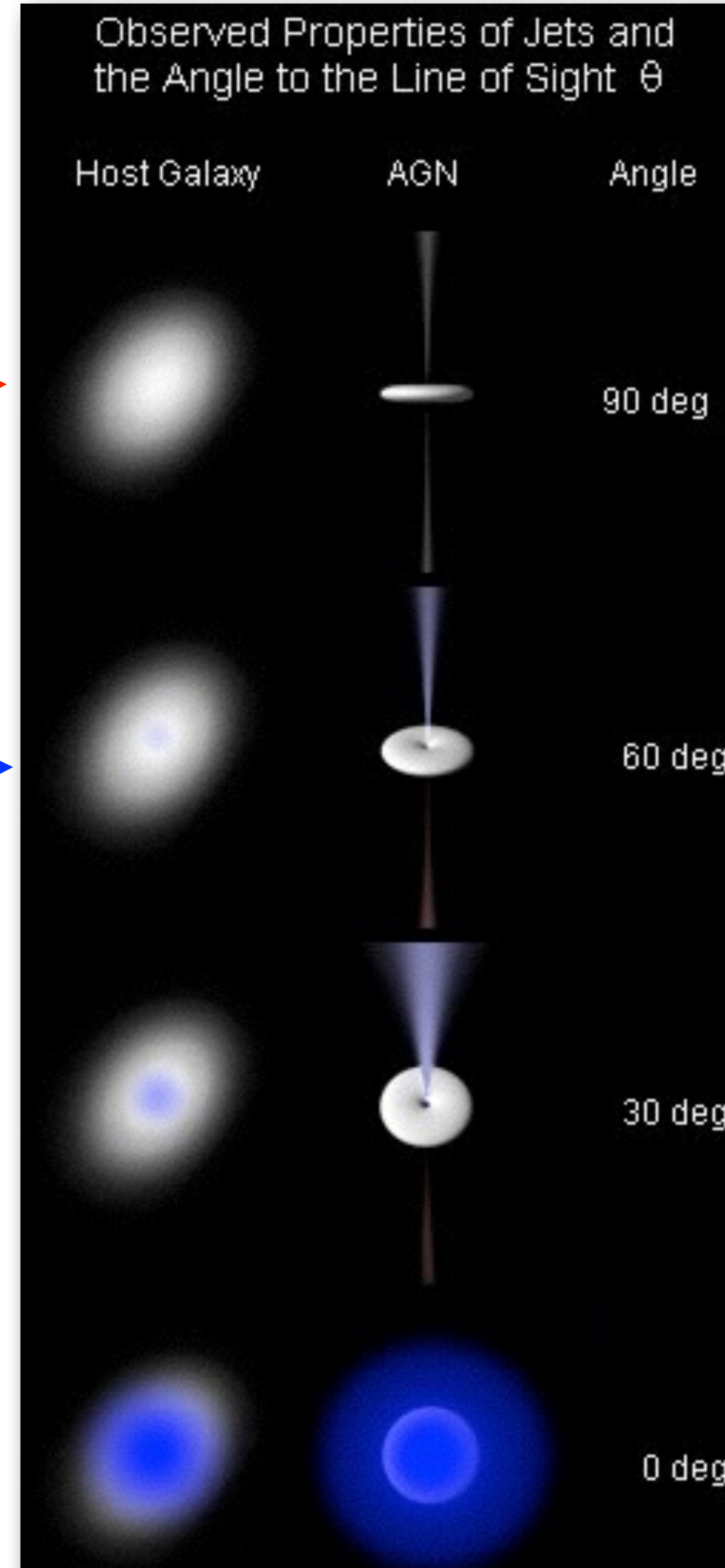

Abbr.	Meaning	Ref
NLRG	Narrow-line radio galaxy	1
BLRG	Broad-line radio galaxy	2
WLRG	Weak-line radio galaxy	3
SLRG	Strong-line radio galaxy	4
Quasar	Quasi-stellar radio source	5
LEG	Low-excitation galaxy	6
HEG	High-excitation galaxy	6
ELEG	Extreme low-excitation galaxy	6
BLRQ/Q	Broad-line radio galaxy or quasar	7
BLO	Broad-line object	6
OVV	Optically violently variable (quasar)	8
FRI	Fanaroff-Riley class I source	9
FRII	Fanaroff-Riley class II source	9
FR0	Fanaroff-Riley class 0 source	10
FSRQ	Flat-spectrum radio-loud quasar	11
SSRQ	Steep-spectrum radio-loud quasar	11
CSS	Compact steep spectrum radio source	12
GPS	Gigahertz-peaked radio source	13
FD	Fat-double radio source	14
RD	Relaxed-double radio source	15

Optical

Radio

Table 2 Summary of the main abbreviations of the labels used to classify radio AGN. The top half of the table relates to optical classifications, while the lower half relates to radio classifications. The final column gives references to some of the first uses of the labels. Reference key: 1. Costero & Osterbrock (1977); 2. Osterbrock, Koski & Philips (1976); 3.Tadhunter et al. (1998); 4. Dicken et al. (2014); 5. Schmidt (1963); 5. Buttiglione et al. (2010); 7. Dicken et al. (2009); 8. Penston & Cannon (1971); 9. Fanaroff & Riley (1974); 10. Ghisellini (2011); 11. Urry & Padovani (1995); 12. Fanti et al. (1990); 13. O'Dea, Baum & Stanghellini (1991); 14. Owen & Laing (1989); 15. (Leahy, 1993). Note that LEGs and HEGs are sometimes labelled LERGs (low excitation radio galaxies) and HERGs (high excitation radio galaxies) in the literature.

Tadhunter 2016

Radio

FRI/FRII classification (Fanaroff & Riley 1974)

RADIO MORPHOLOGY

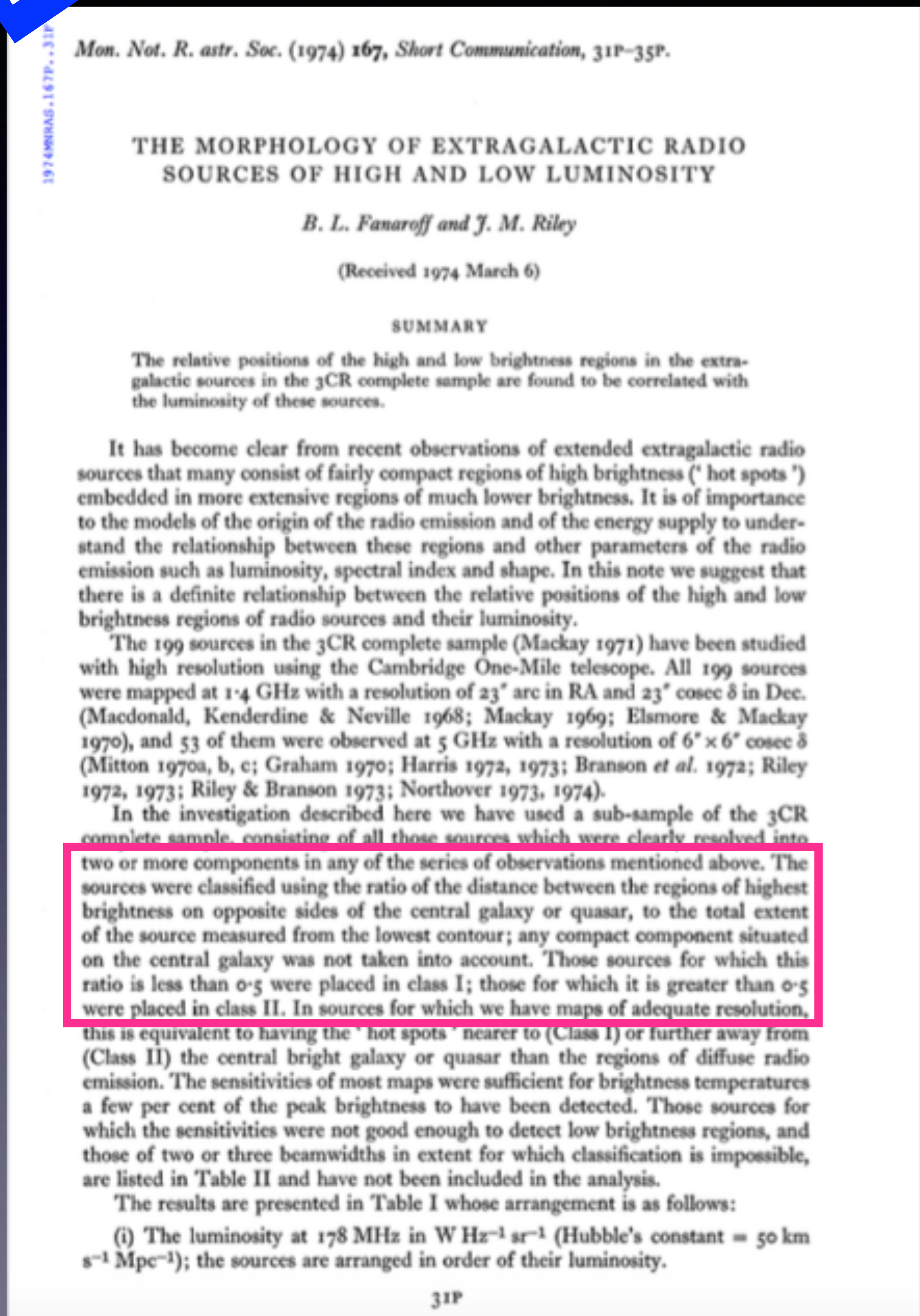

Mon. Not. R. astr. Soc. (1974) **167**, *Short Communication*, 31P–35P.

THE MORPHOLOGY OF EXTRAGALACTIC RADIO SOURCES OF HIGH AND LOW LUMINOSITY

B. L. Fanaroff and J. M. Riley

(Received 1974 March 6)

SUMMARY

The relative positions of the high and low brightness regions in the extra-galactic sources in the 3CR complete sample are found to be correlated with the luminosity of these sources.

It has become clear from recent observations of extended extragalactic radio sources that many consist of fairly compact regions of high brightness (' hot spots ') embedded in more extensive regions of much lower brightness. It is of importance to the models of the origin of the radio emission and of the energy supply to understand the relationship between these regions and other parameters of the radio emission such as luminosity, spectral index and shape. In this note we suggest that there is a definite relationship between the relative positions of the high and low brightness regions of radio sources and their luminosity.

The 199 sources in the 3CR complete sample (Mackay 1971) have been studied with high resolution using the Cambridge One-Mile telescope. All 199 sources were mapped at 1·4 GHz with a resolution of 23" arc in RA and 23" cosec δ in Dec. (Macdonald, Kenderdine & Neville 1968; Mackay 1969; Elsmore & Mackay 1970), and 53 of them were observed at 5 GHz with a resolution of 6" × 6" cosec δ (Mitton 1970a, b, c; Graham 1970; Harris 1972, 1973; Branson *et al.* 1972; Riley 1972, 1973; Riley & Branson 1973; Northover 1973, 1974).

In the investigation described here we have used a sub-sample of the 3CR complete sample, consisting of all those sources which were clearly resolved into two or more components in any of the series of observations mentioned above. The sources were classified using the ratio of the distance between the regions of highest brightness on opposite sides of the central galaxy or quasar, to the total extent of the source measured from the lowest contour; any compact component situated on the central galaxy was not taken into account. Those sources for which this ratio is less than 0·5 were placed in class I; those for which it is greater than 0·5 were placed in class II. In sources for which we have maps of adequate resolution, this is equivalent to having the ' hot spots ' nearer to (Class I) or further away from (Class II) the central bright galaxy or quasar than the regions of diffuse radio emission. The sensitivities of most maps were sufficient for brightness temperatures a few per cent of the peak brightness to have been detected. Those sources for which the sensitivities were not good enough to detect low brightness regions, and those of two or three beamwidths in extent for which classification is impossible, are listed in Table II and have not been included in the analysis.

The results are presented in Table I whose arrangement is as follows:

(i) The luminosity at 178 MHz in W Hz^{-1} sr^{-1} (Hubble's constant = 50 km s^{-1} Mpc^{-1}); the sources are arranged in order of their luminosity.

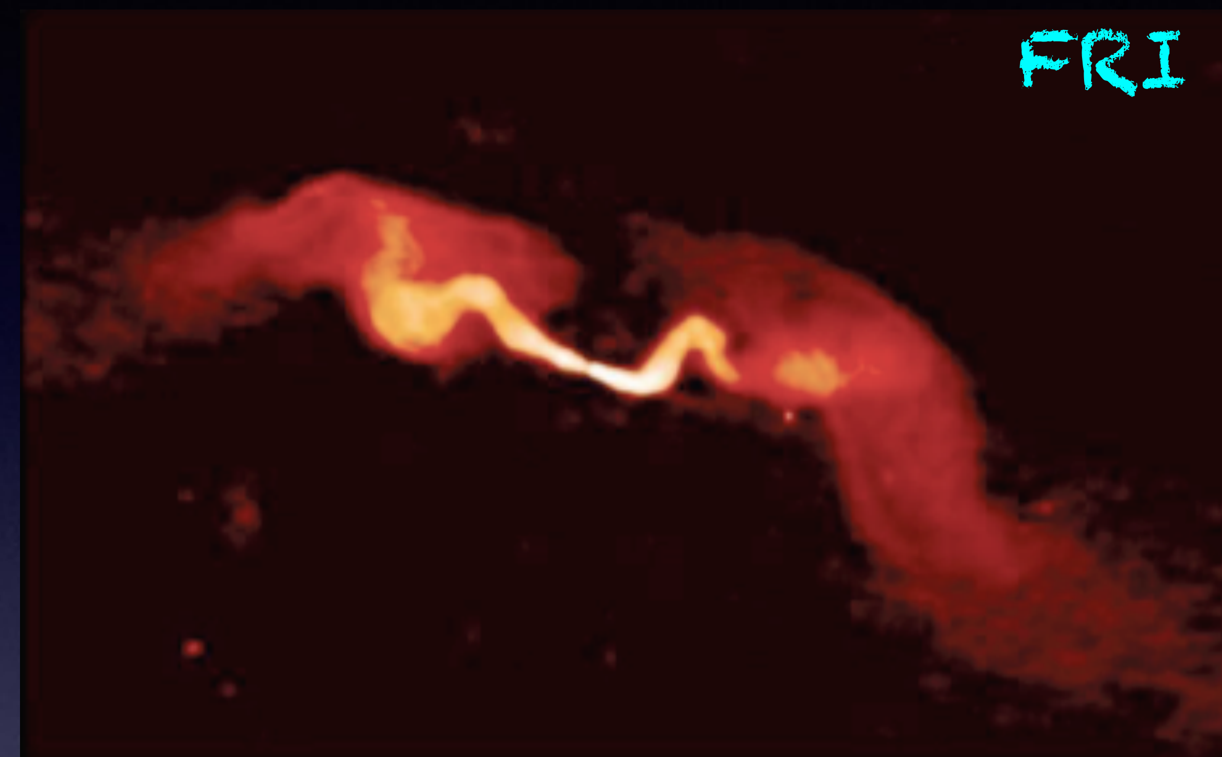

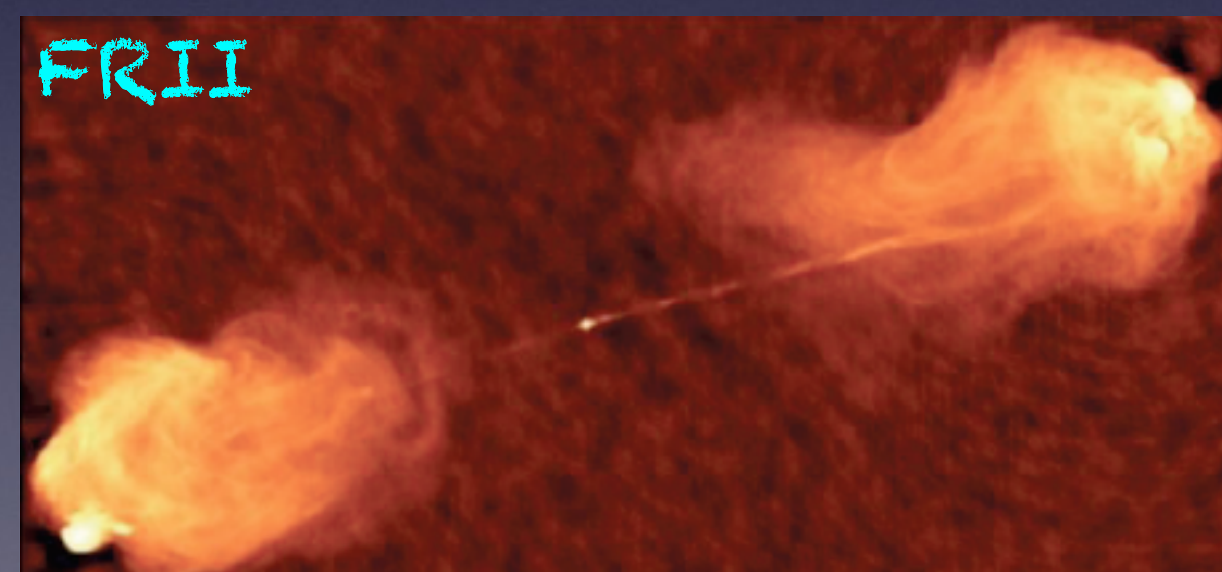

FRI - $L_{178MHz} < 2\times10^{25}$ W Hz^{-1} sr^{-1}

FRII - $L_{178MHz} > 2\times10^{25}$ W Hz^{-1} sr^{-1}

Radio

FRI/jet dominated

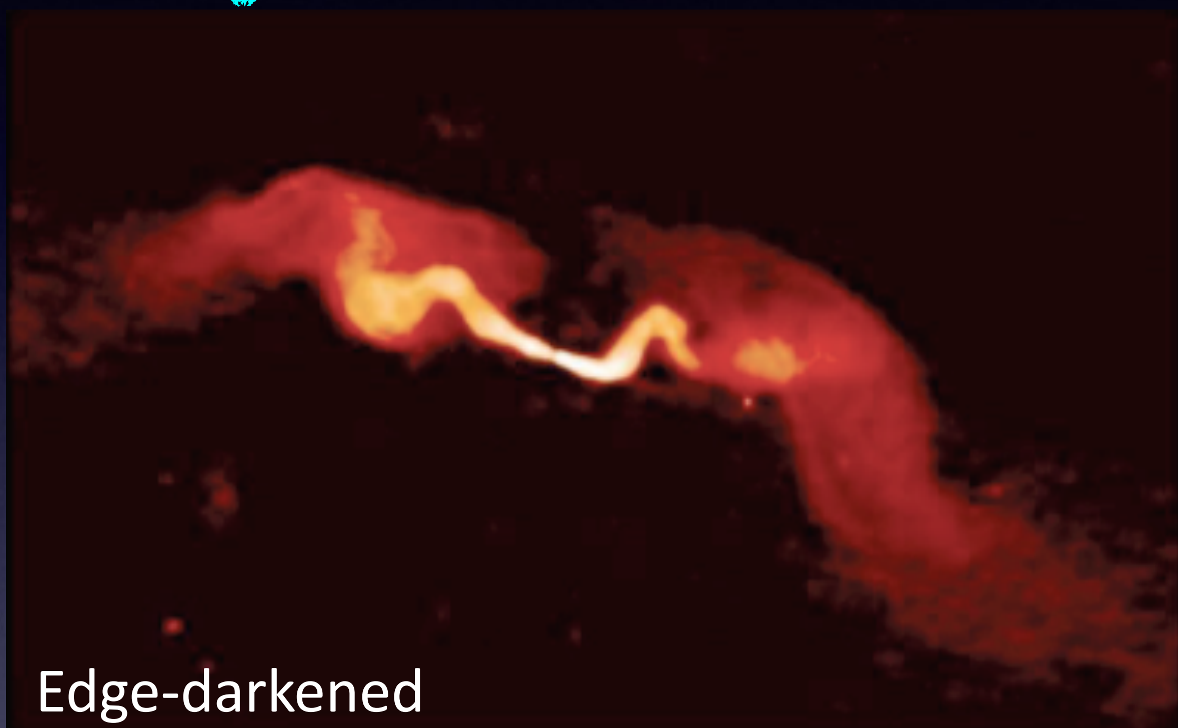

In FRI the jets are thought to decelerate and become sub-relativistic on scales of hundred of pc to kpc.

The nuclei of FRI are not generally absorbed and probably powered by inefficient accretion flows.

FRII/lobe dominated

The jets in FRII are at least moderately relativistic and supersonic from the core to the hot spots.

Most FRII are thought to have an efficient engine and a dusty torus.

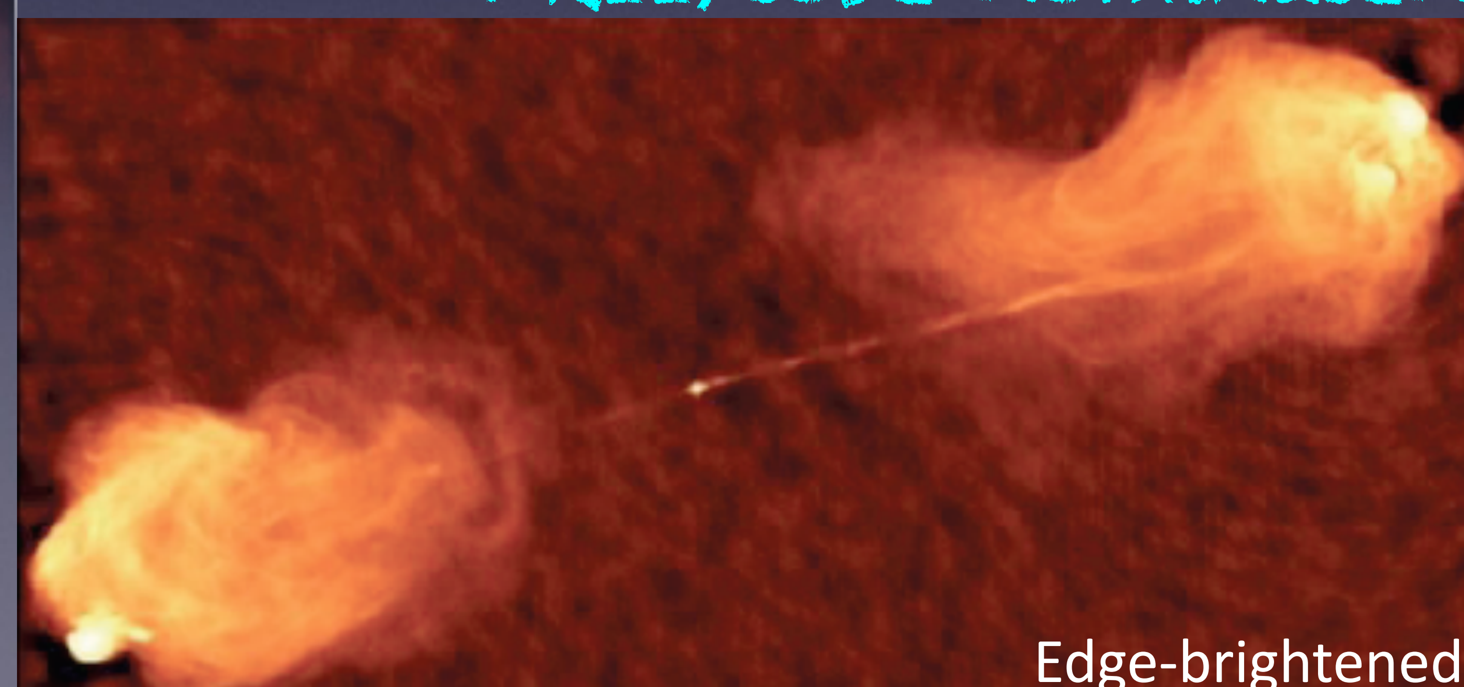

Optical

High-excitation (HERG) and low-excitation (LERG) RG ACCRETION MODE

This classification is related to the excitation modes of the gas in the Narrow Line Regions: different excitation modes correspond to different accretion rates

Laing et al. (1994)

HERG: $EW_{[OIII]}$>3 Å

[OIII]/Ha > 0.2

Excitation Index

(Buttiglione et al. 2010)

EI=log([OIII]/Hb)-1/3[log([NII])/Ha)+log([SII]/Ha)+log([OI]/Ha)]

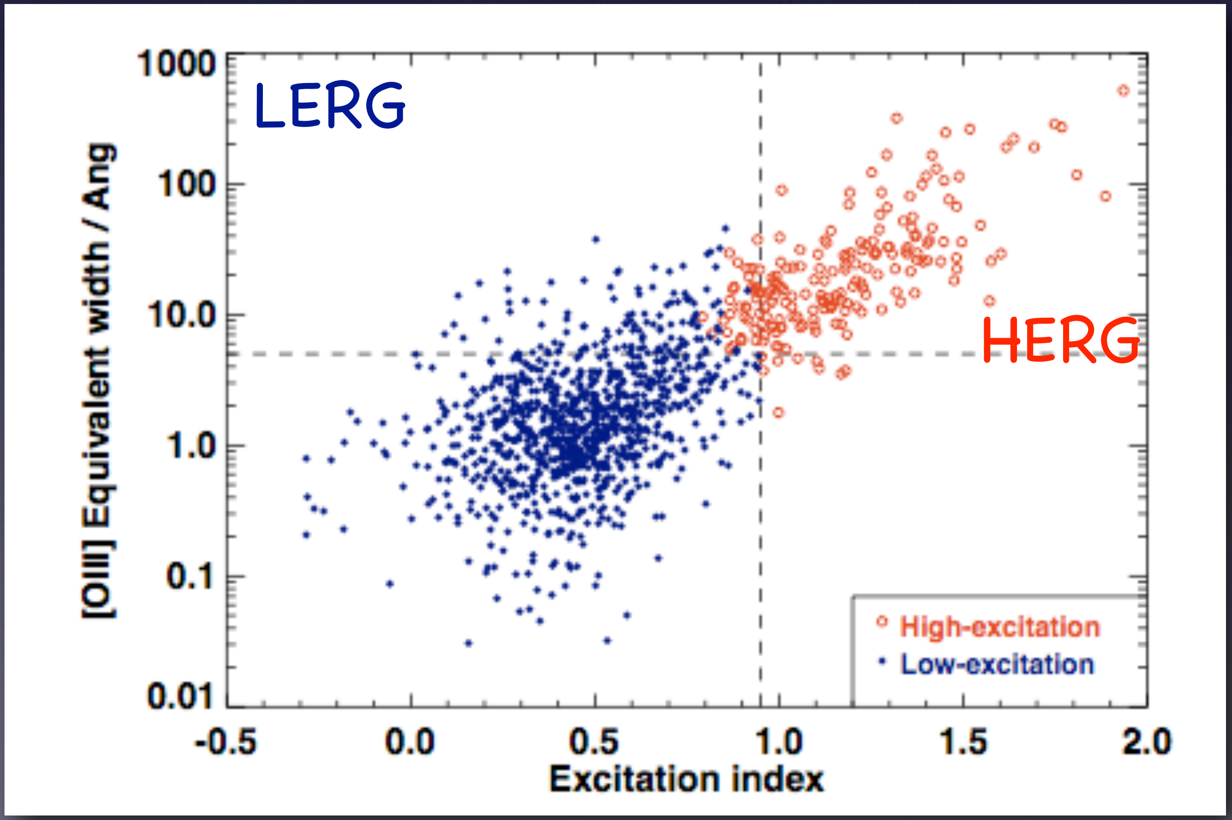

HERG: almost FRII

LERG: both FRI and FRII

Best & Heckman 2012

FRI/FRII not one-to-one correspondence with HERG/LERG

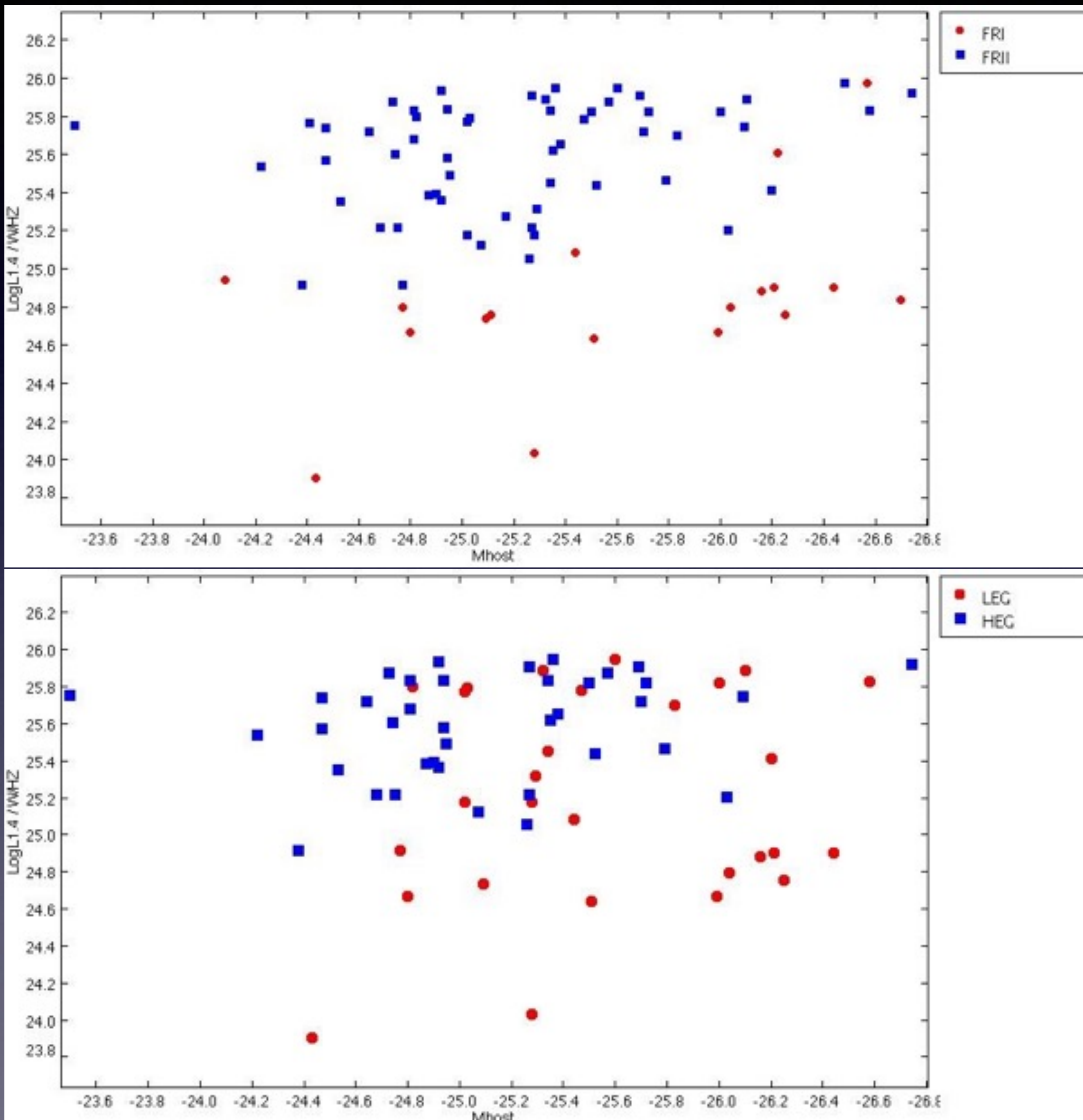

Log $L_{1.4GHz}$ (W Hz^{-1})

M_{host}

HERG: almost FRII

LERG: both FRI and FRII

FR0 radio galaxies

✳ FR0 are compact sources and lack extended radio emission

✳ From the optical point of view they share similar nuclear and host properties with FRI

- host galaxy;
- black hole masses (M_{BH}>$10^8 M_{\odot}$)
- spectroscopic classification (LEG)
- X-ray spectral behavior

✳ FR0 represent the bulk of the Radio-Loud AGN population in the local Universe (the number density of the FR0Cat sources is ~5 times higher than that of FRI Baldi et al. 2017)

FRI (size > 30 kpc), sFRI (10 < size < 30 kpc) and FR0 (size < 5 kpc)

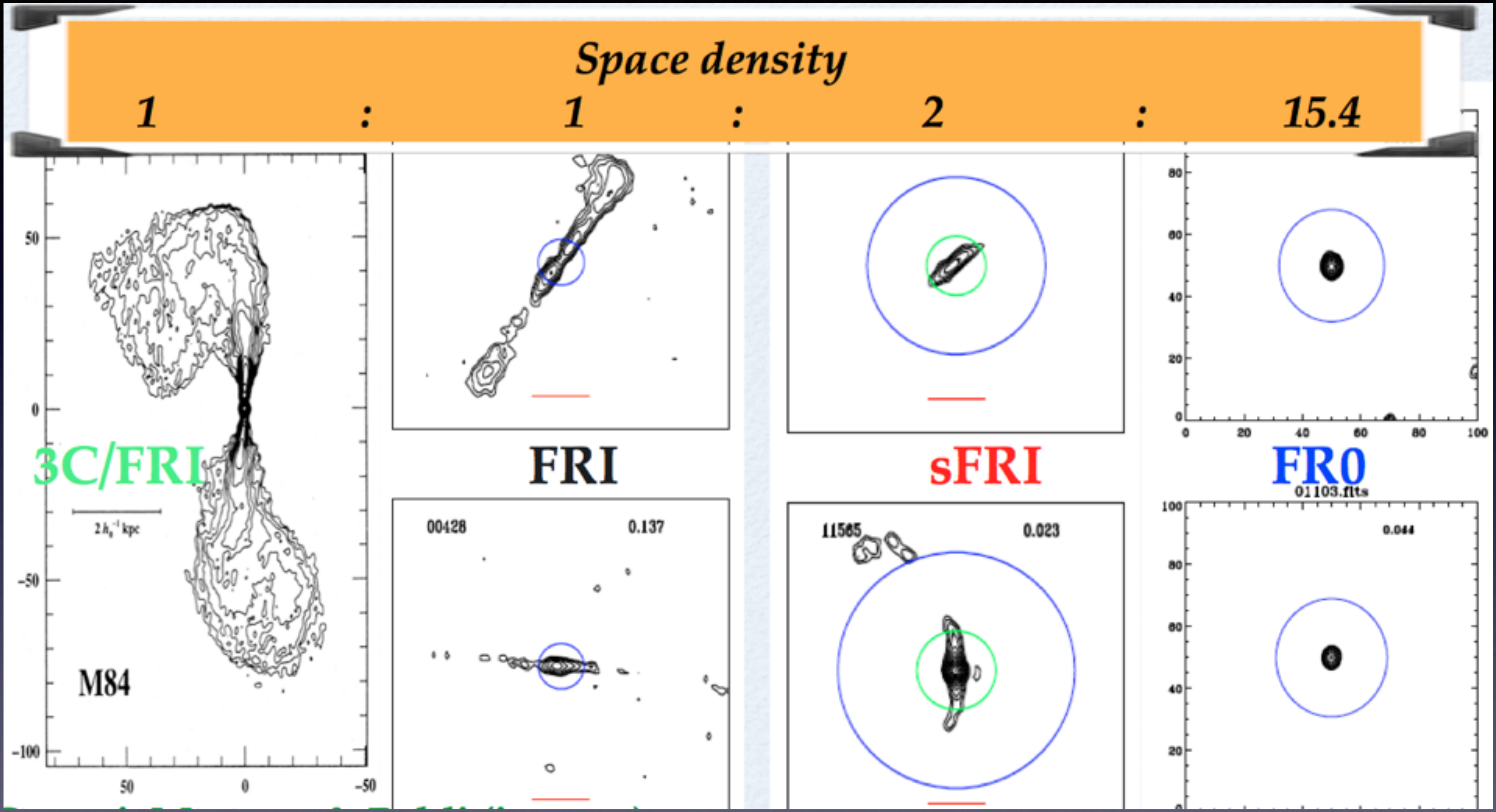

courtesy: R.D. Baldi

In the same volume 108 FR0, 21 FRI and 1 FRII

2. Spectral Energy Distribution of a RL AGN

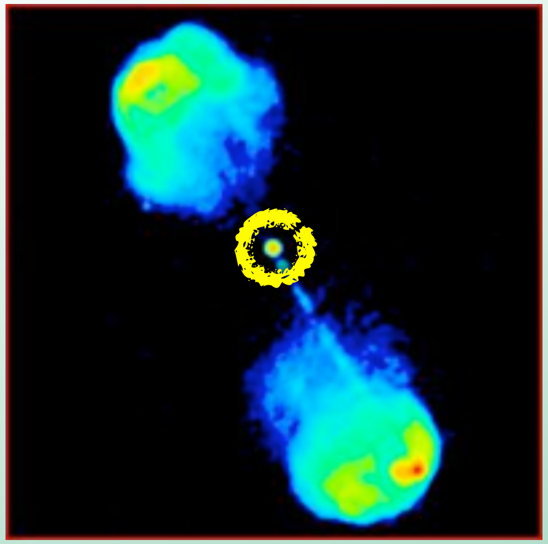

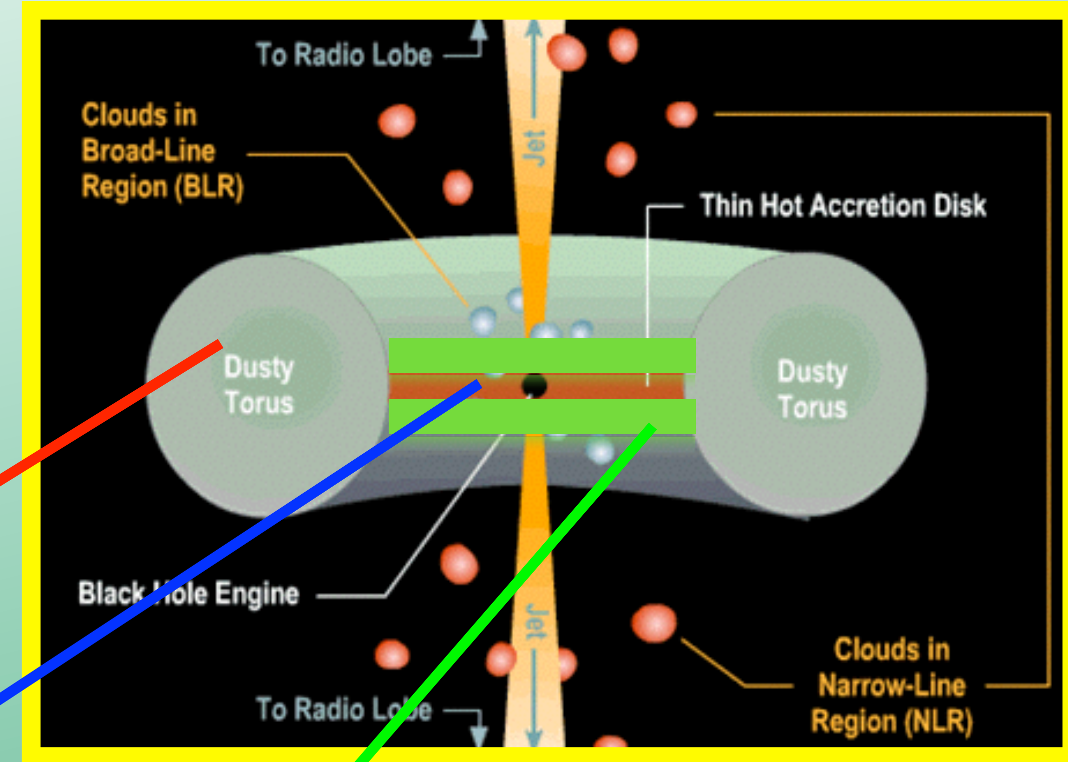

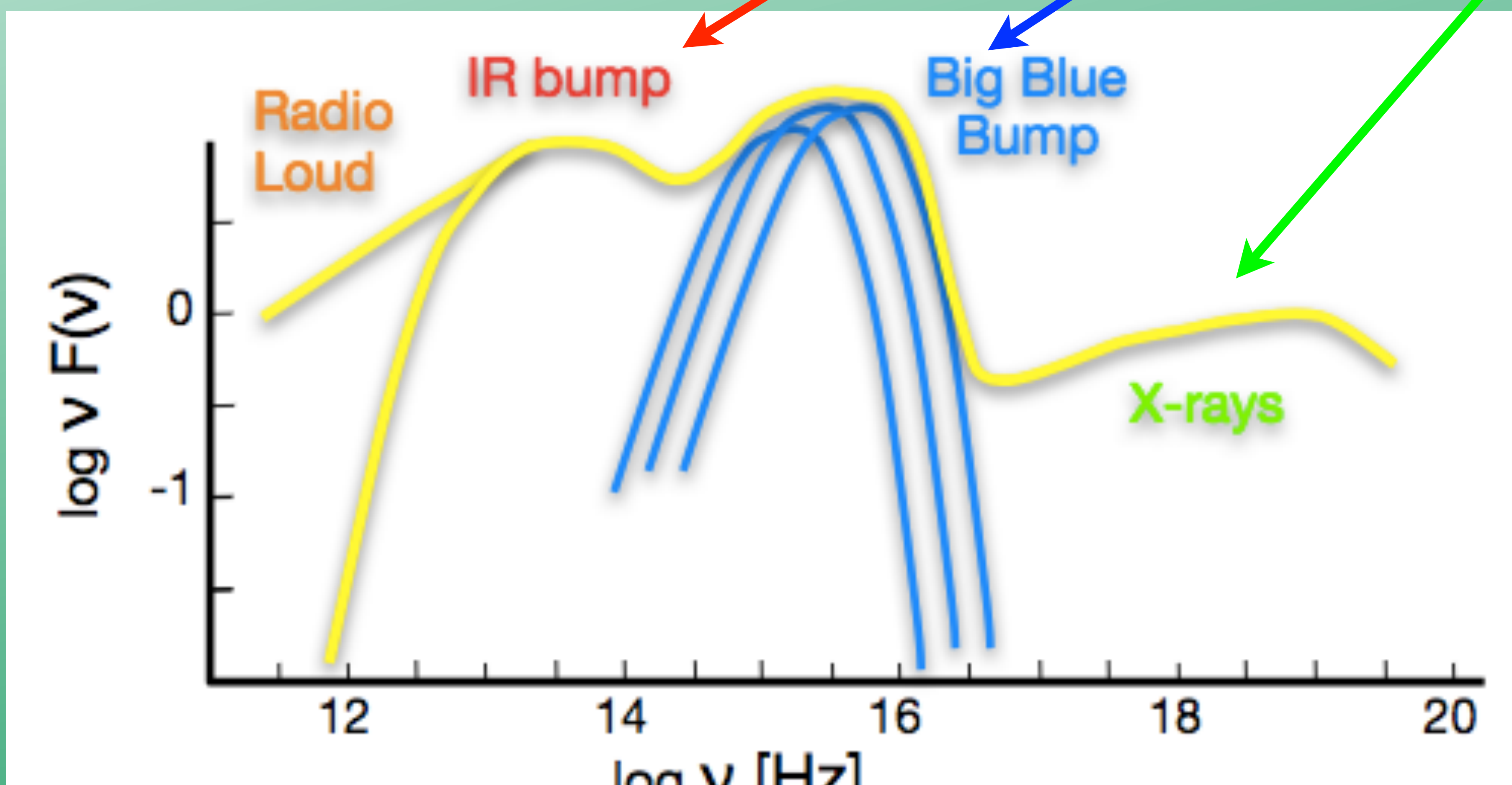

Credits: A. Marconi

Radio Galaxies: kpc components

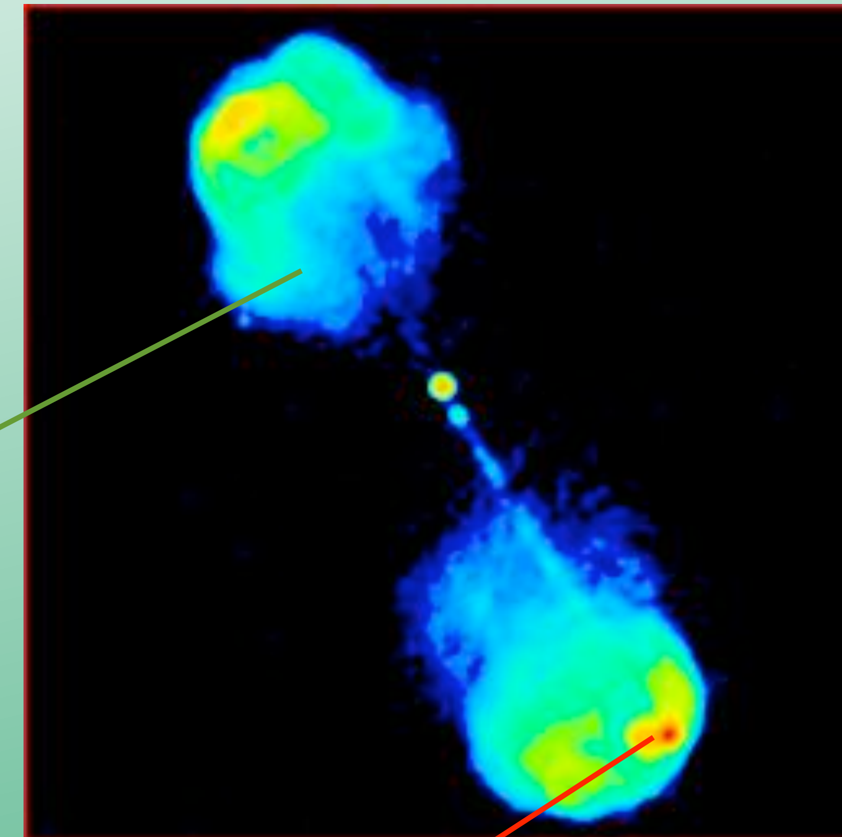

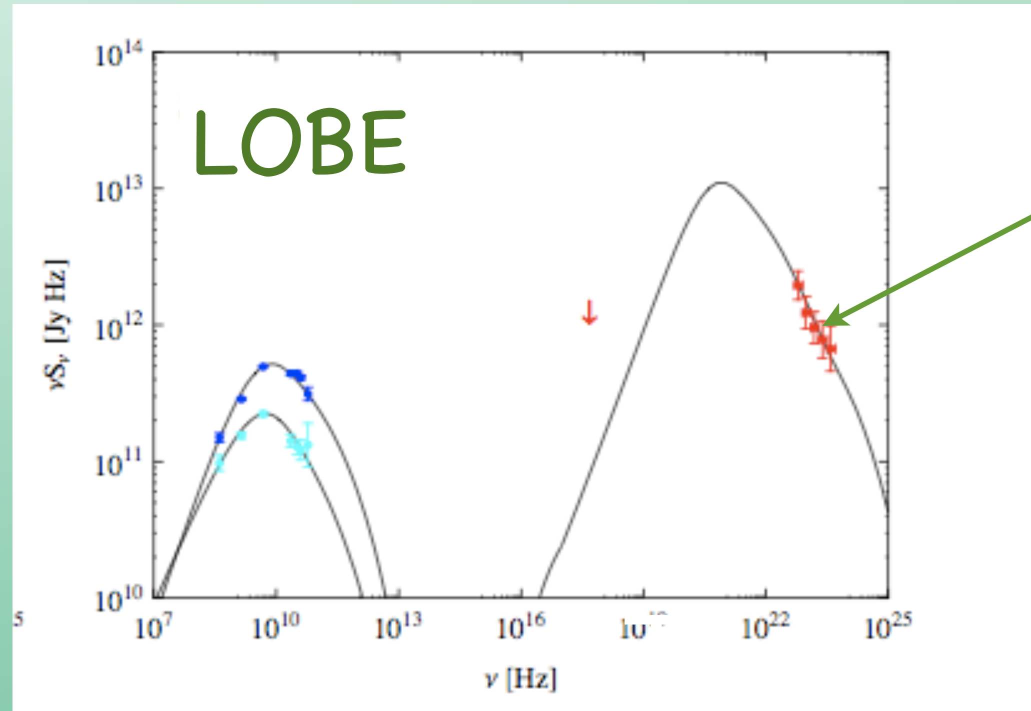

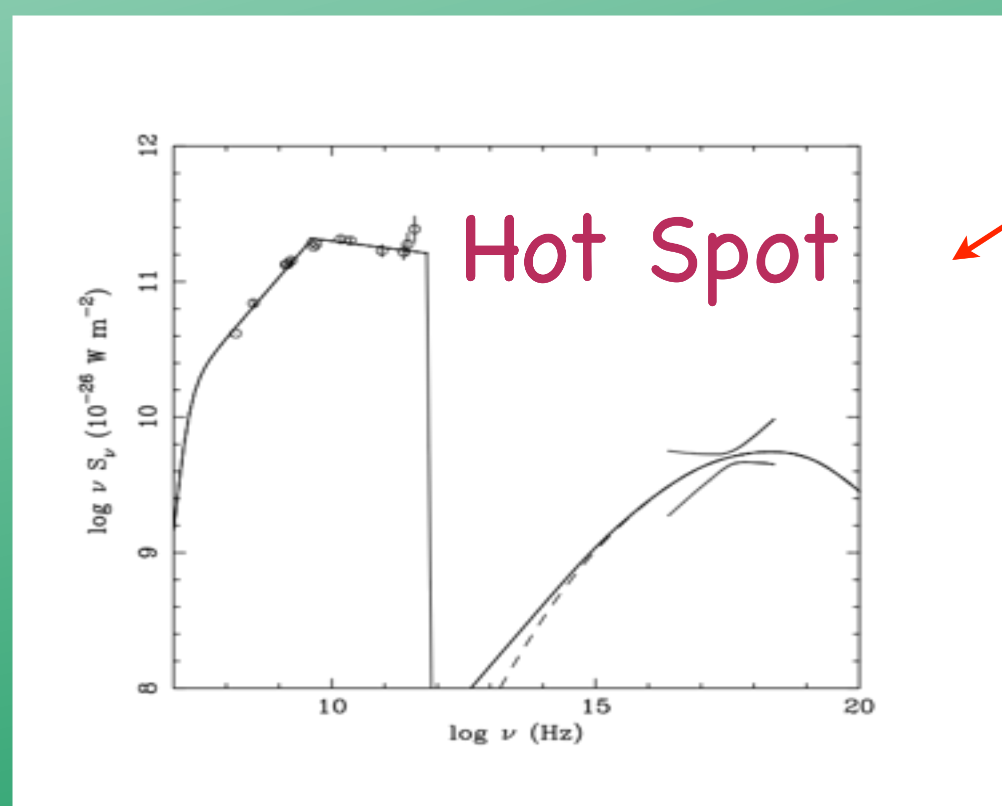

BLAZARS: double peaked SED

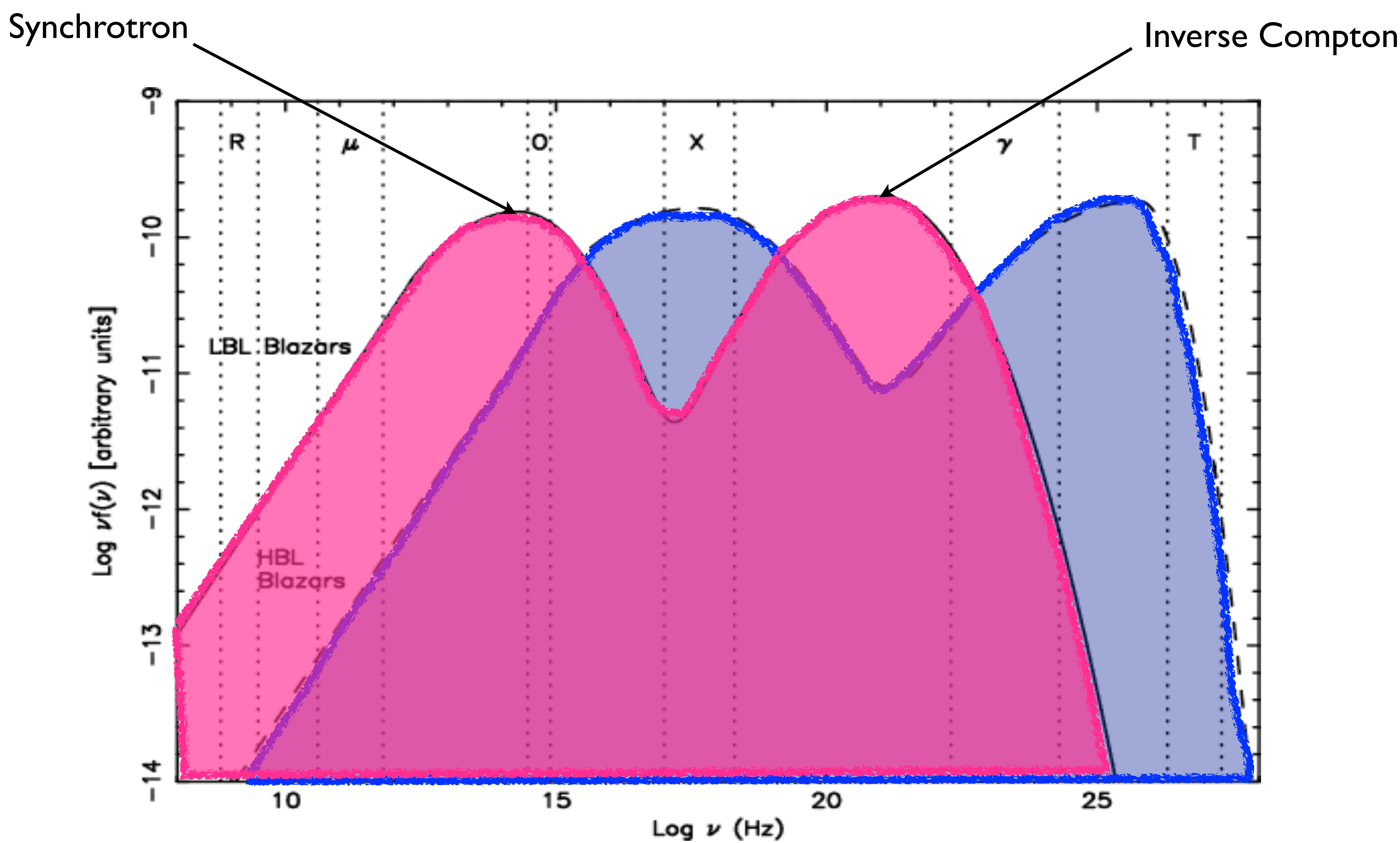

LBL= low-frequency peaked blazars

HBL= high-frequency peaked blazars

The jet emission from blazars is strongly Doppler boosted with respect to radio galaxies

The jet emission from blazars is strongly Doppler boosted with respect to radio galaxies

The key parameter is the Doppler Factor $\delta(\beta, \theta)$

$$\delta = [\gamma(1 - \beta cos\theta)]^{-1}$$

$= \sqrt{(1 - \beta^2)}$

Lorentz factor

=v/c

bulk velo

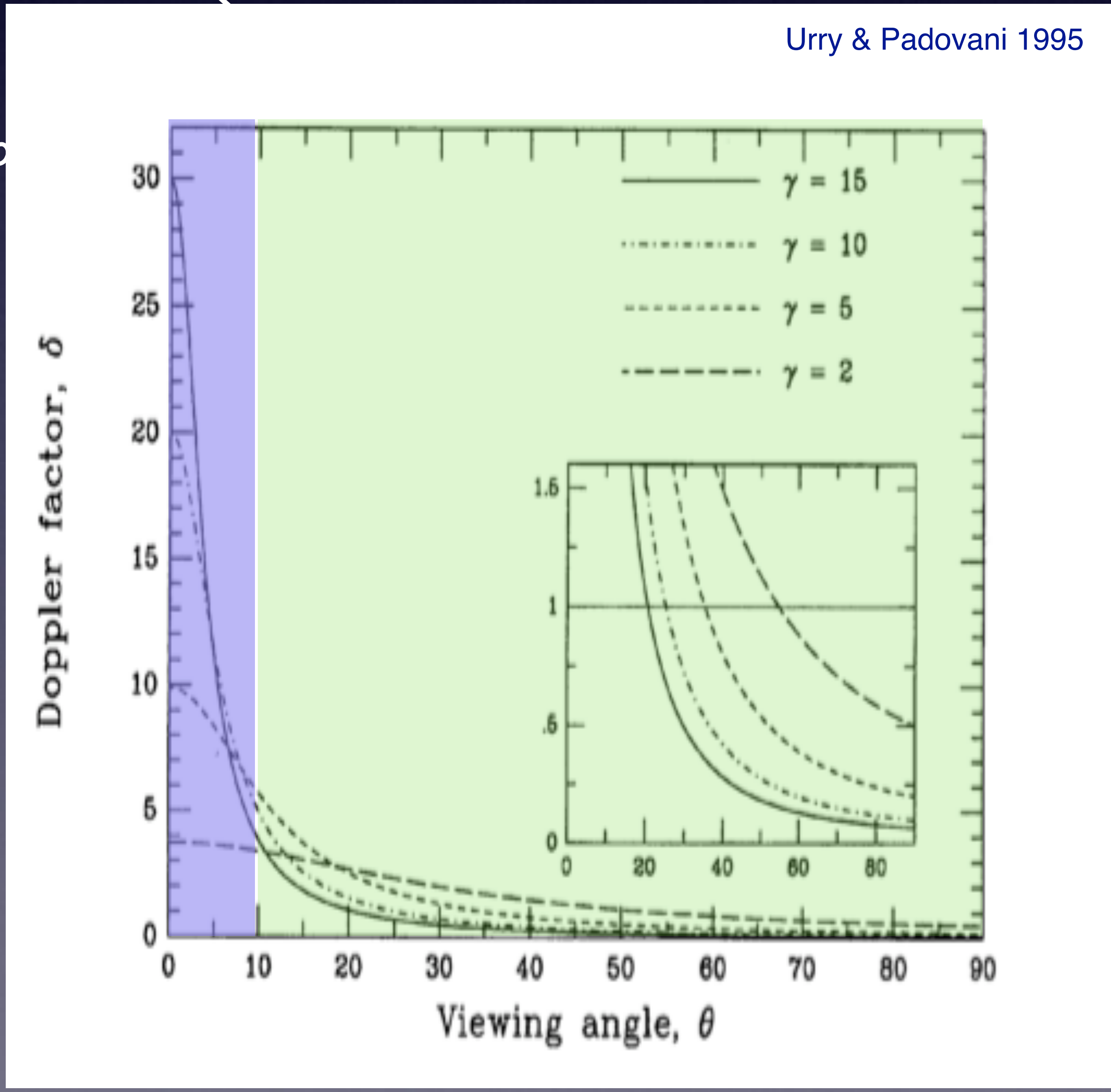

The Doppler factor relates intrinsic and observed flux for a moving source at relativistic speed v=β c.

For an intrinsic power law spectrum: $F'(\nu') = K (\nu')^{-\alpha}$
the observed flux density is

$$F_\nu(\nu) = \delta^{3+\alpha} F'_{\nu'}(\nu)$$

$$\Delta t = \Delta t' / \delta$$

3. The FR dichotomy

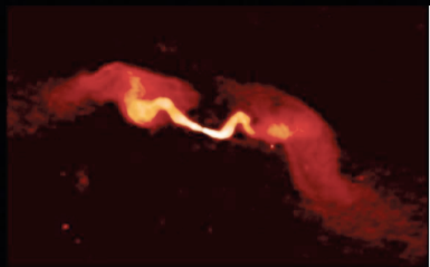

It is still unclear what causes the FRI/FRII dichotomy

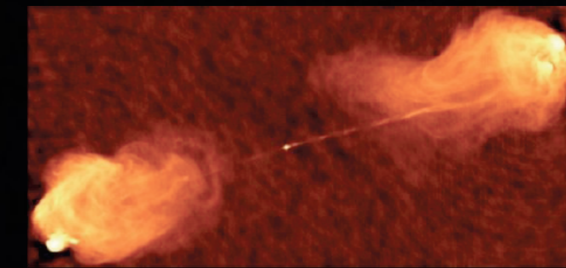

1) Ledlow & Owen (1994) found a correlation between the radio power at the FRI/FRII transition and the host galaxy magnitude

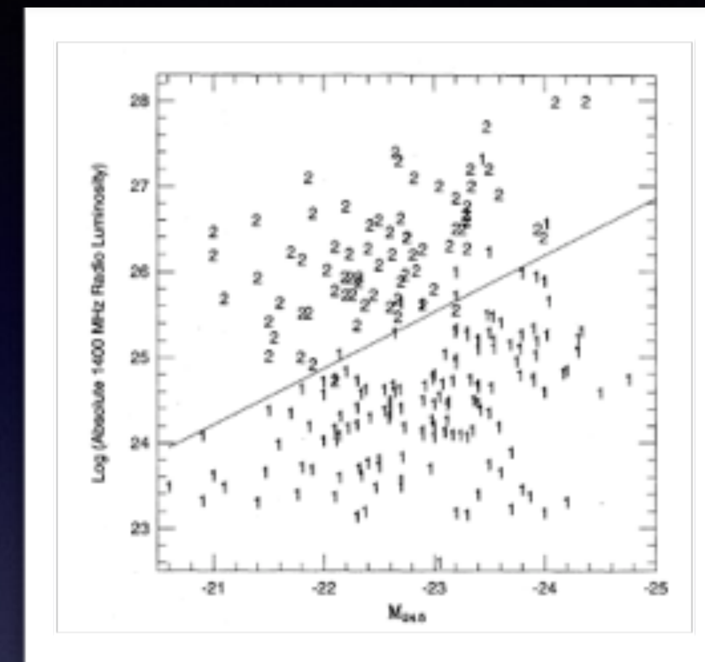

2) Bicknell 1995 points to different ways in which the jet interacts with the ambient medium: the FRI jets start highly relativistic and decelerate between the sub-pc and kpc scales

3) Baum et al. (1995) and Reynolds et al. (1996) suggest different nuclear intrinsic properties of the accretion and jet formation and the jet content

4) Ghisellini & Celotti (2001) indicate that the **accretion process** itself might play a key role in the deceleration and dichotomic behavior by affecting the pc-kpc scale environment

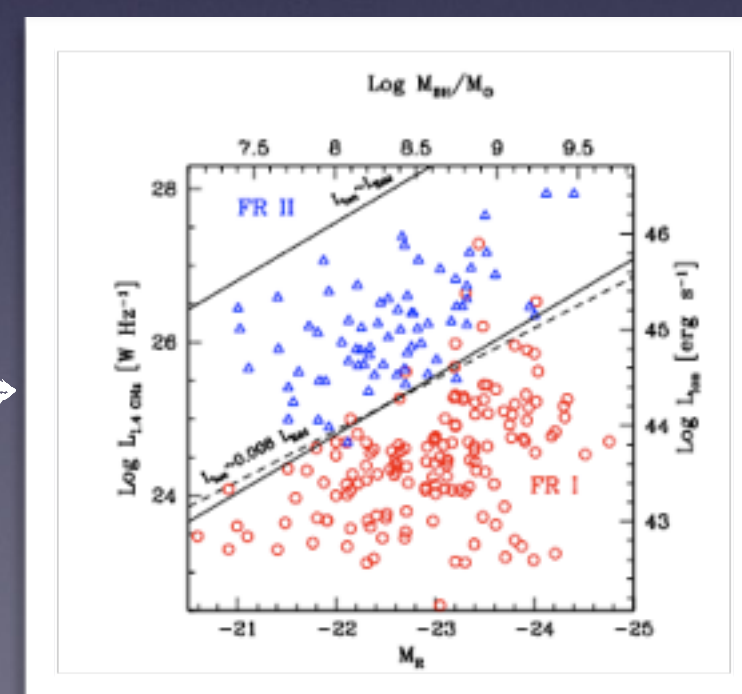

Optical observations seem to indicate that FRIs and FRIIs have different accretion regimes

The optical flux of FRIs shows a strong correlation with the radio core one over four decades, arguing for a non-thermal synchrotron origin of the nuclear emission (Chiaberge et al. 2002)

There is no nuclear absorption in FRI HST images. The weakness of the optical lines is not due to obscuration (Chiaberge et al. 2002)

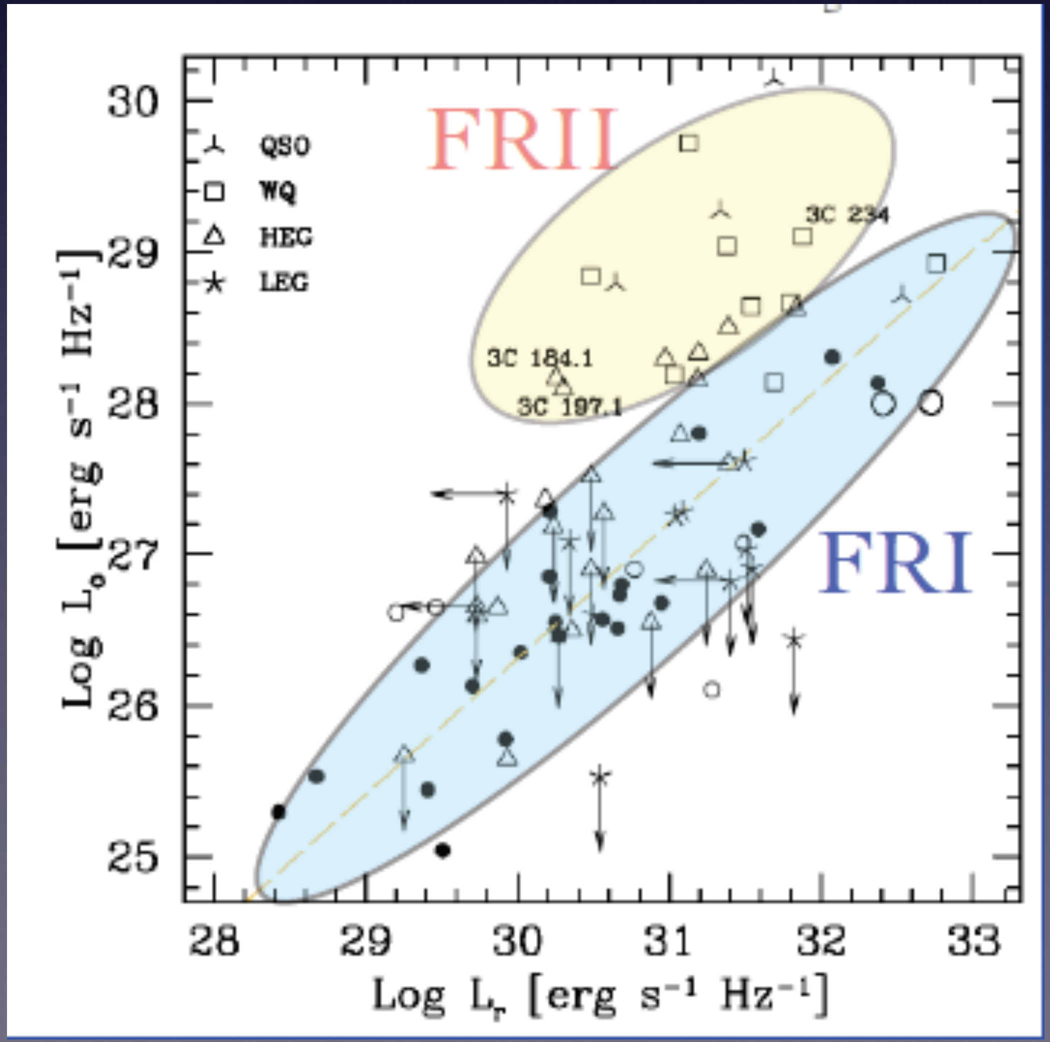

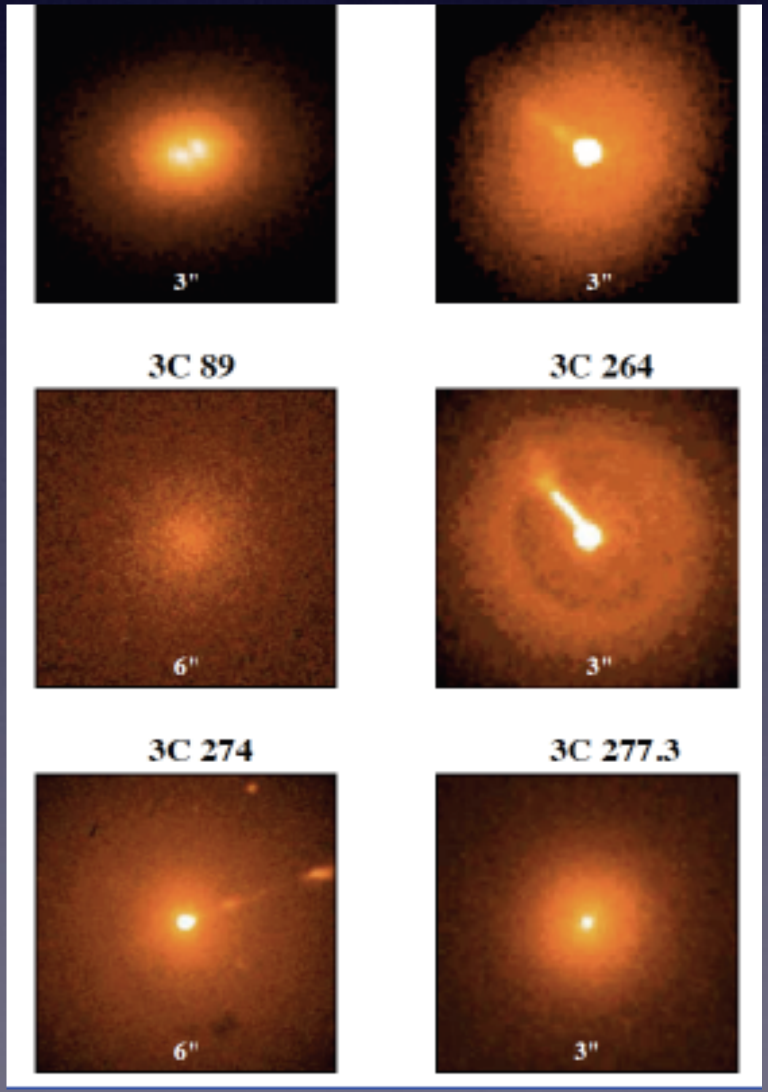

This scenario is also supported by IR observations...

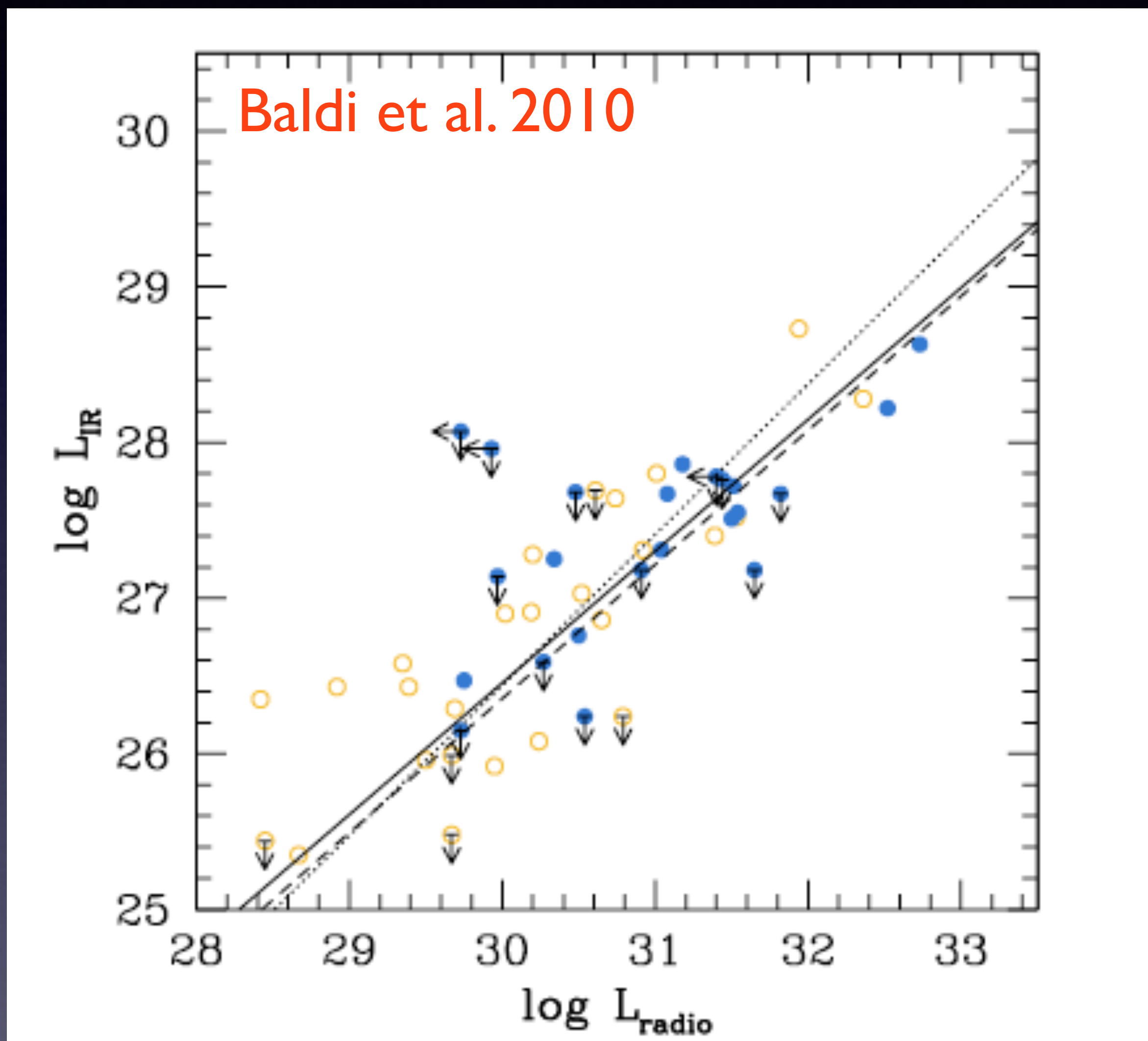

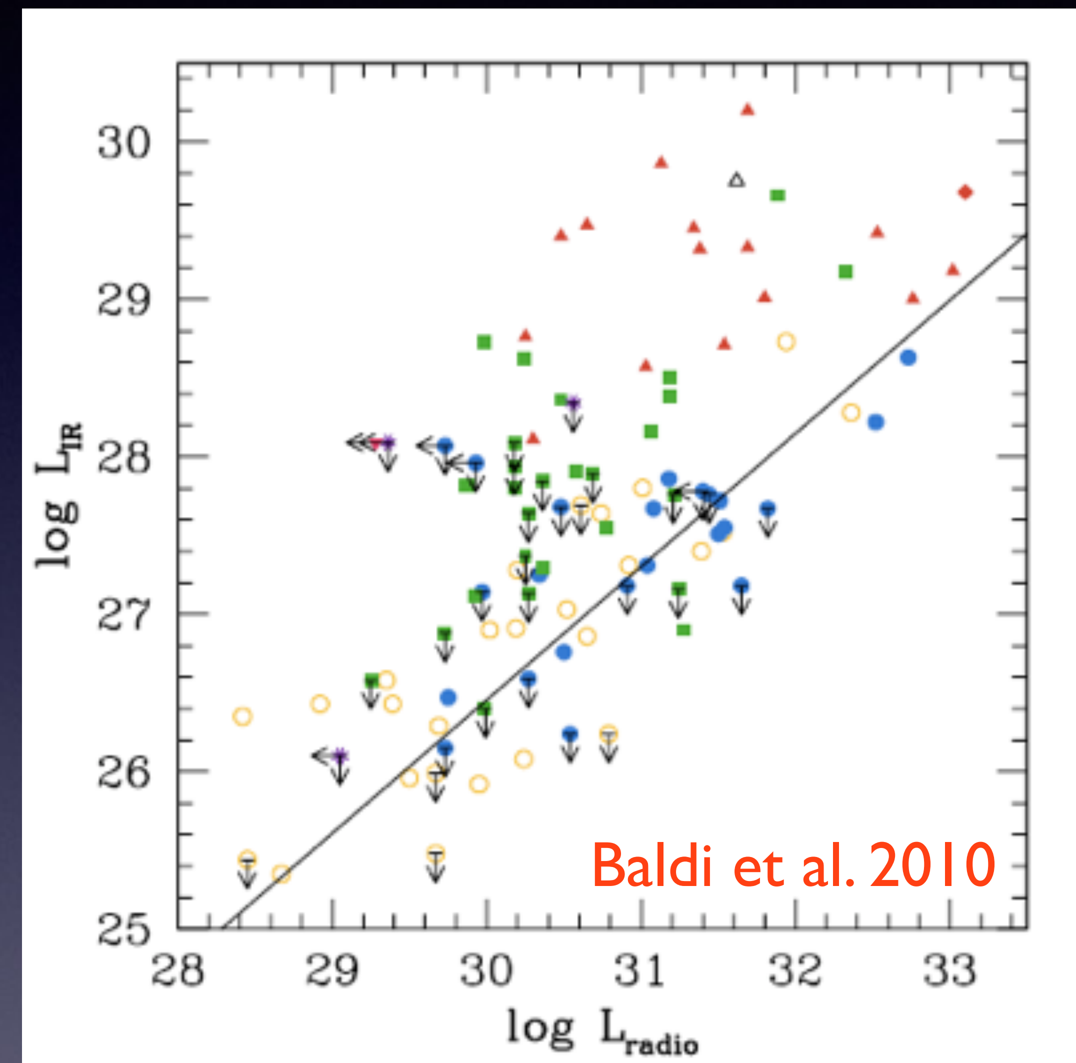

The NIR nuclear emission of FRIs has a non-thermal origin

FRIIs show an unresolved NIR nucleus and a large NIR excess --> hot circumnuclear dust (dusty torus)

…and X-ray observations

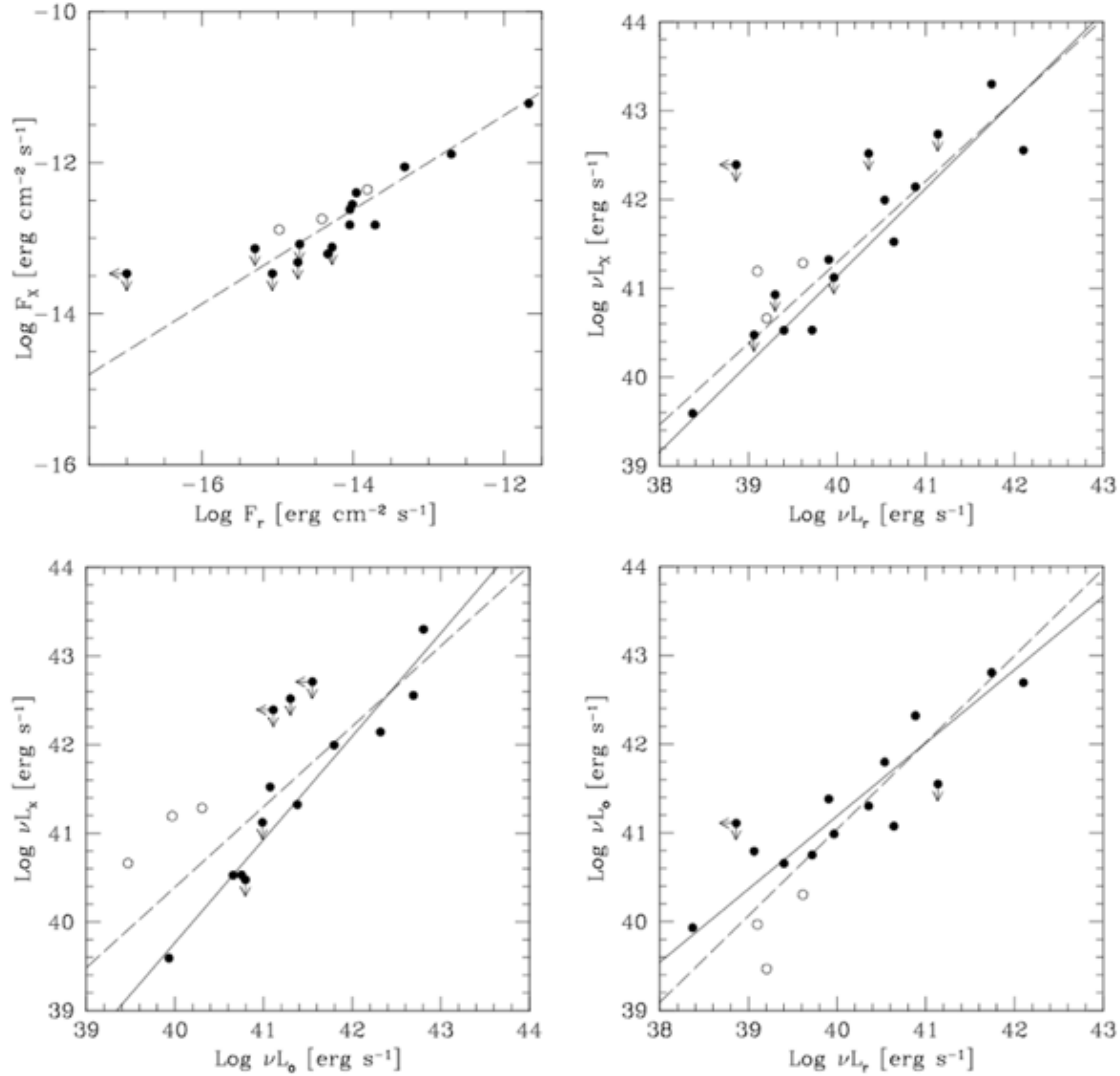

Fig. 2. Comparison of (*top left*) radio (5 GHz) and X-ray (0.5–5 keV) nuclear fluxes, (*top right*) radio and X-ray luminosities, (*bottom left*) optical (5500 Å) and X-ray luminosities, (*bottom right*) optical and radio luminosities. The empty circles represent the objects for which we have detected an intrinsic absorption $>10^{22}$ cm^{-2}. The solid line reproduces the best linear fit after having excluded the 3 X-ray absorbed nuclei, while the dashed line is the fit on the whole sample.

Balmaverde, Capetti & Grandi 2006

Radiative processes

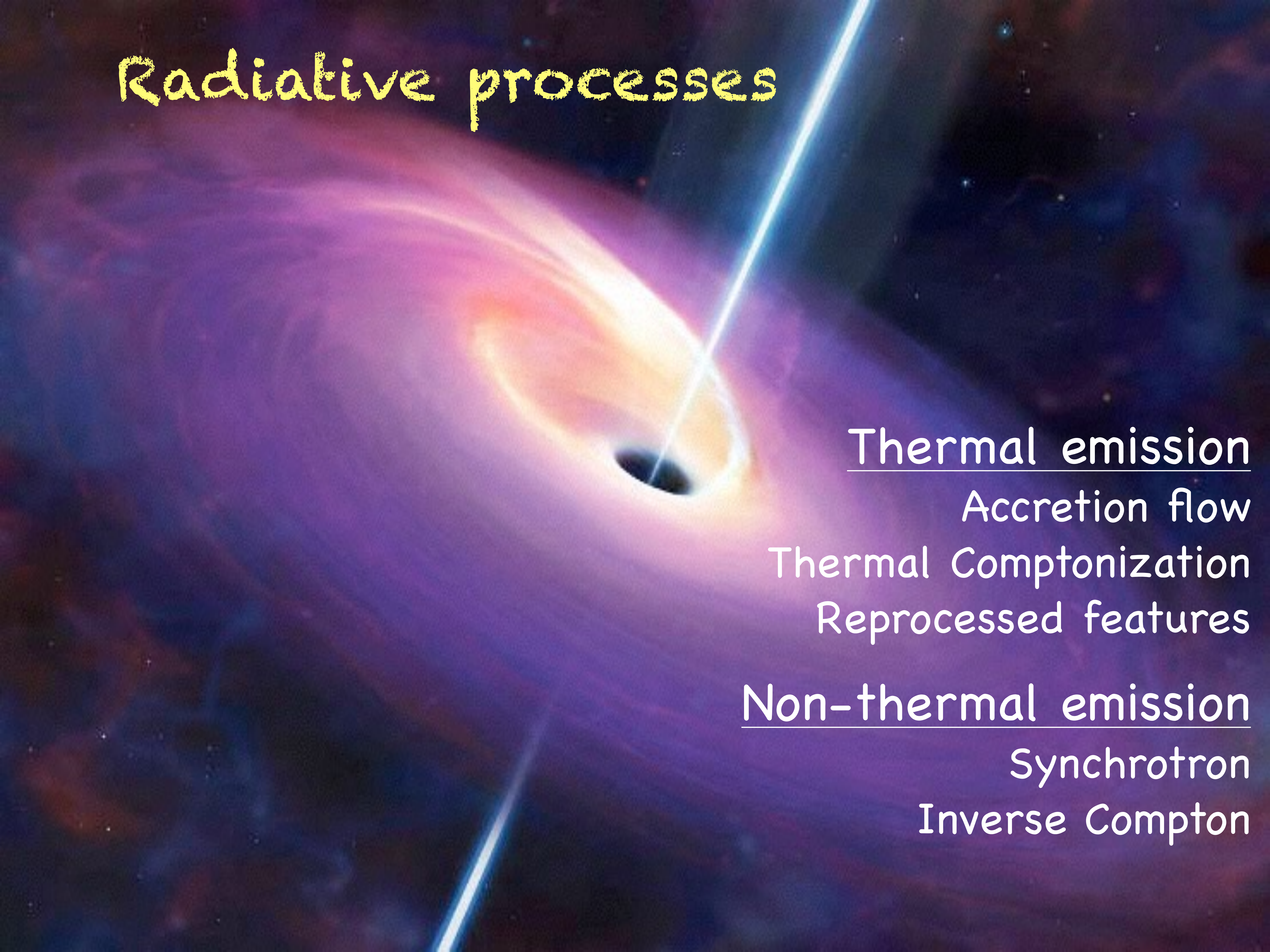

Thermal emission

Accretion flow

Thermal Comptonization

Reprocessed features

Non-thermal emission

Synchrotron

Inverse Compton

Thermal Processes

Accretion

Accretion as a source of energy

- Gravitational potential energy release for an object with mass *M* and with radius *R* by accretion of a test particle with mass *m*

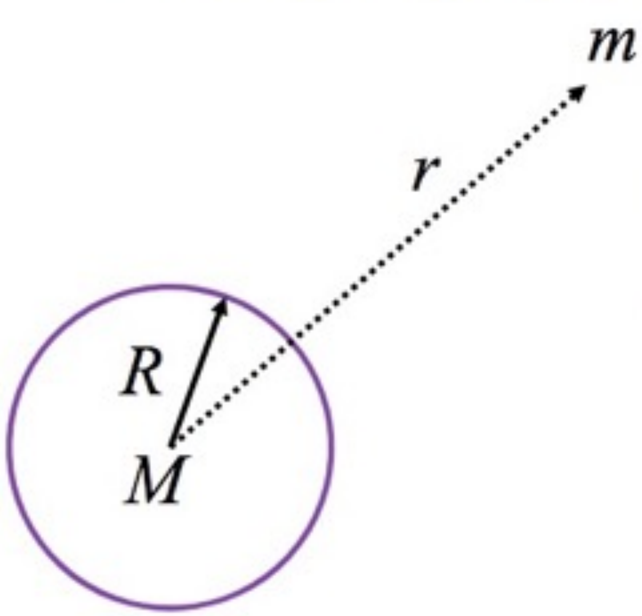

$$\left.\begin{matrix} E_r = -\frac{GMm}{r} \\ E_R = -\frac{GMm}{R} \end{matrix}\right\} \Delta E = Er - E_p = -\frac{GMm}{r} + \frac{GMm}{R}$$

$$\Longrightarrow E_{acc} = \frac{GMm}{R} \text{ for } r \gg R$$

- ***M/R is the compactness of the accretor***
  - ***The more compact, the more energy can be released***

Accretion luminosity

The accretion luminosity is given by

$$L_{acc} = \frac{dE_{acc}}{dt} = \frac{GM}{R}\frac{dm}{dt} \Rightarrow L_{acc} = \frac{GM\dot{m}}{R}$$

With M and R the mass and radius of the accreting star and $\dot{m}$ the *accretion rate*

For a Black Hole

$$L_{rad} = \epsilon \frac{GM\dot{m}}{R} = \eta \dot{m} c^2$$

with

$$R = \frac{GM}{c^2} \sim 3 \times 10^{13} M_8 \text{ cm}$$

$$\eta \propto \frac{M}{R}$$ process efficiency

Black hole radius can be derived by the escape velocity of the light

$$v_{escape} = c = \left(\frac{2GM}{R_S}\right)^{\frac{1}{2}}$$

Schwarzschild radius

$$R_S = \frac{2GM}{c^2}$$

Eddington Luminosity L_E is the luminosity at which the outward force of the radiation pressure is balanced by the inward gravitational force

$$L_{Edd} = \frac{4\pi G m_p M c}{\sigma_T} \sim 1.3 \times 10^{38} (\frac{M}{M_\odot}) \text{ erg/s}$$

$$L_{\mathrm{Edd}} = \frac{4\pi G M c m_{\mathrm{p}}}{\sigma_{\mathrm{T}}}$$

$$L = \eta \dot{m} c^2$$

from which

$$M = 7 \times 10^8 M_\odot.$$

And from our Eddington accretion rate, using $\eta = 0.1$ we have

$$\dot{M}_{\mathrm{Edd}} = \frac{4\pi G M m_{\mathrm{p}}}{\epsilon c \sigma_{\mathrm{T}}} \approx 3 M_\odot \mathrm{yr}^{-1}$$

Disks usually rotate such that each fluid element is moving almost in a circular orbit. As the angular velocity is a function of radius, there is a shearing flow. This means that coupling between adjacent radii exerts a force. Given that the outer parts rotate more slowly, inner try to speed up outer, giving it a higher velocity. This increases the angular momentum of the outer, decreases the angular momentum of the inner, so net result is that angular momentum is transferred outwards and mass flows inwards.

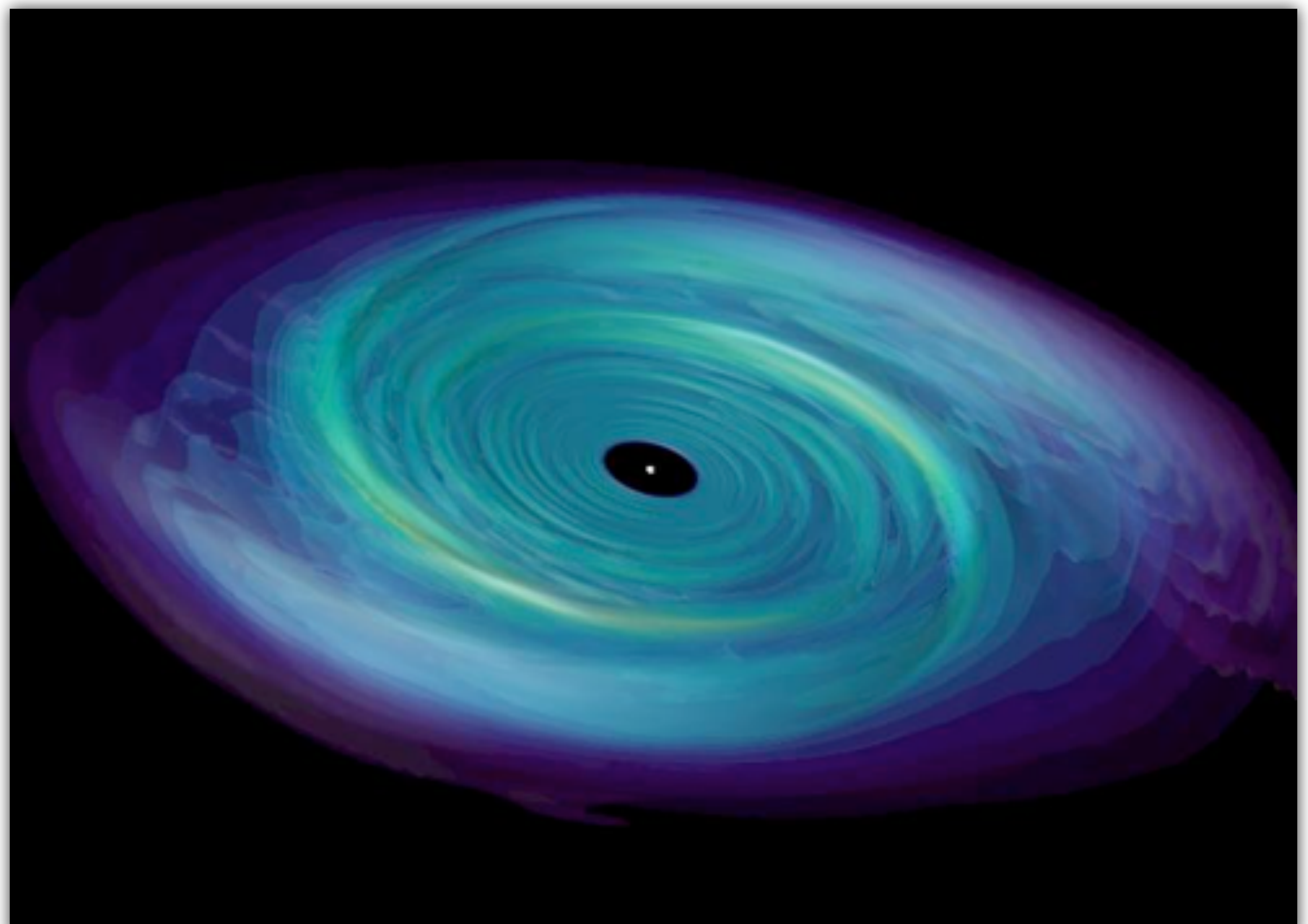

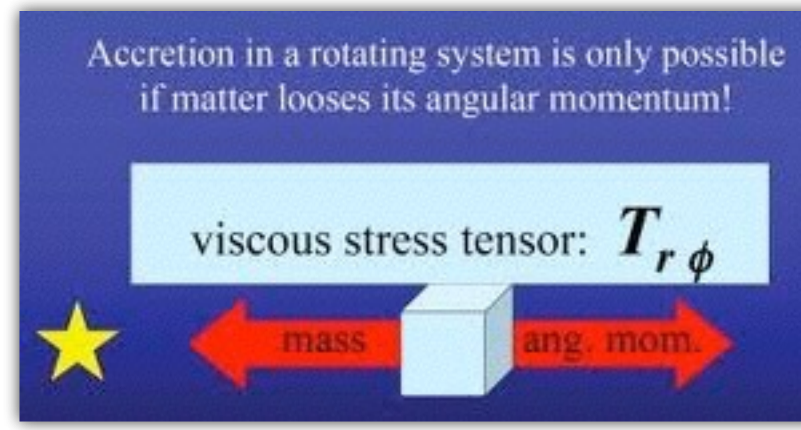

Viscosity transports angular momentum outward, allowing the accretion gas to spiral in toward the BH. Viscosity acts as a source of heat that is radiated away.

Accretion processes around black holes involve rotating gas flow. Therefore the accretion flow structure is determined by solving simultaneously four conservation equations:

conservation of vertical momentum
conservation of mass
conservation of energy
conservation of angular momentum

Four solutions are currently known. In these solutions viscosity transports angular momentum outward, allowing the accretion gas to spiral in toward the BH. Viscosity acts a source of heat that is radiated away.

The most famous solutions are:

i) Shakura & Sunyaev thin optically thick disk model (standard model)
ii) Optically thick Advection-Dominated Accretion Flow (ADAF)

Shakura & Sunyaev thin optically thick disk model (standard model)

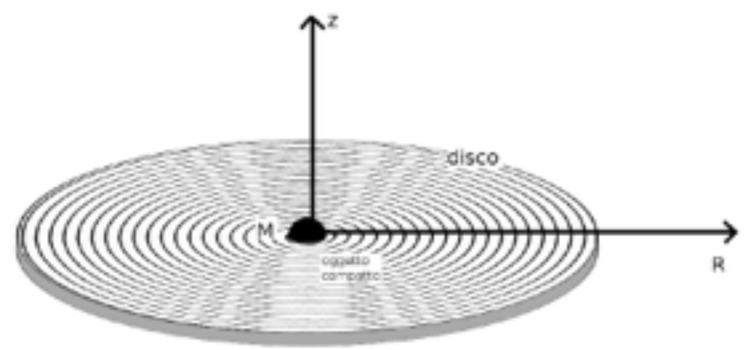

Thin $H/R \ll 1$

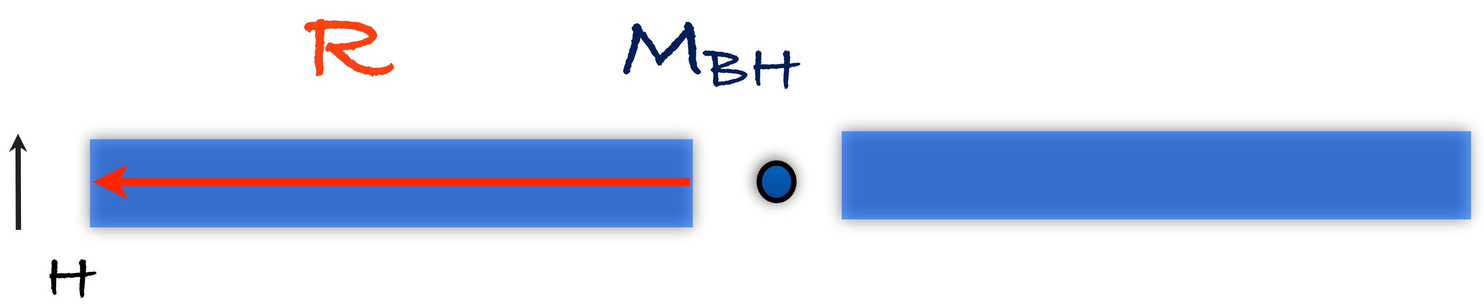

Thick, in the sense that each element of the disk radiates as a black body

If the the disk is optically thick, we can approximate the local emission as blackbody and the effective temperature of the photosphere

$$T(r) \sim 6.3 \times 10^5 \left(\frac{\dot{M}}{\dot{M}_E}\right)^{1/4} M_8^{-1/4} \left(\frac{r}{R_s}\right)^{-3/4} \quad K$$

For AGN with $M_{BH} = 10_8 = 10^8 M_\odot$ $\quad \dot{M} \sim \dot{M}_E = \frac{L_E}{\eta c^2}$

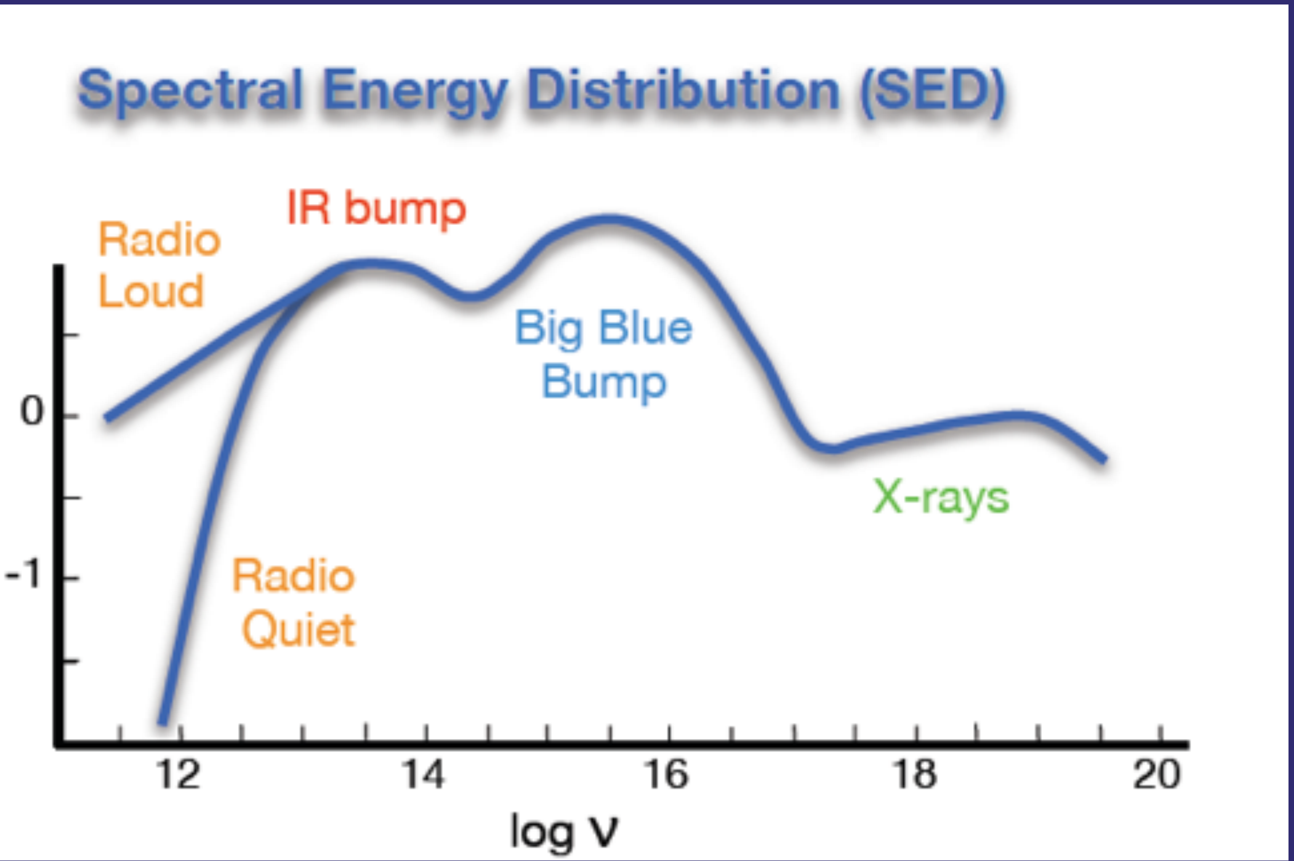

the peak occurs at UV-soft-X-ray region

$$\frac{\partial B}{\partial \nu} = 0 \qquad B(\nu) \propto \nu^3 [e^{\frac{h\nu}{kT}} - 1]^{-1}$$

$$\nu_{max} = 2.8kT/h \sim 10^{16} \quad Hz$$

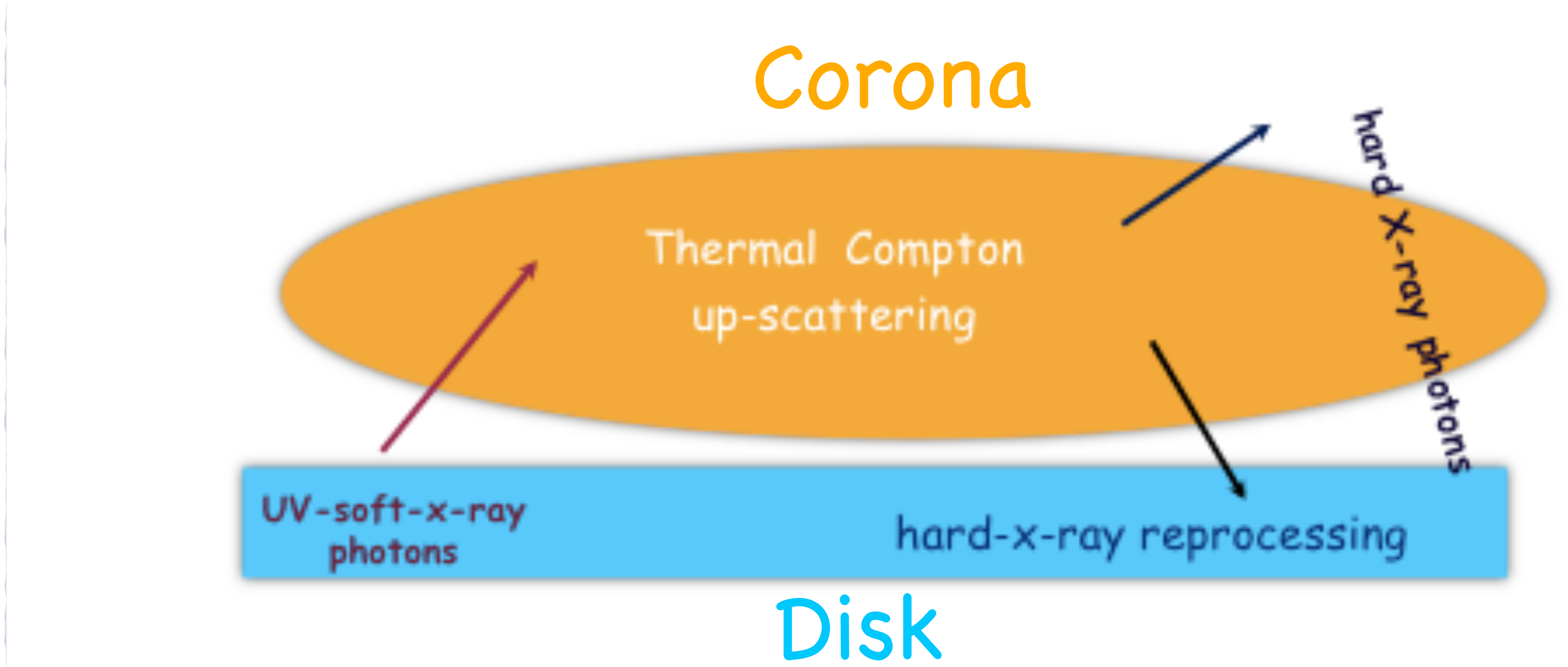

Thermal Comptonization

With this term we mean the process of multiple scattering of a photon due to a **thermal (Maxwellian)** distribution of electrons.

There is one fundamental parameter measuring the importance of the Inverse Compton process in general, and of multiple scatterings in particular: the Comptonization parameter, usually denoted with the letter **y**.

y = [average # of scatt.] x[average fractional energy gain for scatt.]

Thermal Comptonization

Comptonization on a thermal plasma of electrons characterized by a temp. T and optical depth τ

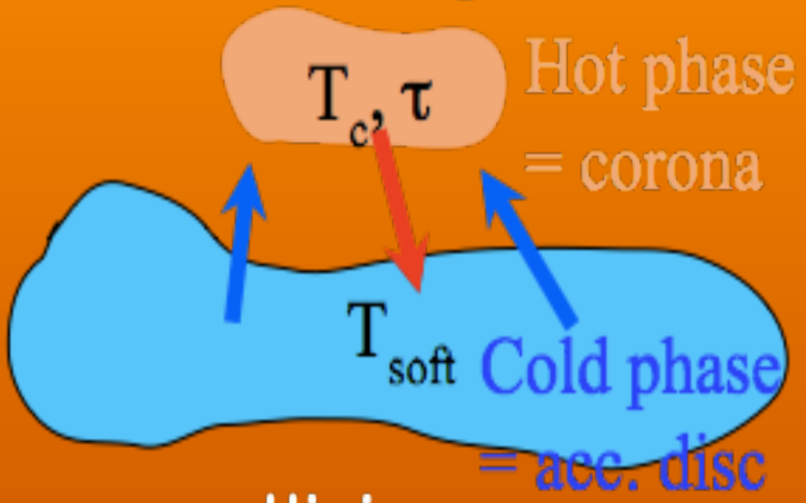

✓ mean relative energy gain per collision

$$\frac{\Delta E}{E} \simeq \left(\frac{4kT}{mc^2}\right) + 16\left(\frac{kT}{mc^2}\right)^2 \quad \text{for } E \ll kT$$

$$\leq \quad 0 \quad \text{for } E \gtrsim kT$$

✓ mean number of scatterings

$$N \simeq (\tau + \tau^2)$$

➡ Compton parameter $y = \frac{\Delta E}{E} N$

$E_f = E_i\, e^y$

Thermal Comptonization Spectrum: the continuum

$$F_E \propto E^{-\Gamma(kT,\tau)} \exp\left(-\frac{E}{E_c(kT,\tau)}\right)$$

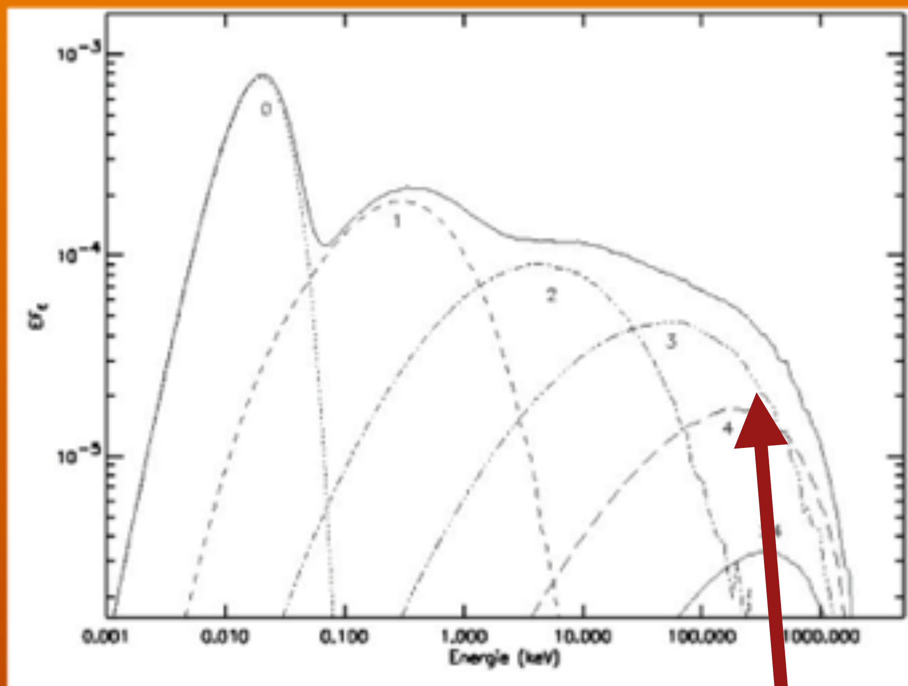

$$\Gamma(\tau, kT)$$

The exact relation between spectral index and optical depth depends on the geometry of the scattering region.

$$E_c \simeq kT$$

As photons approach the electron thermal energy, they no longer gain energy from scattering, and a sharp rollover is expected in the spectrum.
The observed high energy spectral cutoff yields information about the temperature of the underlying electron distribution.

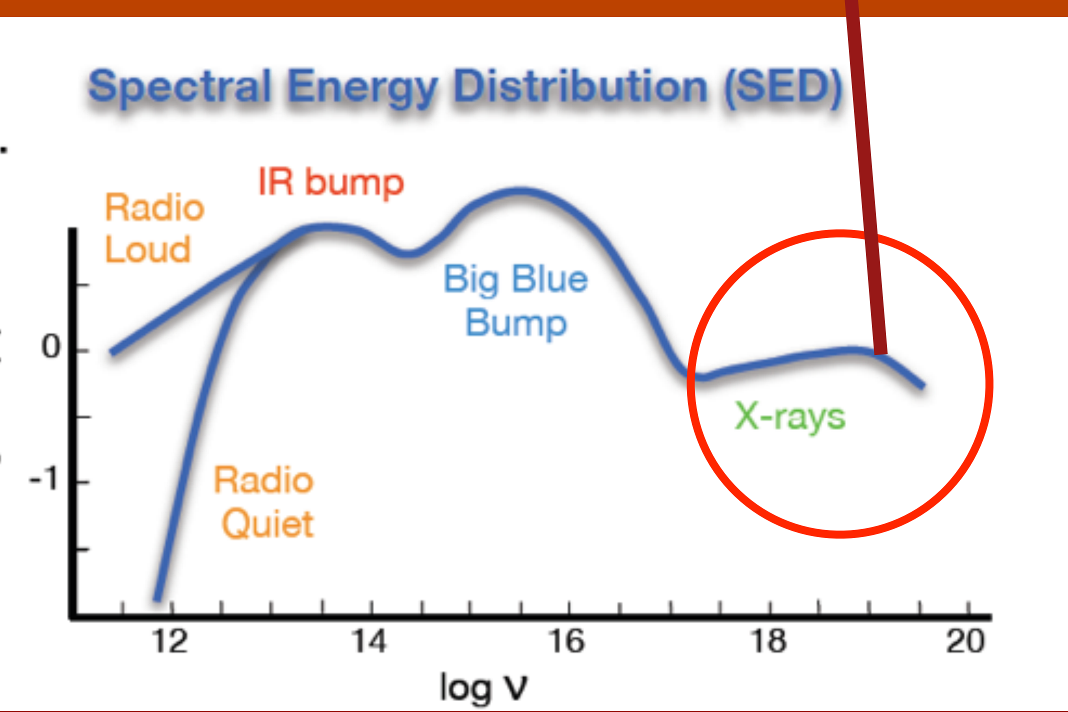

Ec ~ 100-200 keV

1 keV ~ 10^7 K

Ec =?

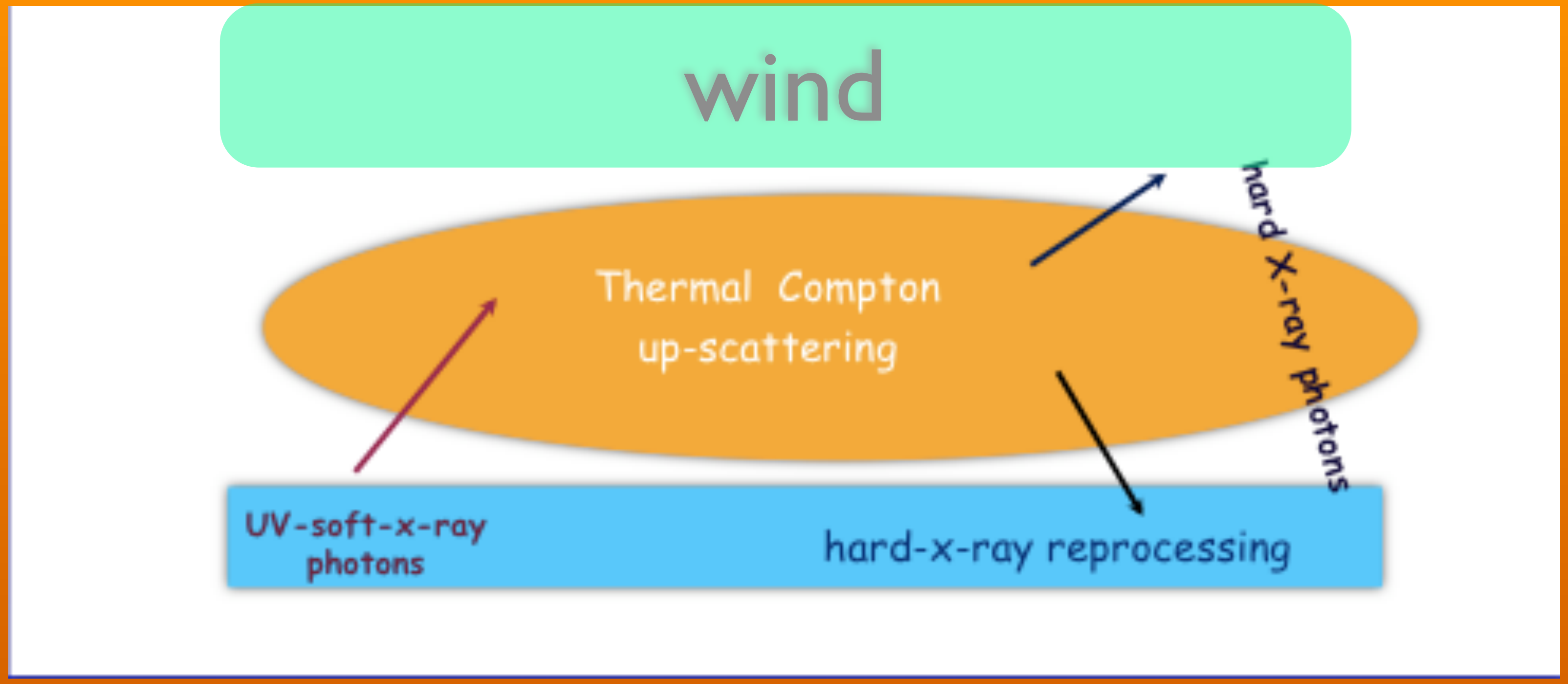

- Thermal Comptonization
- Hard X-ray reprocessing

Iron line

Compton hump

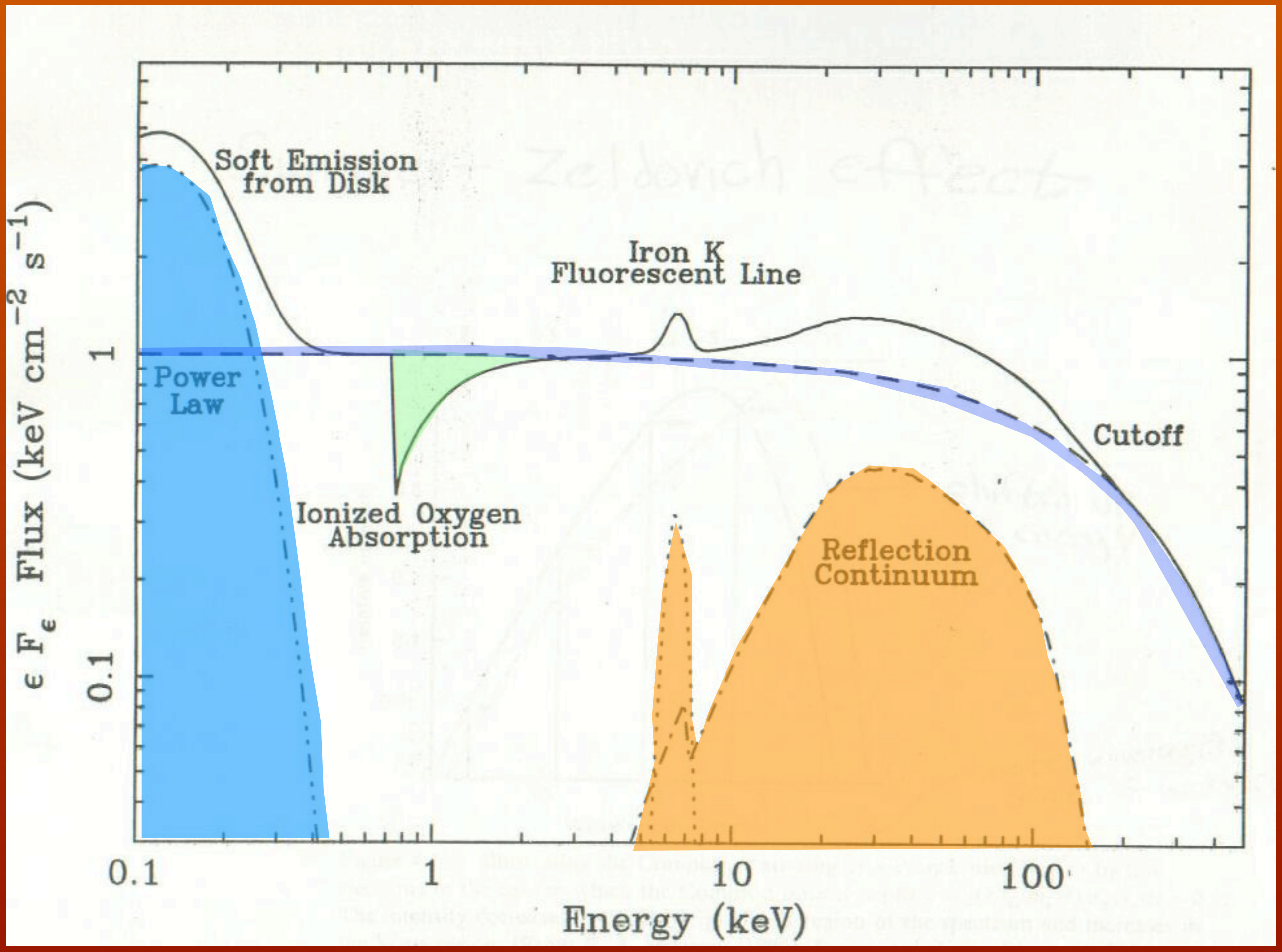

Reflection

At low energies <10 keV the high-Z ions absorb the X-rays. A major part of the opacity above 7 keV is due to Fe K-edge opacity.

At high energies the Compton shift of the incident photons becomes important.

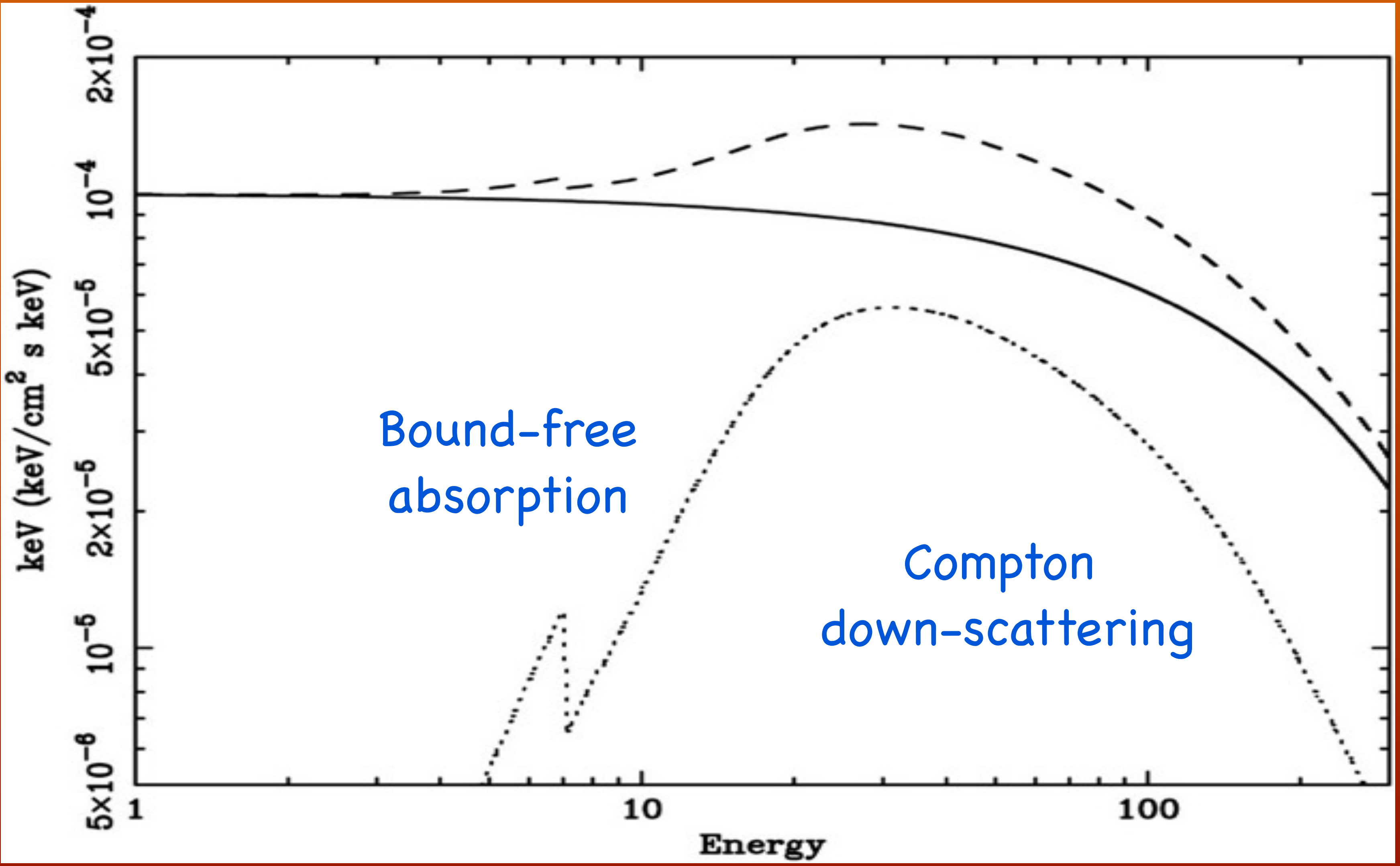

Photon-electron interaction

Direct Compton Scattering

In this process the photon is absorbed and immediately re-radiated by the electron into a different direction but it looses part of its initial energy. It can be thought as an heating mechanism.

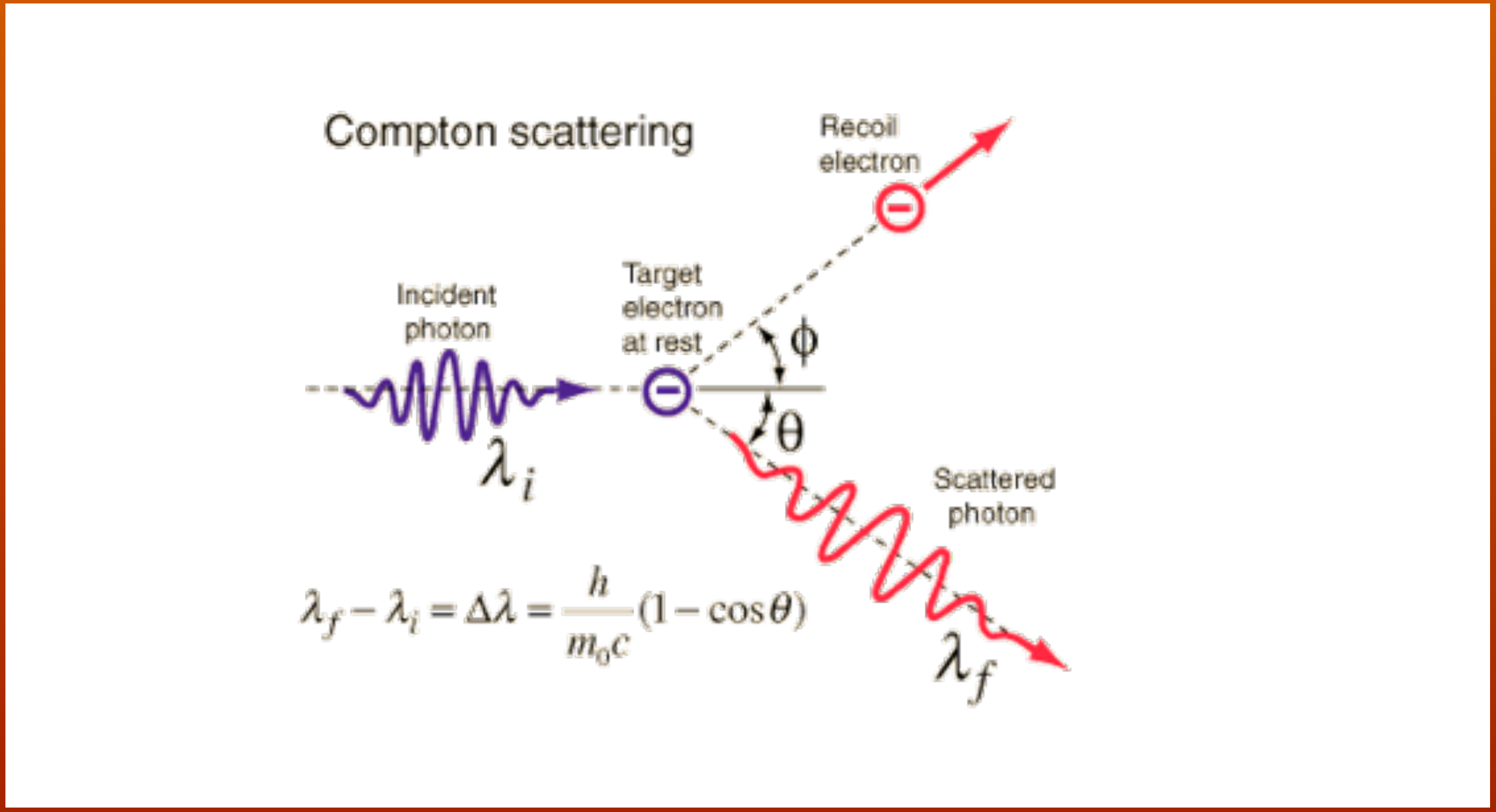

Iron Line

The fluorescent iron line is produced when one of the 2 K-shell (n=1) electrons of an iron atom (or ion) is ejected following photoelectric absorption of an X-ray. Following the photoelectric event, the resulting excited state can decay in one of two ways. An L-shell (n=2) electron can then drop into the K-shell releasing 6.4 keV of energy either as an emission line photon (34 % probability) or an Auger electron (66 % probability).

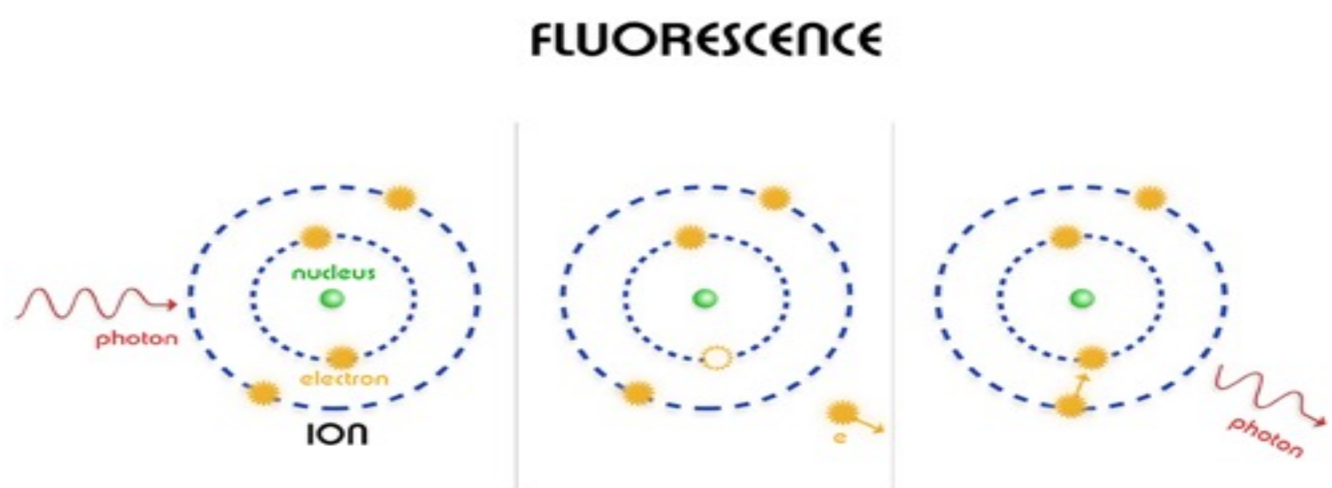

For ionized iron, the outer electrons are less effective at screening the inner K-shell from the nuclear charge and the energy of both the photoelectric threshold and the K line are increased.

BROAD LINE

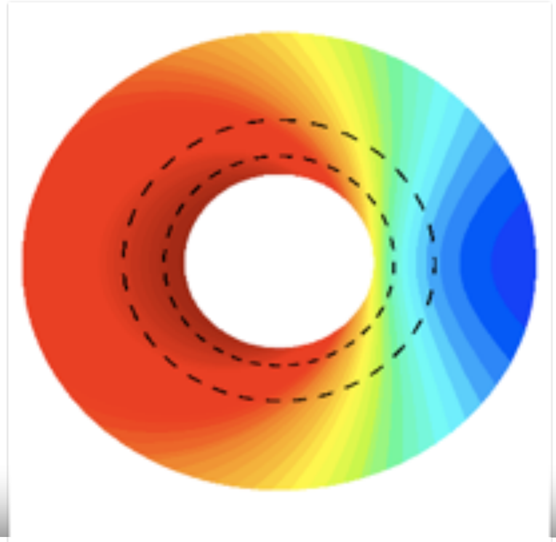

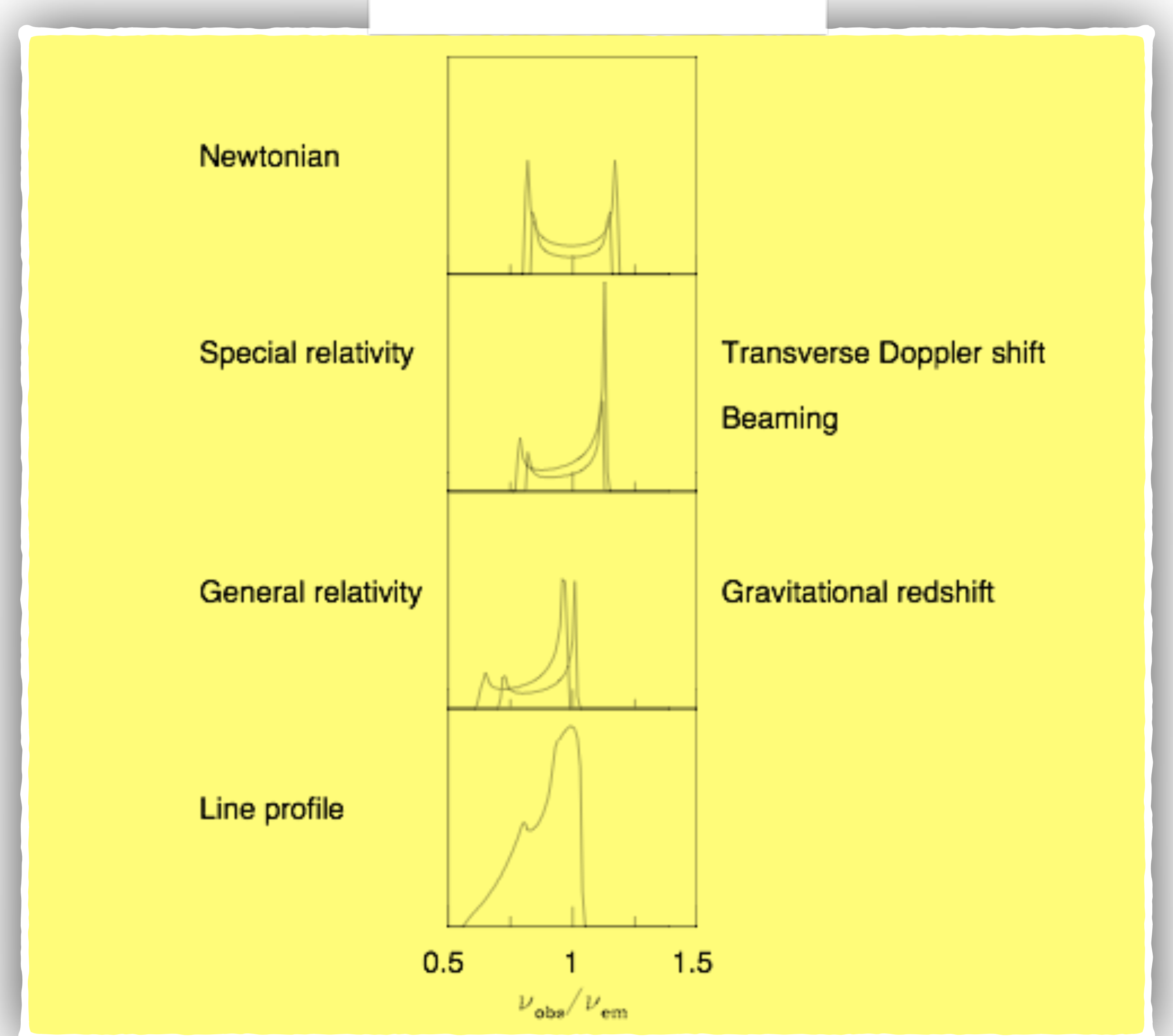
Newtonian
Special relativity
Transverse Doppler shift
Beaming
General relativity
Gravitational redshift
Line profile
0.5
1
1.5
ν_{obs}/ν_{em}

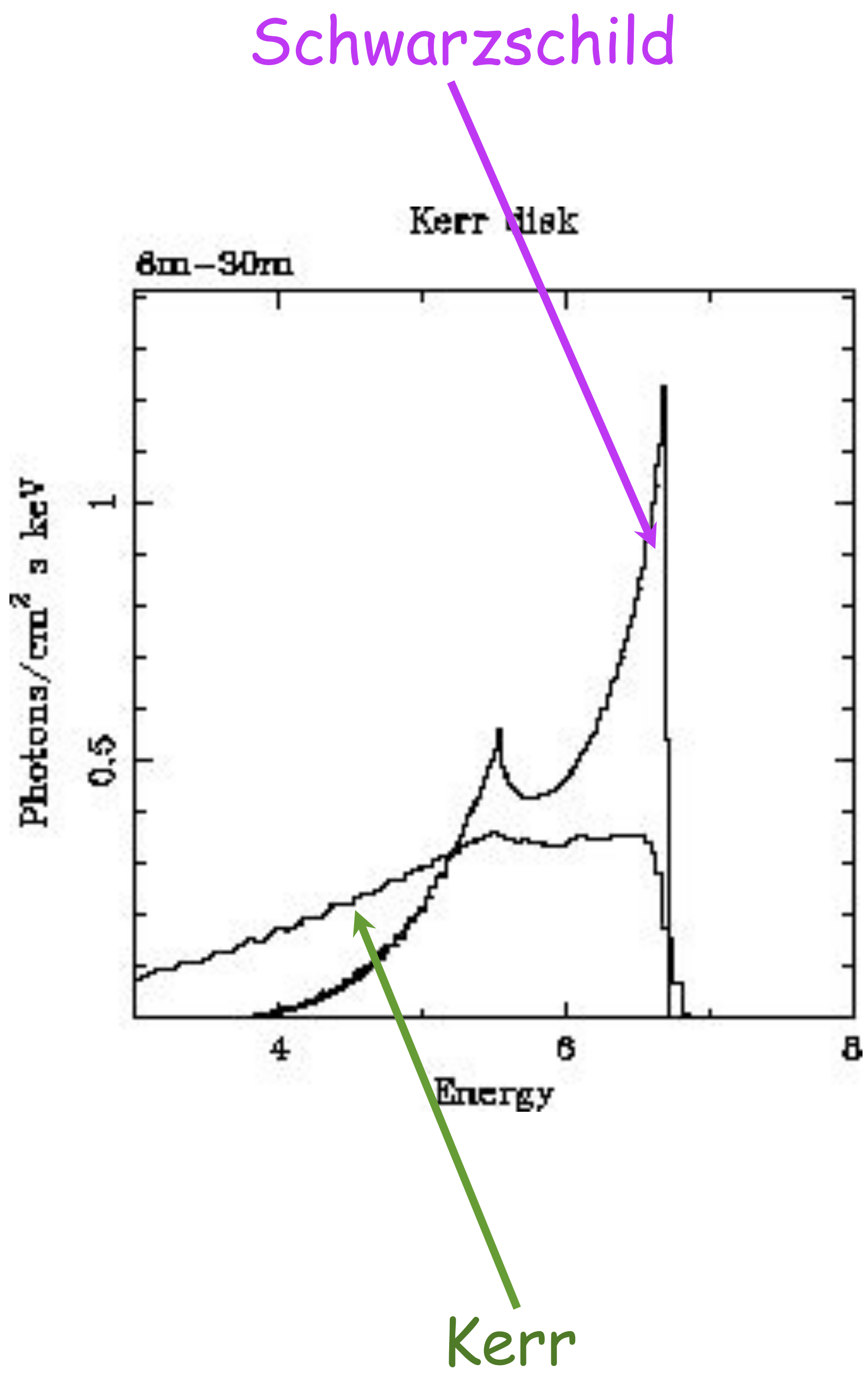
Schwarzschild
Kerr disk
6m–30m
Photons/cm^2 s keV
1
0.5
4
6
8
Energy
Kerr

Energy Equation

$$q^+ = q^- + q^{adv}$$

Thin Accretion Disk

(Shakura & Sunyaev 1973; Novikov & Thorne 1973;...)

Most of the viscous heat energy is radiated

$$q^- \approx q^+ \gg q^{\mathrm{adv}}$$

$$L_{\mathrm{rad}} : \quad 0.1\dot{M}c^2$$

Advection-Dominated Accretion Flow (ADAF)

(Ichimaru 1977; Narayan & Yi 1994, 1995; Abramowicz et al. 1995)

Most of the heat energy is retained in the gas

$$q^- \ll q^+ \approx q^{\mathrm{adv}}$$

$$L_{\mathrm{rad}} \ll 0.1\dot{M}c^2$$

$$L_{\mathrm{adv}} : \quad 0.1\dot{M}c^2$$

q+ is the energy generated by viscosity per unit volume
q- is the radiative cooling per unit volume
q_{adv} represents the advective transport of energy

ADAF

In this solution the accreting gas has a very low density and is unable to cool efficiently. The viscous energy is stored in the gas as thermal energy instead of being radiated and is advected onto the BH. Ions and electrons are thermally decoupled.

- Very Hot: Ti~ 10^{12}K (R_S/R), Te~ 10^{9-11}K (since ADAF loses very little heat).
- Geometrically thick: H~R (most of the viscosity generated energy is stored in the gas as internal energy rather than being radiated, the gas puffes up
- Optically thin (because of low density)

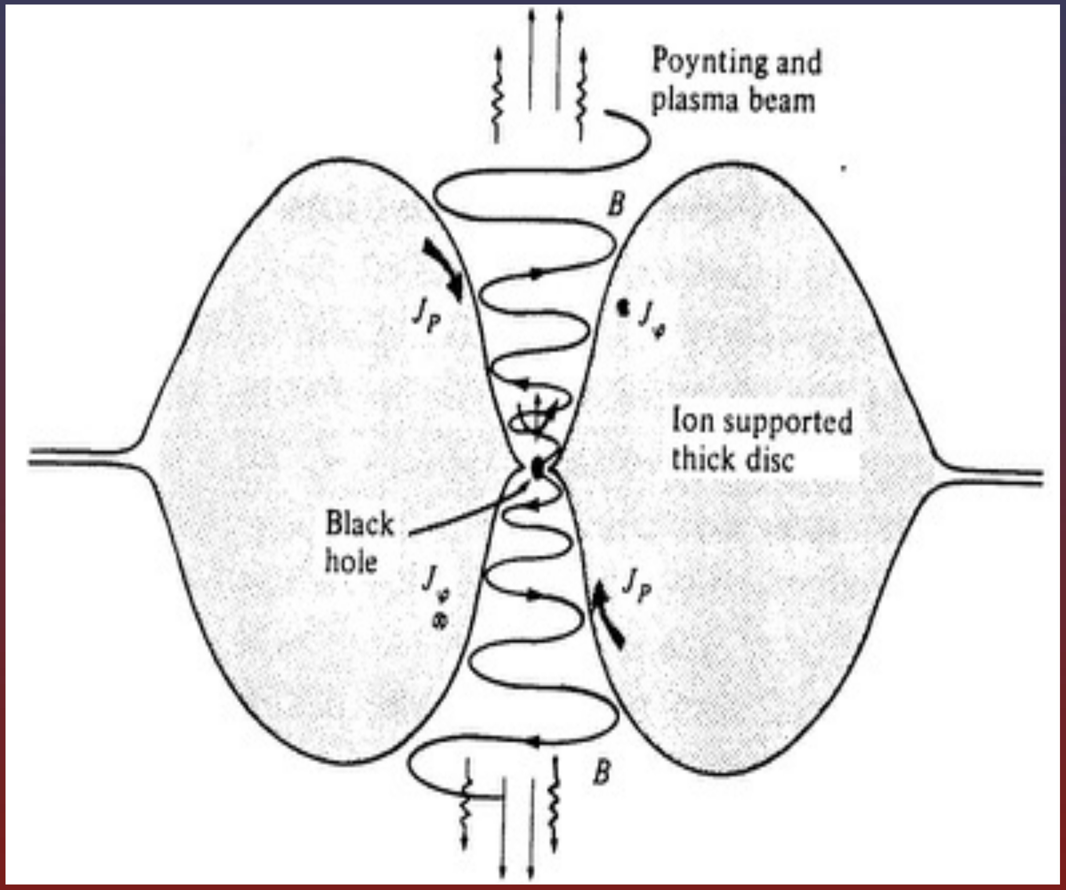

ADAF

The ADAF solution exists only for $\frac{\dot{M}}{\dot{M}_E} \leq 0.05 - 0.1$

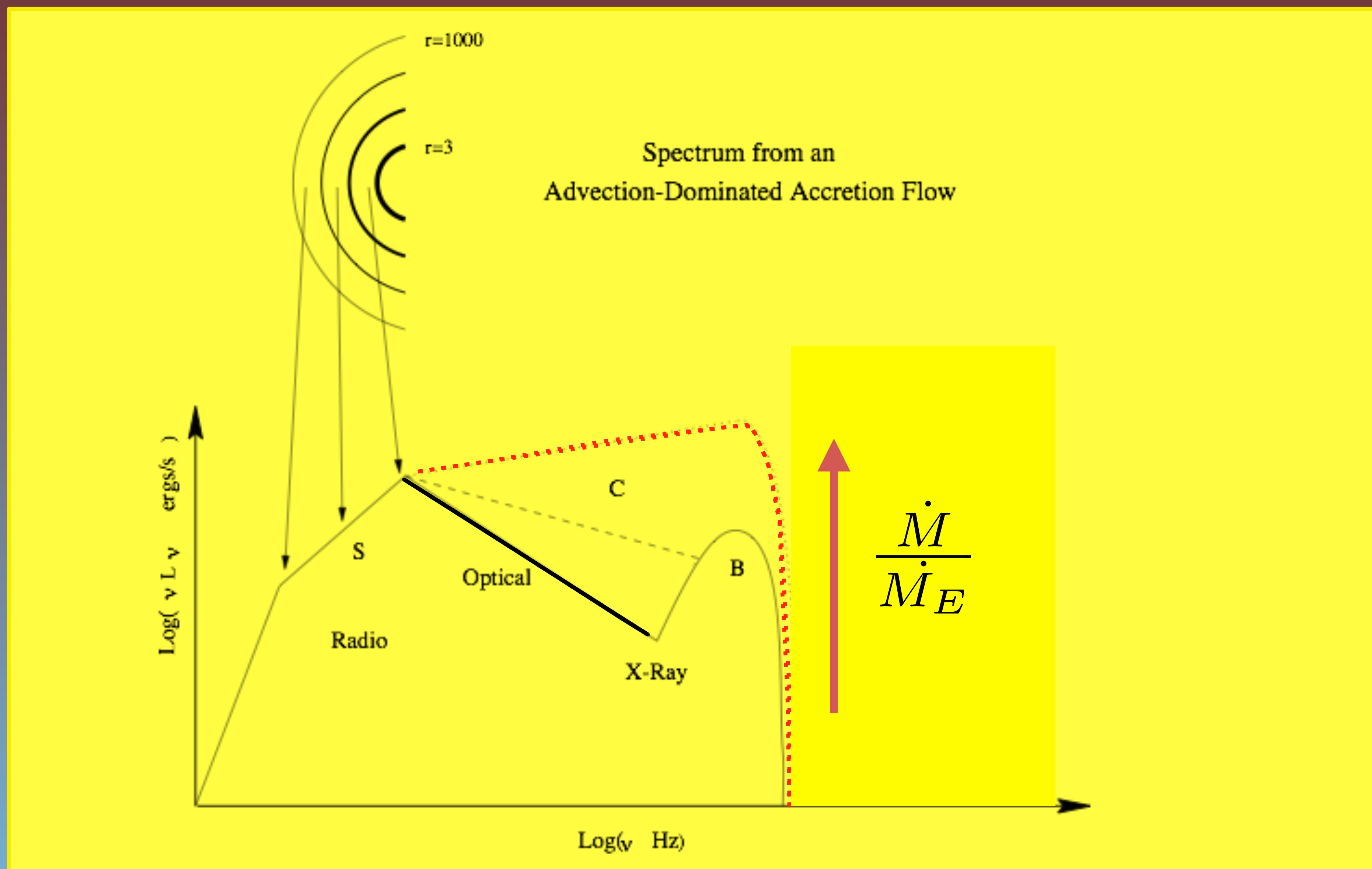

Schematic spectrum of an ADAF around a black hole. S, C, and B refer to electron emission by synchrotron radiation, inverse Compton scattering, and bremsstrahlung, respectively. The solid line corresponds to a low accretion, the dashed line to an intermediate accretion , and the dotted line to the highest (possible) accretion.

Jets, Lobes

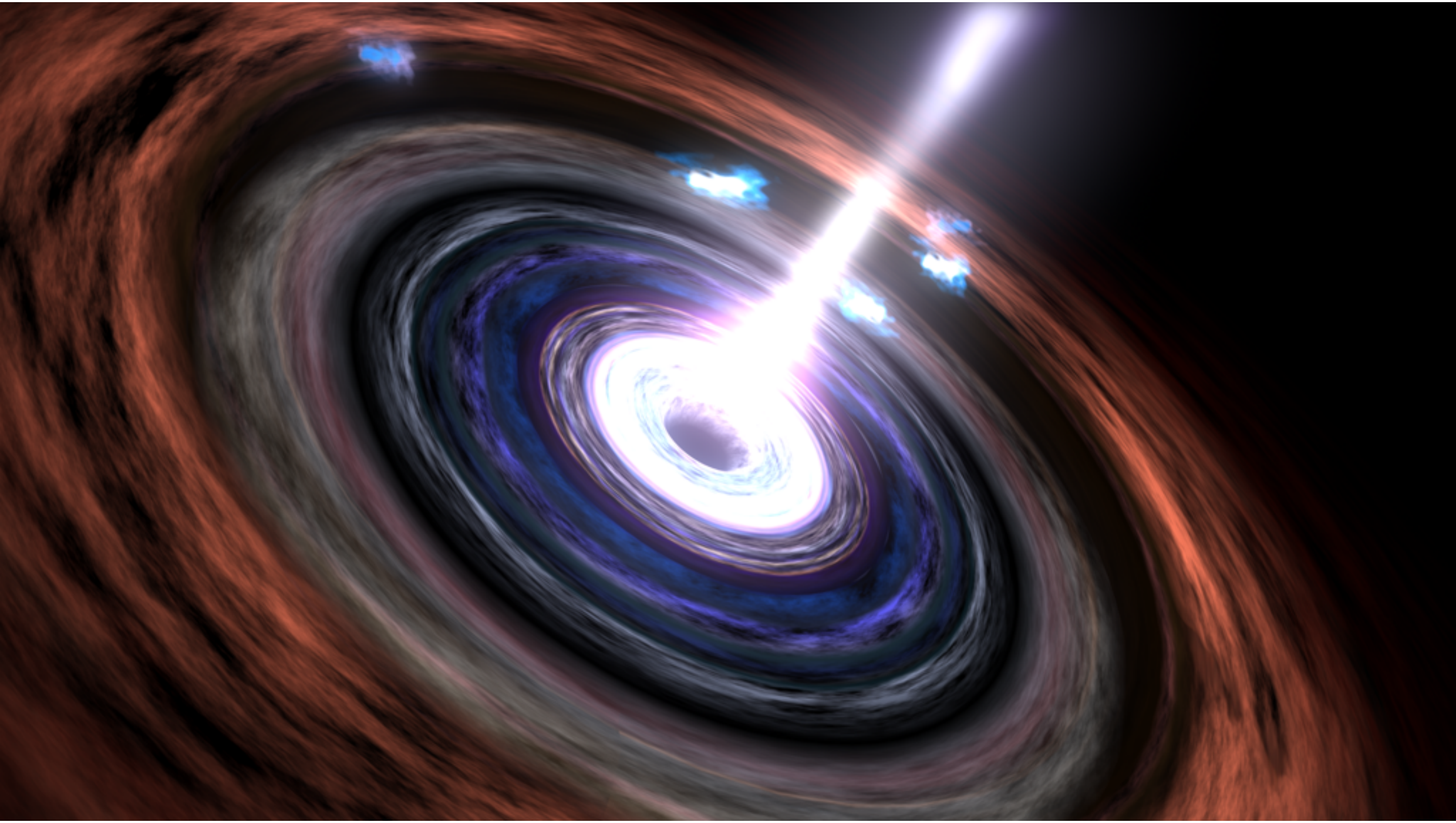

Non-Thermal Processes

Synchrotron Radiation

Synchrotron radiation is due to the movement of an electron charge in a magnetic field. As a particle gyrates around a magnetic field, it will emit radiation at a frequency proportional to the strength of the magnetic field and its velocity.

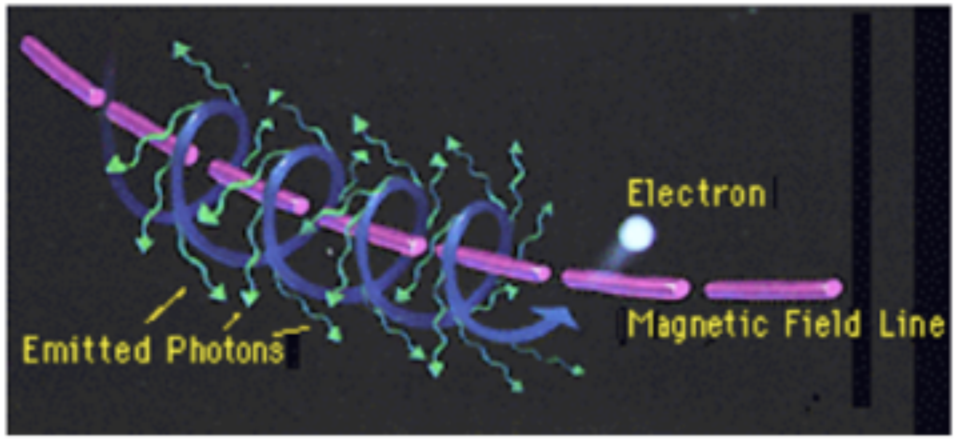

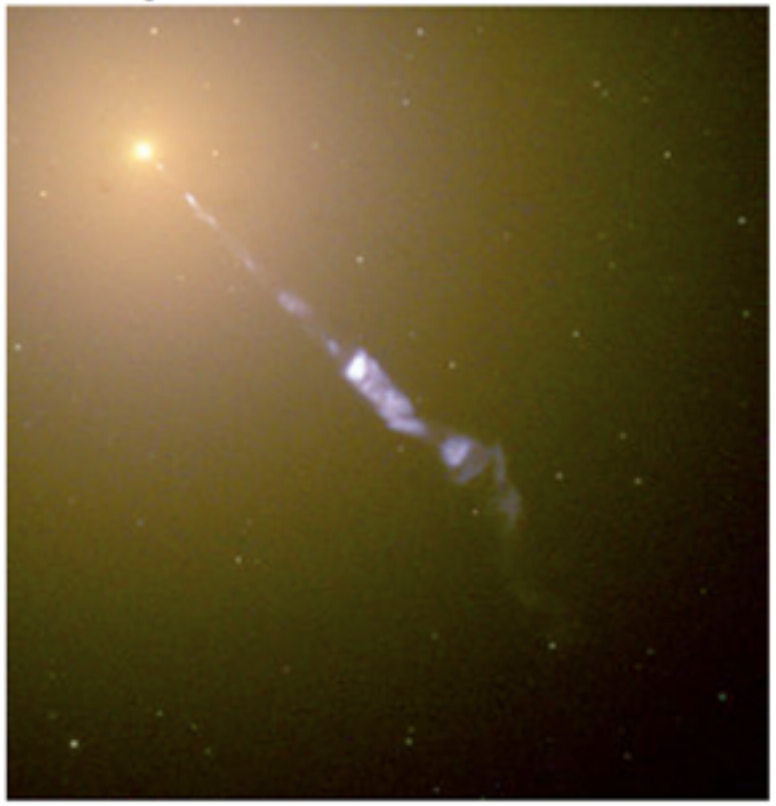

Synchrotron radiation is highly polarized and is seen at all wavelengths. At relativistic speeds, the radiation can also be beamed. It is very common in radio spectrum, but can be seen in x-rays. It is usually fit as a power law. For full details, see the review by Ginzburg & Syrovatskii (1969)

The synchrotron radiation of a power law distribution of electron energies

Synchrotron

$$N(\gamma_e) = K\gamma_e^{-p}, \quad \gamma_{min} < \gamma_e < \gamma_{max}, \; p = 1 + 2\alpha$$

$$\epsilon_{sin}(\nu) \propto KB^{\alpha+1}\nu^{-\alpha} \quad \text{erg cm}^{-3}\ \text{s}^{-1}\ \text{sr}^{-1}$$

Inverse Compton scattering

When the electron is not at rest, but has an energy greater that the typical photon energy, there can be a transfer of energy from the electron to the photon. This process is called Inverse Compton to distinguish it from the direct Compton scattering, in which the electron is at rest, and it is the photon to give part of its energy to the electron.

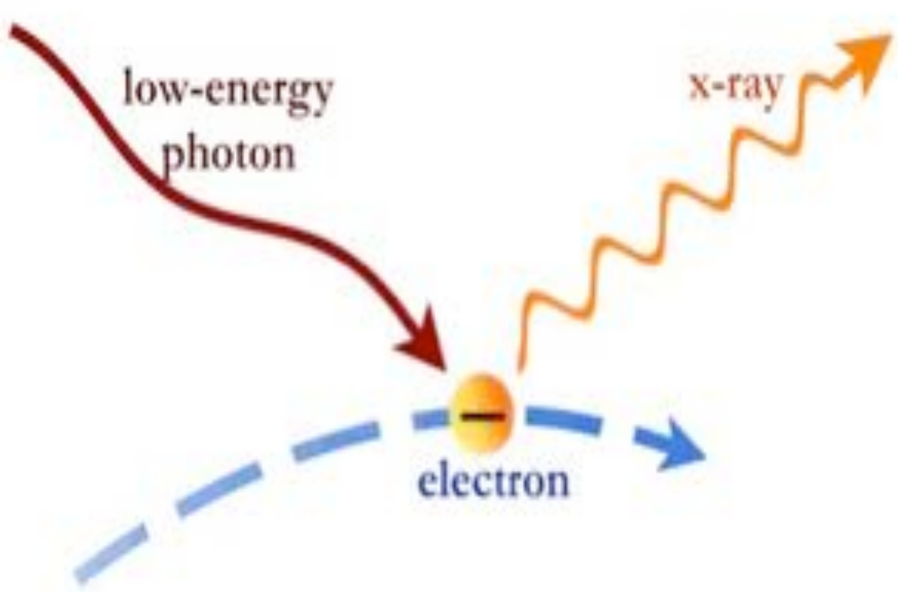

$$< \nu >= \frac{4}{3}\gamma^2\nu$$

Inverse Compton Radiation

The general result that the frequency of the scattered photons is $\nu \approx \gamma^2 \nu_0$ is of profound importance in high energy astrophysics. We know that there are electrons with Lorentz factors $\gamma \sim 100 - 1000$ in various types of astronomical source and consequently they scatter any low energy photons to very much higher energies. Consider the scattering of radio, infrared and optical photons scattered by electrons with $\gamma = 1000$.

Waveband	*Frequency (Hz)* ν_0	*Scattered Frequency (Hz) and Waveband*
Radio	10^9	$10^{15} =$ UV
Far-infrared	3×10^{12}	$3 \times 10^{18} =$ X-rays
Optical	4×10^{14}	$4 \times 10^{21} \equiv 1.6$MeV $= \gamma$-rays

Thus, inverse Compton scattering is a means of creating very high energy photons indeed. It also becomes an inevitable drain of energy for high energy electrons whenever they pass through a region in which there is a large energy density of photons.

Inverse Compton

For a power law distribution of electrons:

$$N(\gamma_e) = K\gamma_e^{-p}\,, \quad \gamma_{min} < \gamma_e < \gamma_{max}\,, p = 1 + 2\alpha$$

Inverse Compton

$$\epsilon_c(\nu_c) \propto K\nu_c^{-\alpha} \int \frac{Ur(\nu)\nu^\alpha}{\nu} d\nu \qquad \text{erg cm}^{-3}\,\text{s}^{-1}\,\text{sr}^{-1}$$

U_r is the radiation energy density

$$U_r = \int n(\epsilon)\epsilon d\epsilon$$

- Synchrotron photons in the jet
- Environment photons from Accretion Flow, BLR, NLR, Torus
- Cosmic Microwave Background (CMB) photons

6. Journey along the jet

pc-scale jet

kpc-scale jet

lobes

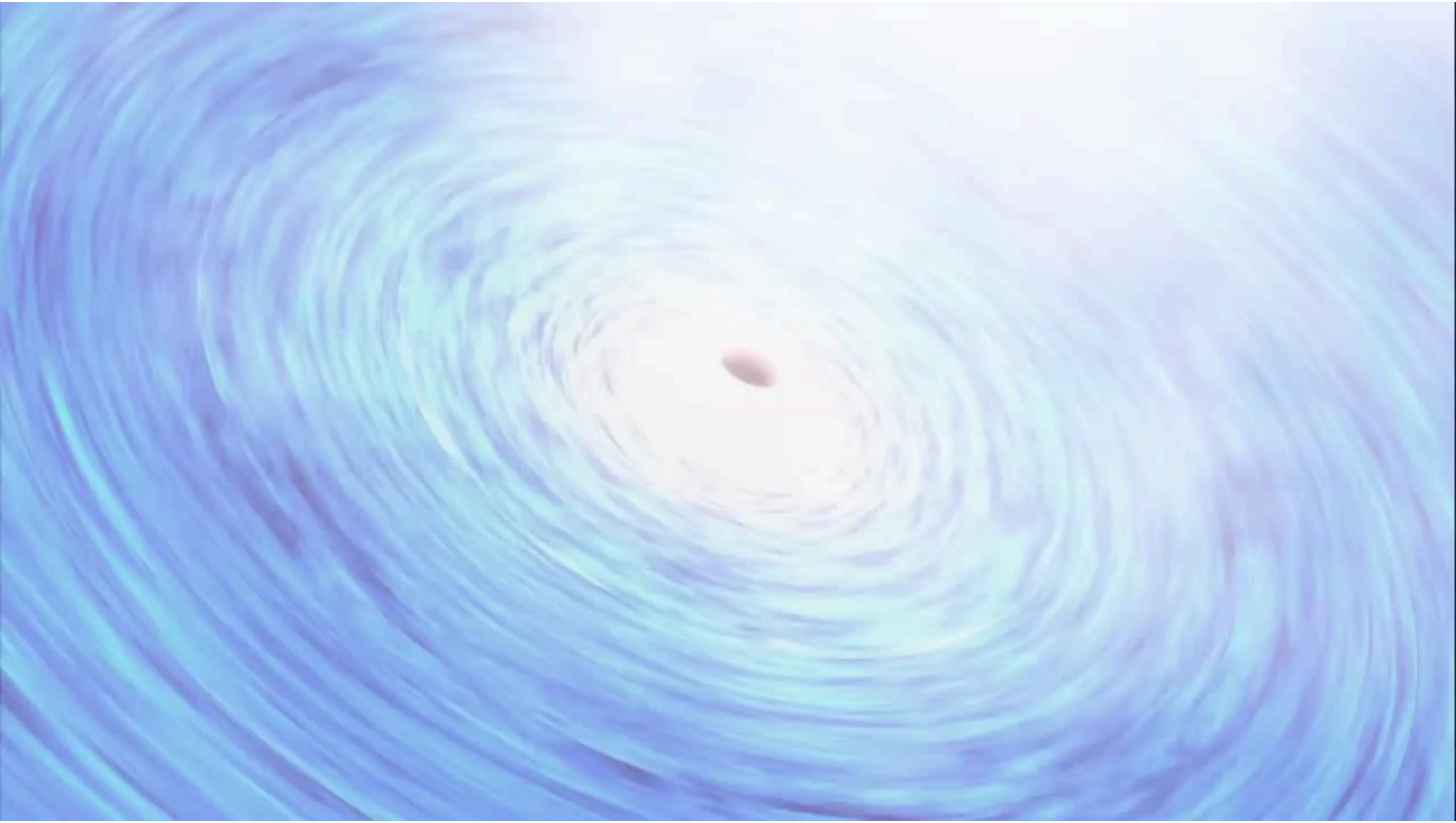

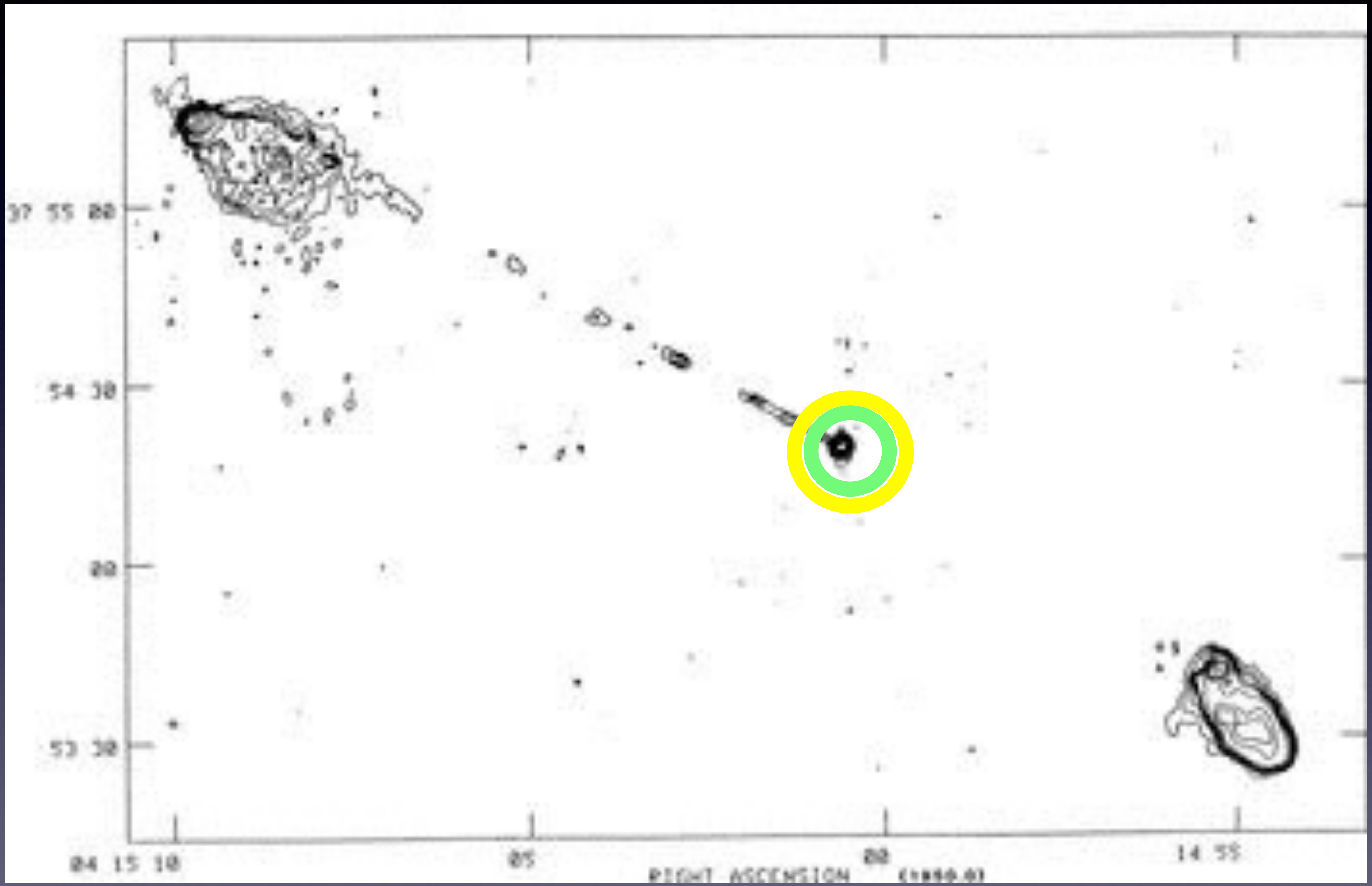

37 55 00
54 30
00
53 30
04 15 10
05
00
14 55
RIGHT ASCENSION

Radio Loud AGNs
JET at sub-pc scale (core)

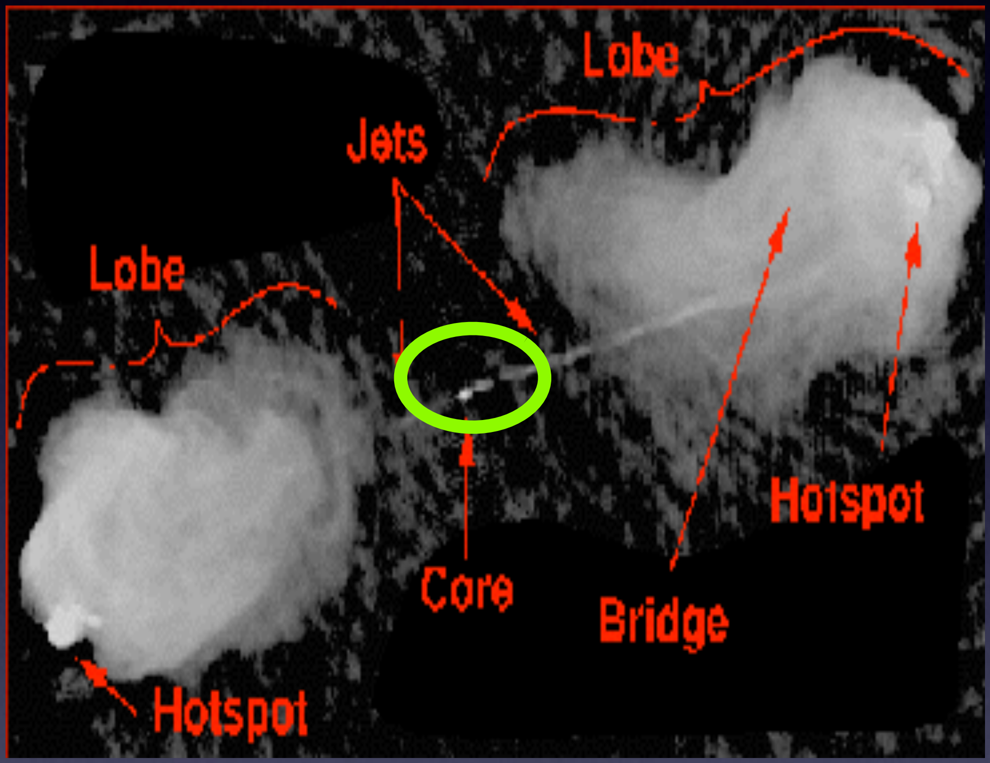

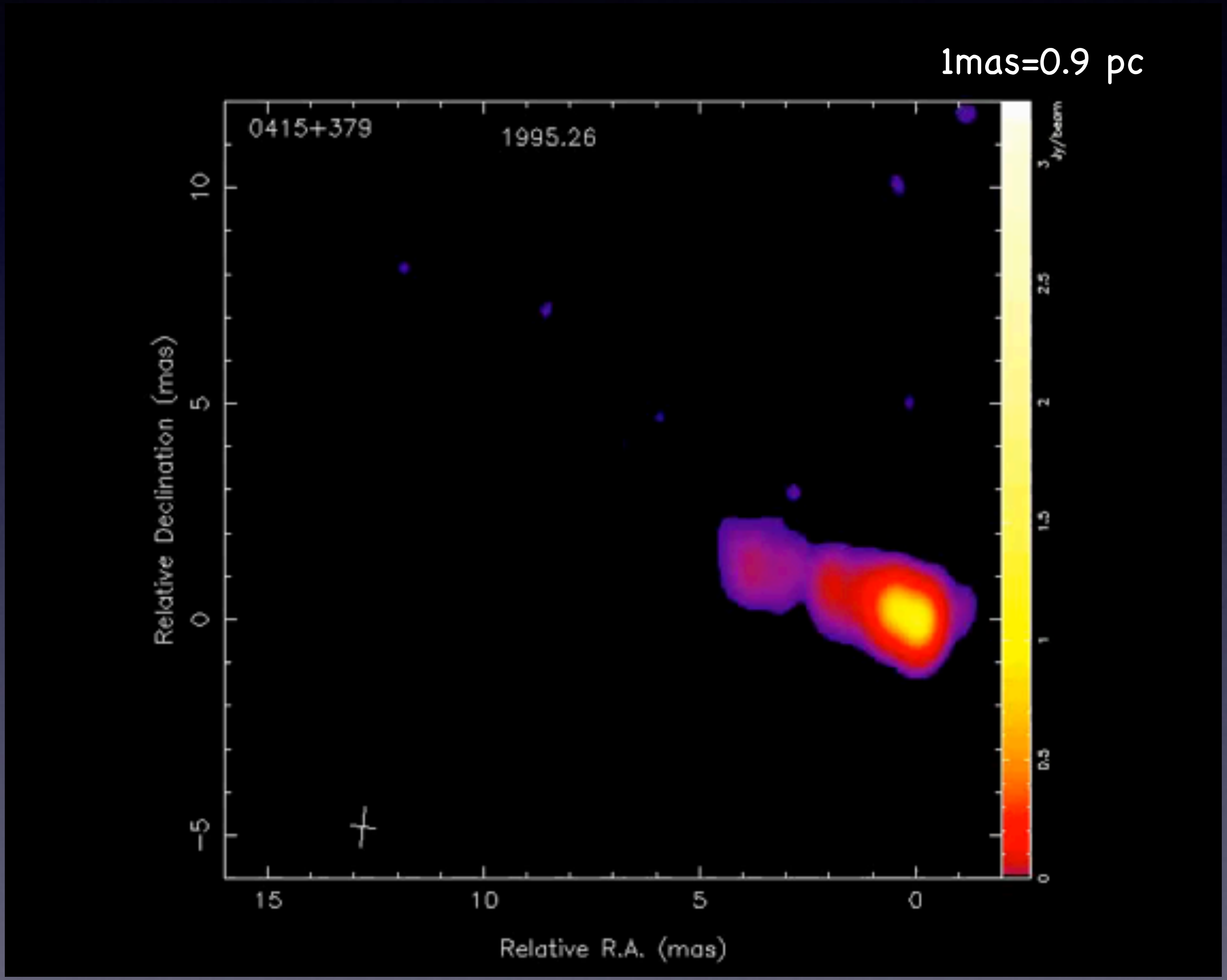

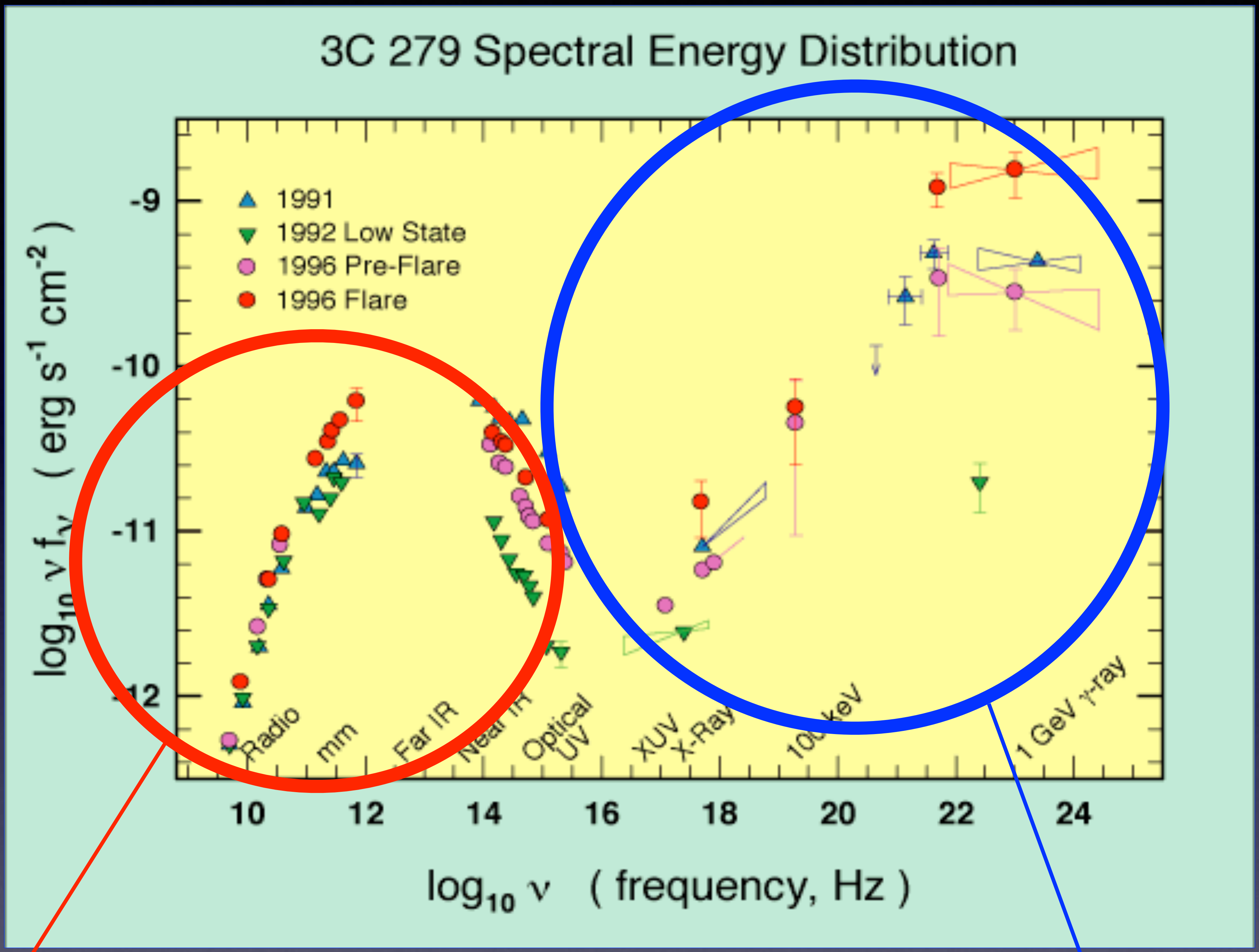

Synchrotron

Inverse Compton

Synchrotron Self–Compton

Consider a population of relativistic electrons in a magnetized region. They will produce synchrotron radiation, and therefore they will fill the region with photons. These synchrotron photons will have some probability to interact again with the electrons, by the Inverse Compton process. Since the electron "work twice" (first making synchrotron radiation, then scattering it at higher energies) this particular kind of process is called synchrotron self–Compton, or SSC for short.

External Compton

The population of relativistic electrons in a magnetized region can also interact with photons externa to the jet produced in the accretion disk, in the broad/narrow line regions in the torus. This particular kind of process is called External Compton, or EC for short.

Emission Models

Simplest scenario: **SSC model**

No external radiation

The simplest model

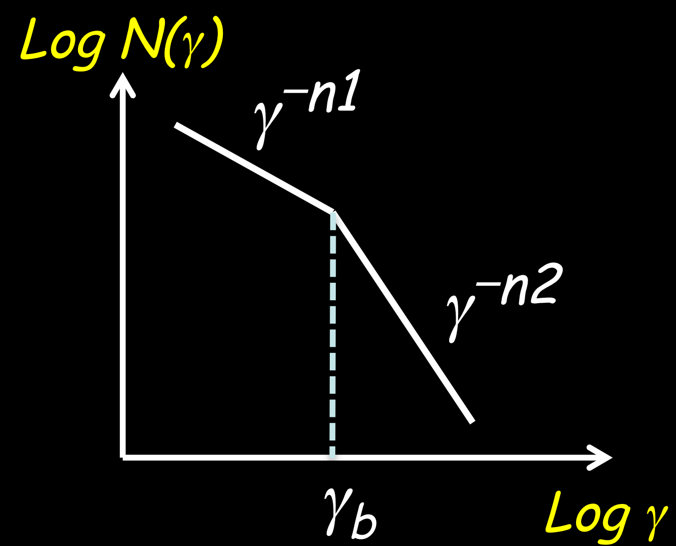

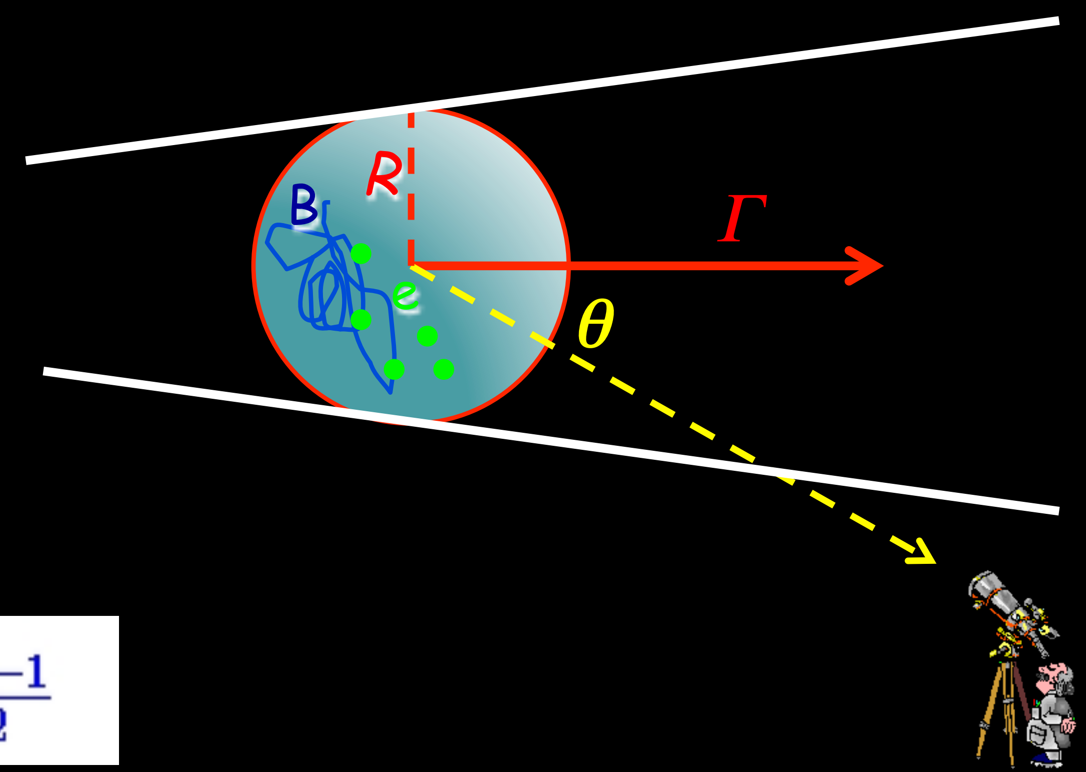

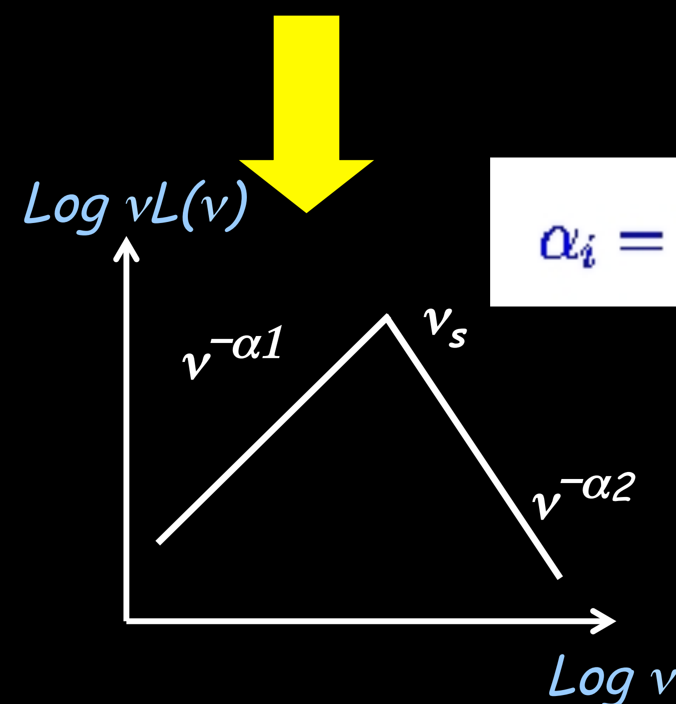

$$\alpha_i = \frac{n_i - 1}{2}$$

$$\nu_s = 3 \times 10^6 B \gamma_b^2 \delta$$

$$\nu_s L(\nu_s) \propto \sigma_T c B^2 N(\gamma_b) \gamma_b \gamma_b^2 V \delta^4$$

The simplest model

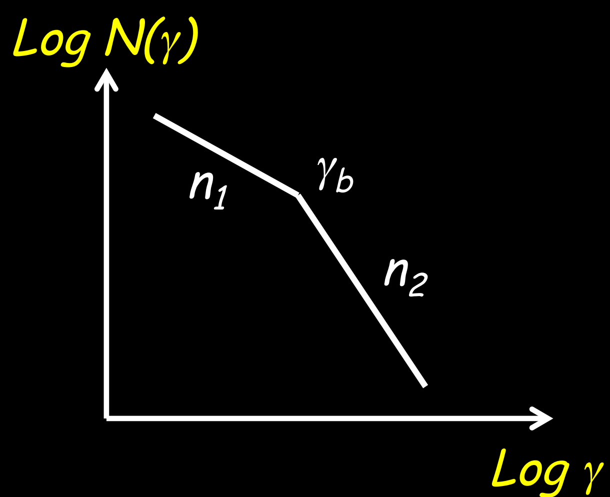

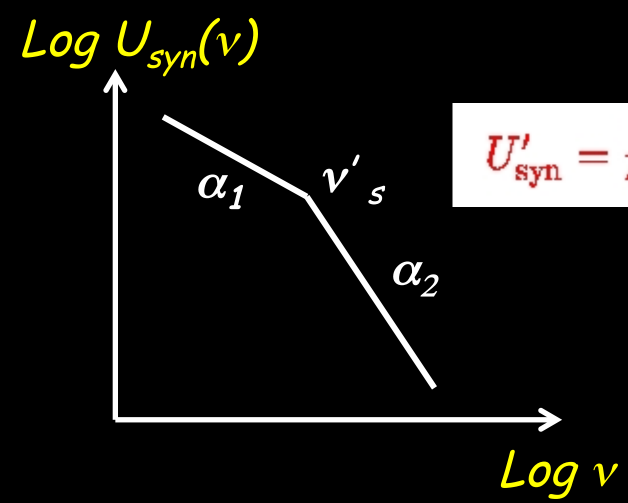

$$U'_{\rm syn} = \frac{\nu_s L(\nu_s)}{4\pi R^2 c \delta^4}$$

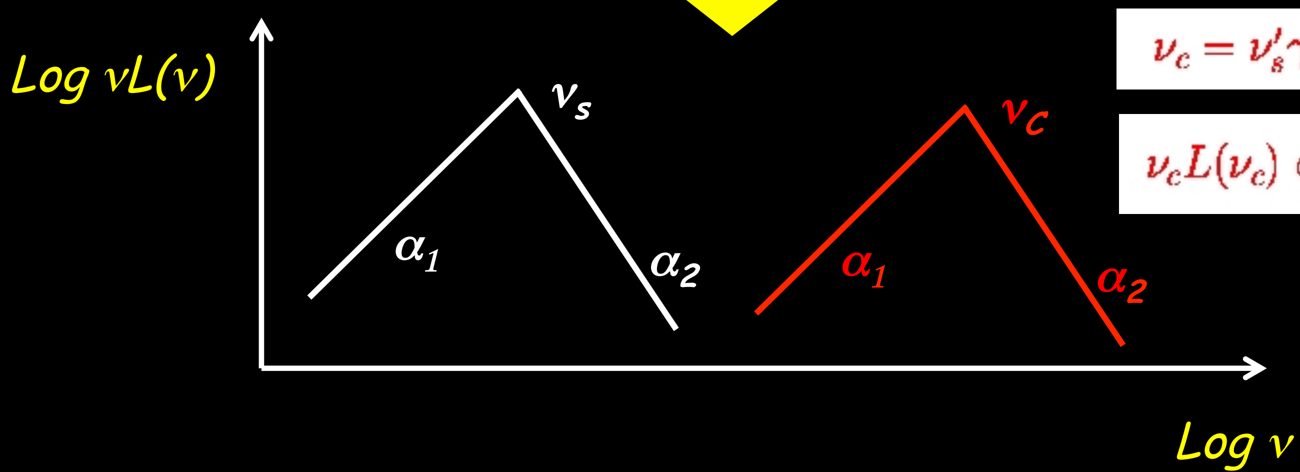

$$\nu_c = \nu'_s \gamma_b^2 \delta \quad \nu'_s = \nu_s/\delta$$

$$\nu_c L(\nu_c) \propto \sigma_T c U'_{\rm syn} N(\gamma_b) \gamma_b \gamma_b^2 V \delta^4$$

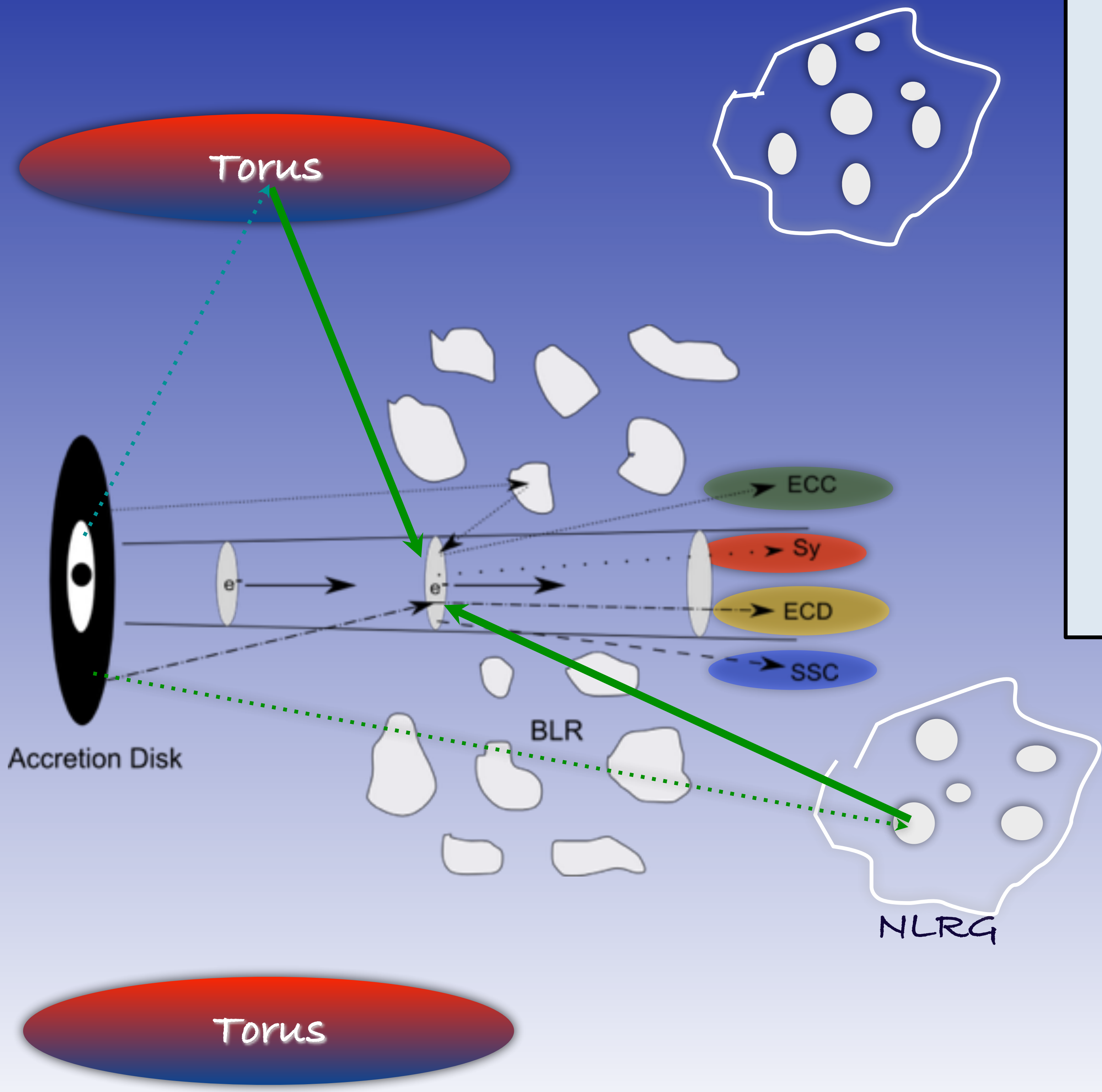
Torus
ECC
Sy
ECD
SSC
BLR
Accretion Disk
NLRG
Torus

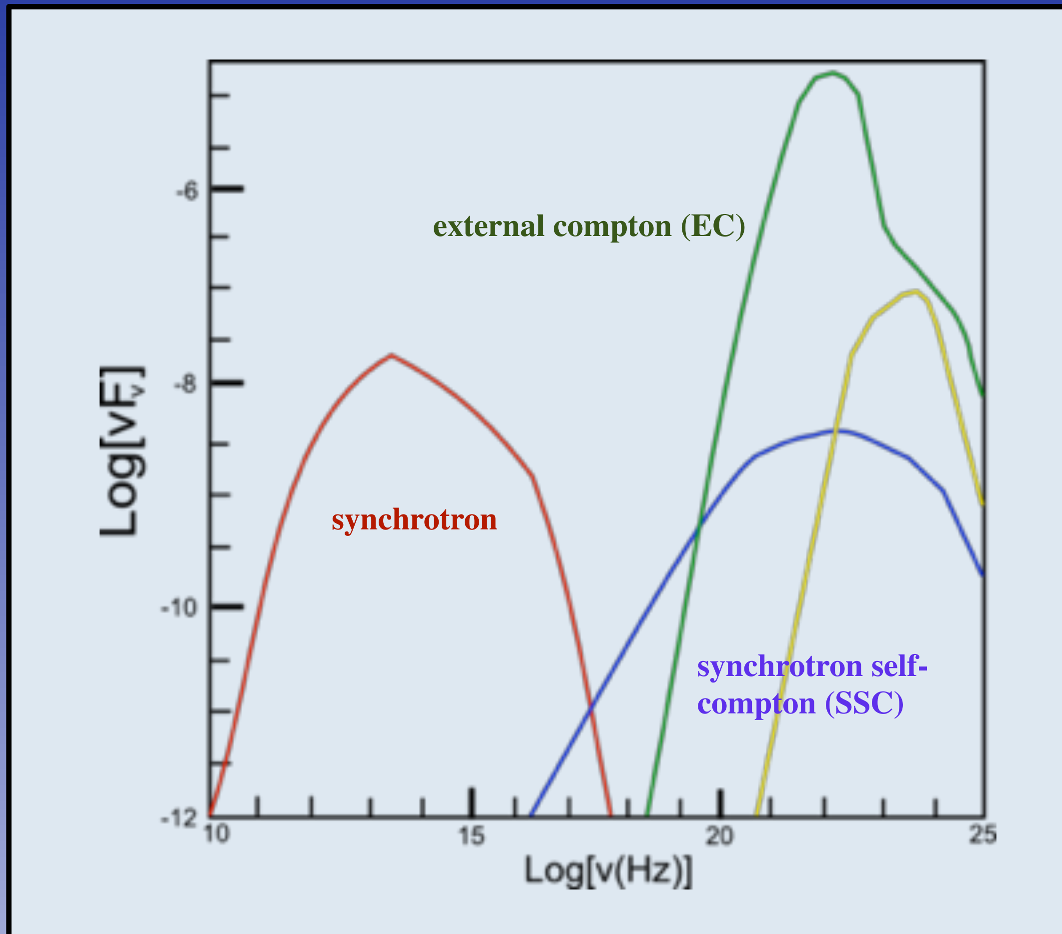
Log[vFv]
-6
-8
-10
-12
10
15
20
25
Log[v(Hz)]
external compton (EC)
synchrotron
synchrotron self-compton (SSC)

Competition between jet and disk

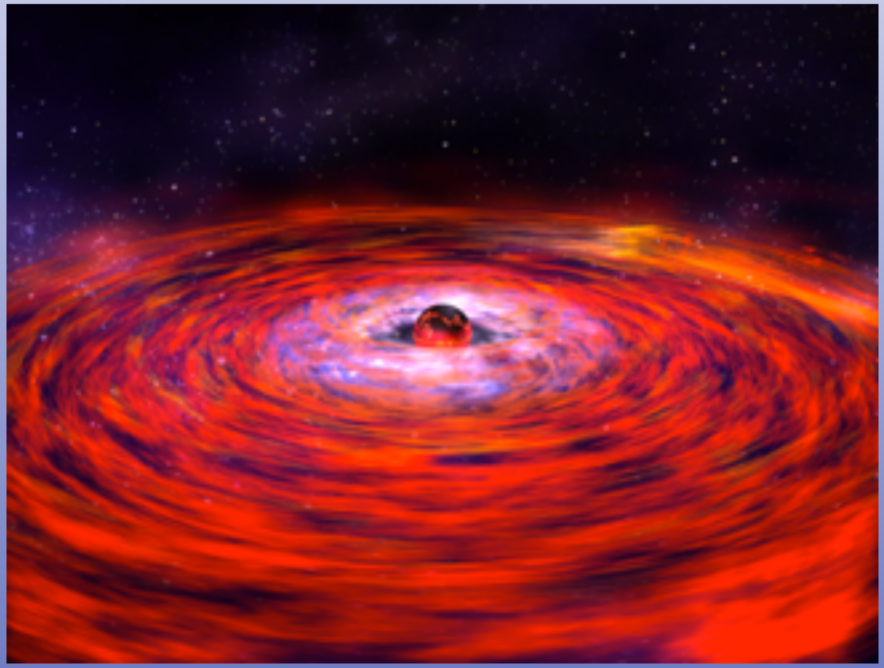

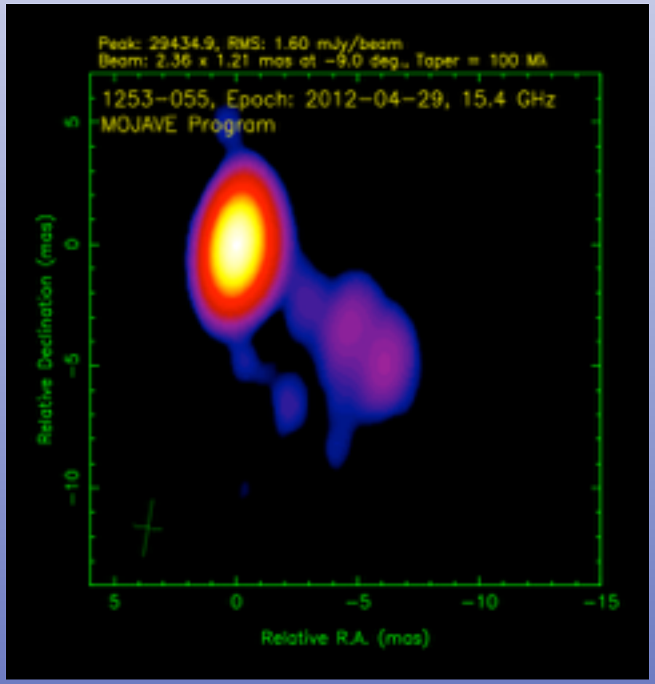

X-ray Spectra:Accretion Disk and pc-scale Jet emission are in competion:

Angle of sight = 0° ==> Jet radiation dominates

Angle of sight = 90° ==> Accretion disk dominates

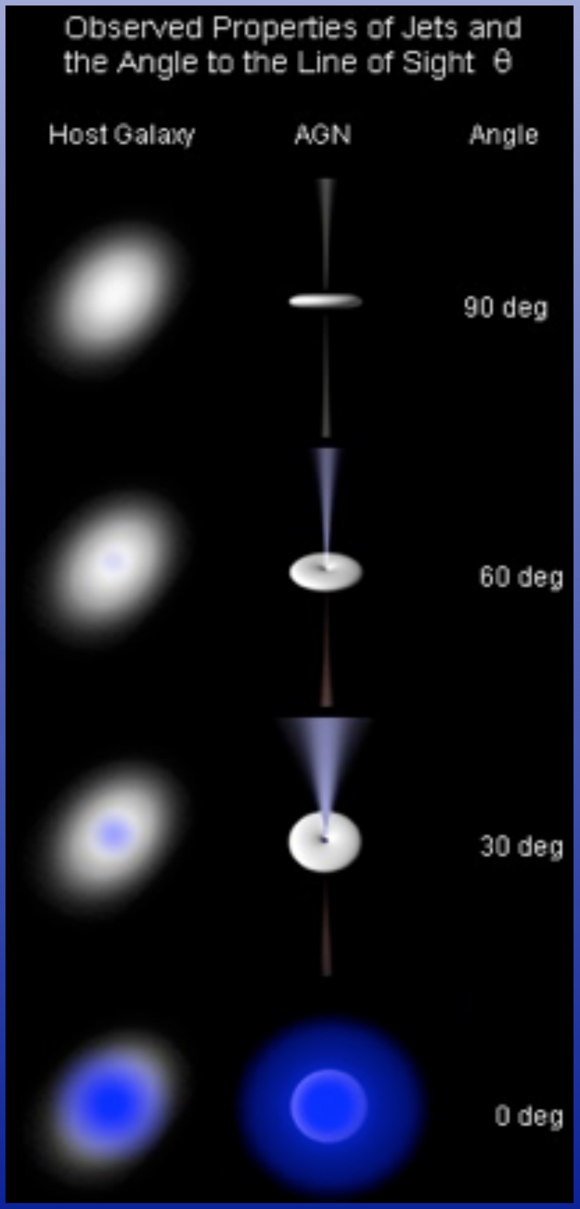

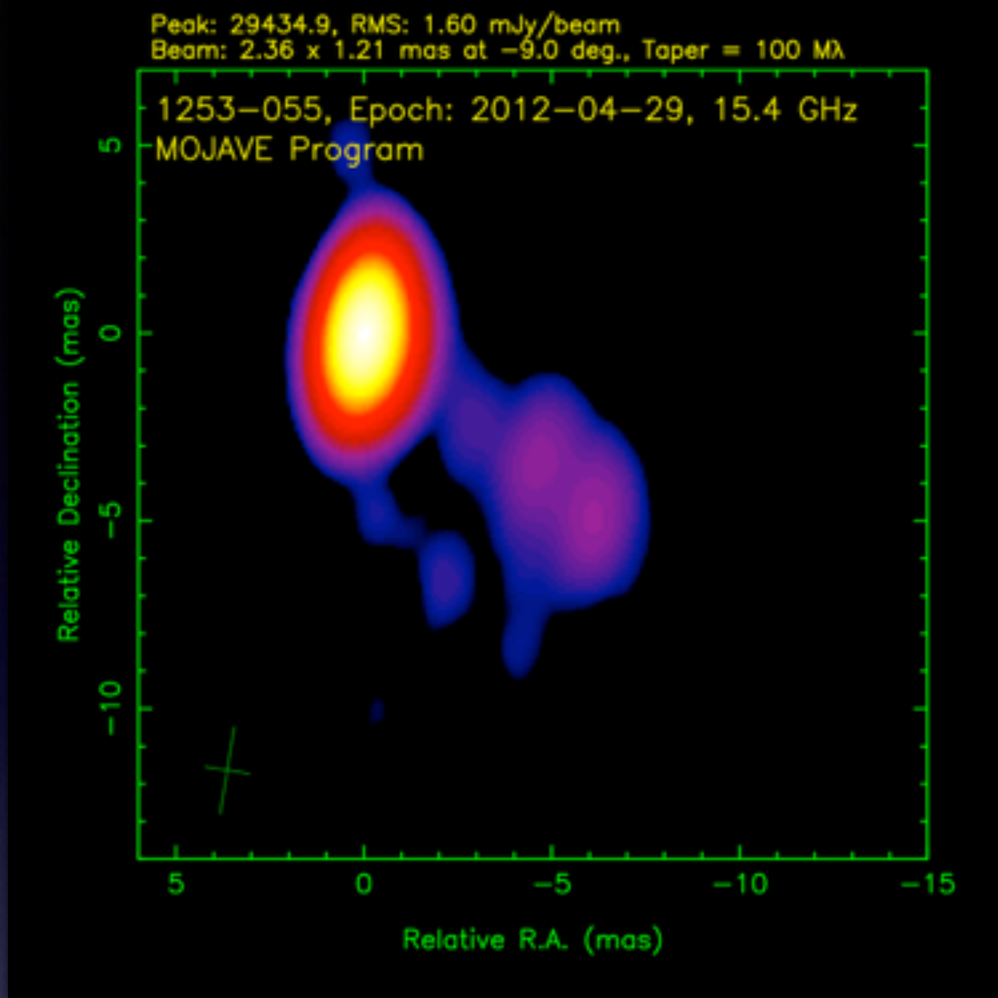
Peak: 29434.9, RMS: 1.60 mJy/beam
Beam: 2.36 x 1.21 mas at −9.0 deg., Taper = 100 Mλ
1253−055, Epoch: 2012−04−29, 15.4 GHz
MOJAVE Program
Relative Declination (mas)
Relative R.A. (mas)

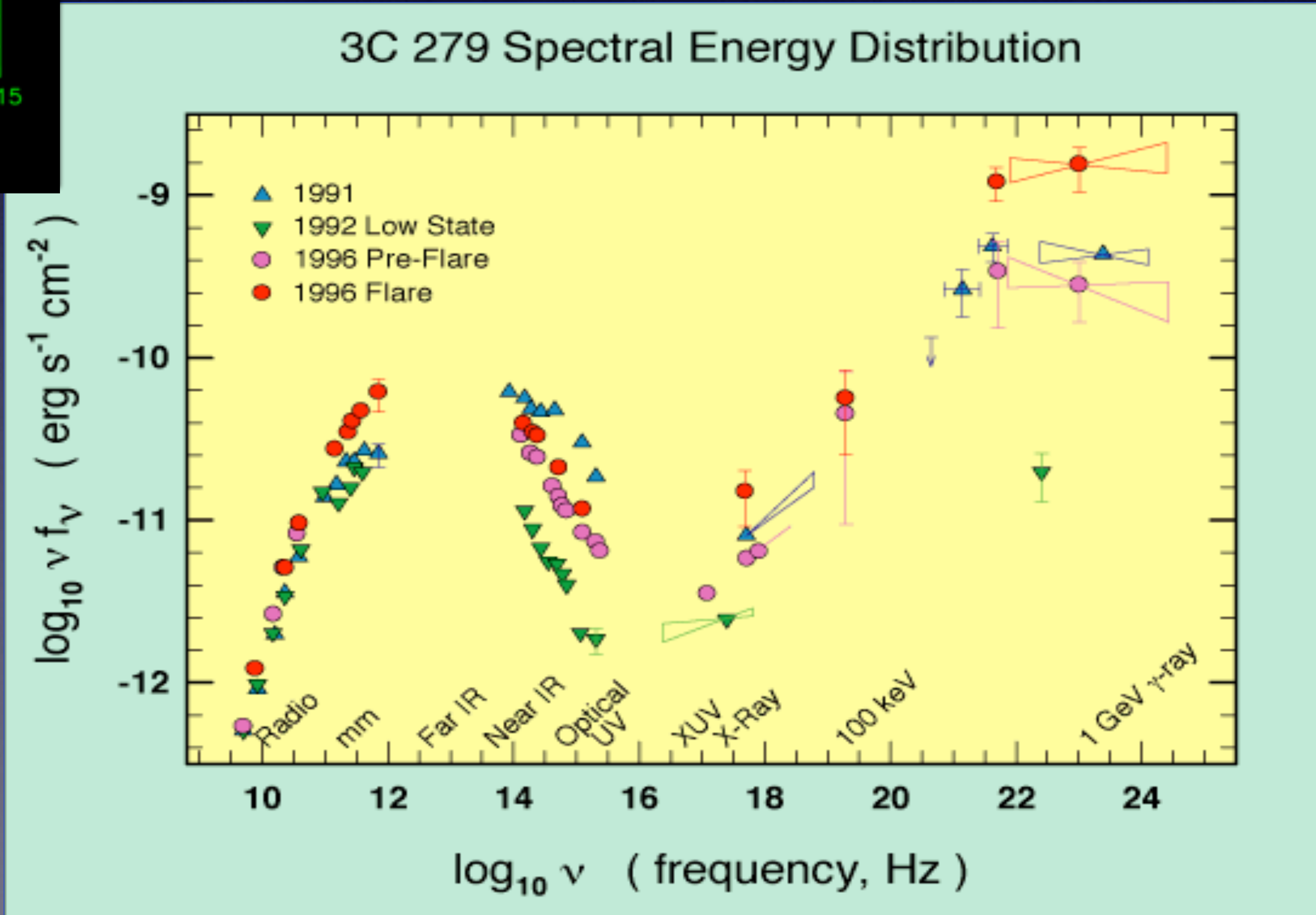
3C 279 Spectral Energy Distribution
1991
1992 Low State
1996 Pre-Flare
1996 Flare
$\log_{10} \nu f_\nu$ (erg s^{-1} cm^{-2})
Radio
mm
Far IR
Near IR
Optical
UV
XUV
X-Ray
100 keV
1 GeV γ-ray
$\log_{10} \nu$ (frequency, Hz)

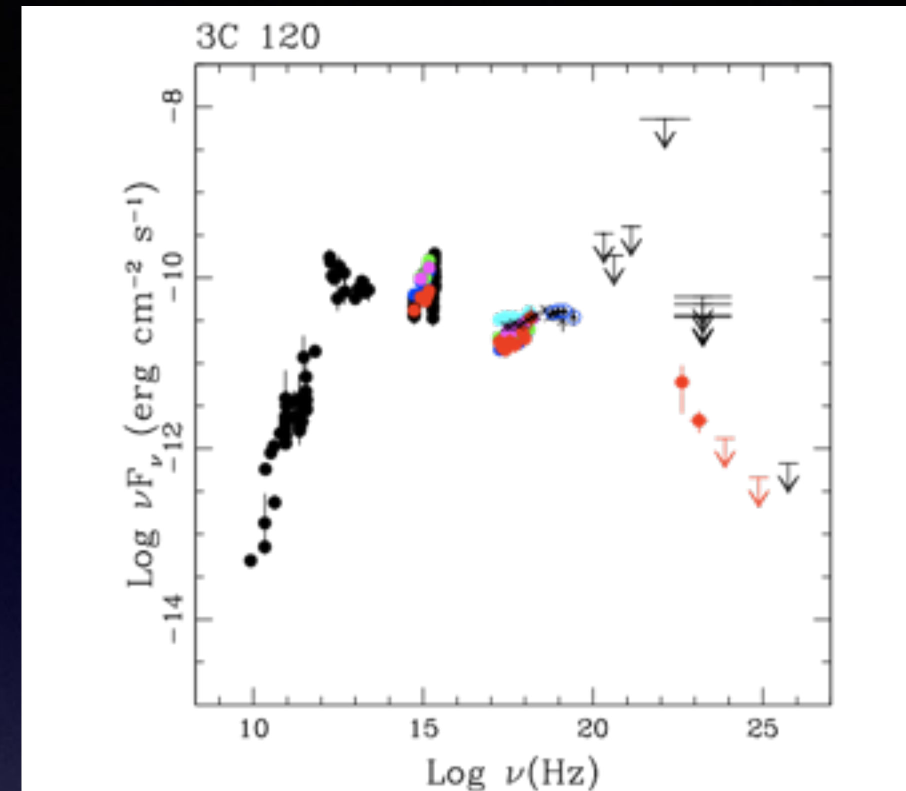

3C 120
Log νF_ν (erg cm^{-2} s^{-1})
Log ν(Hz)
-8
-10
-12
-14
10
15
20
25

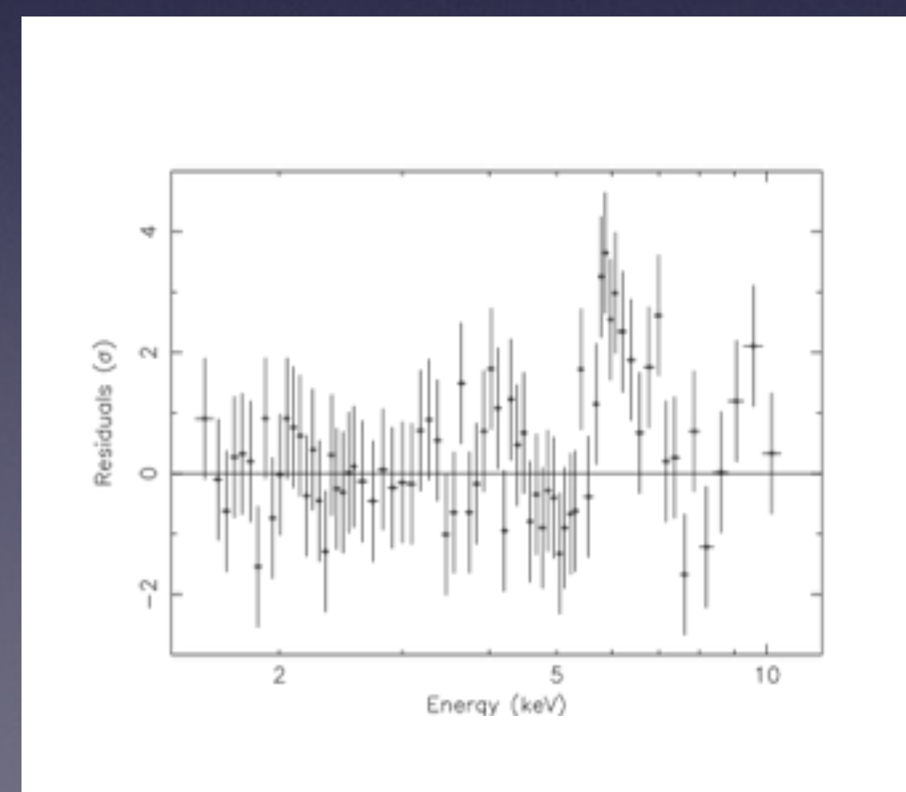

Residuals (σ)
Energy (keV)
4
2
0
-2
2
5
10

kpc-scale Jet

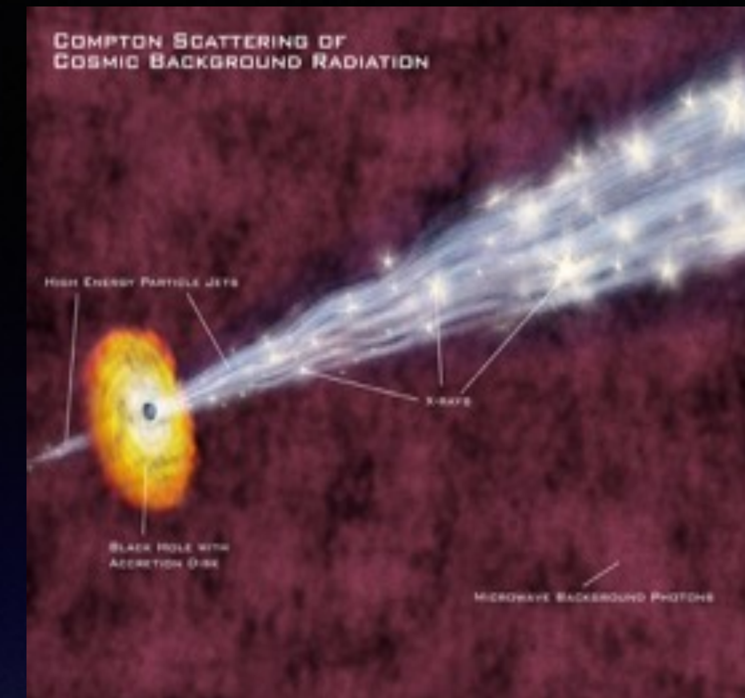

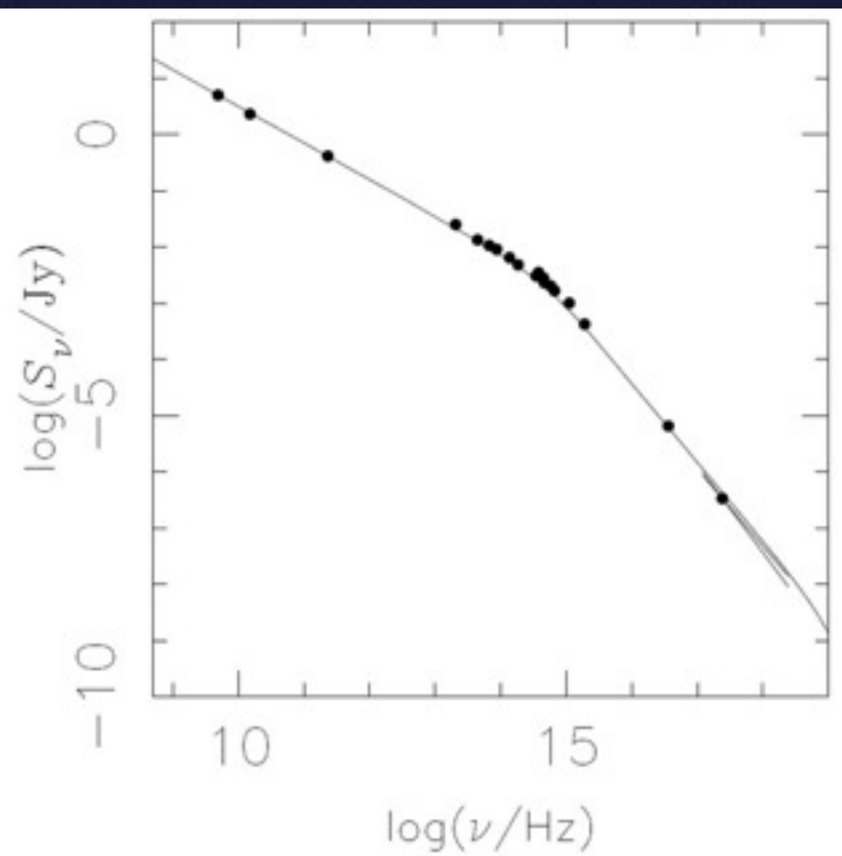

FRI-M87

For low-luminosity (FRI) radio sources, there is strong support for the synchrotron process as the dominant emission mechanism for the X-rays, optical, and radio emissions

Synchrotron process

FRII sources require multi-zone synchrotron models, or synchrotron and IC models (seed photons: CMB).

The most popular model postulates very fast jets with high bulk Lorentz factors Γ.

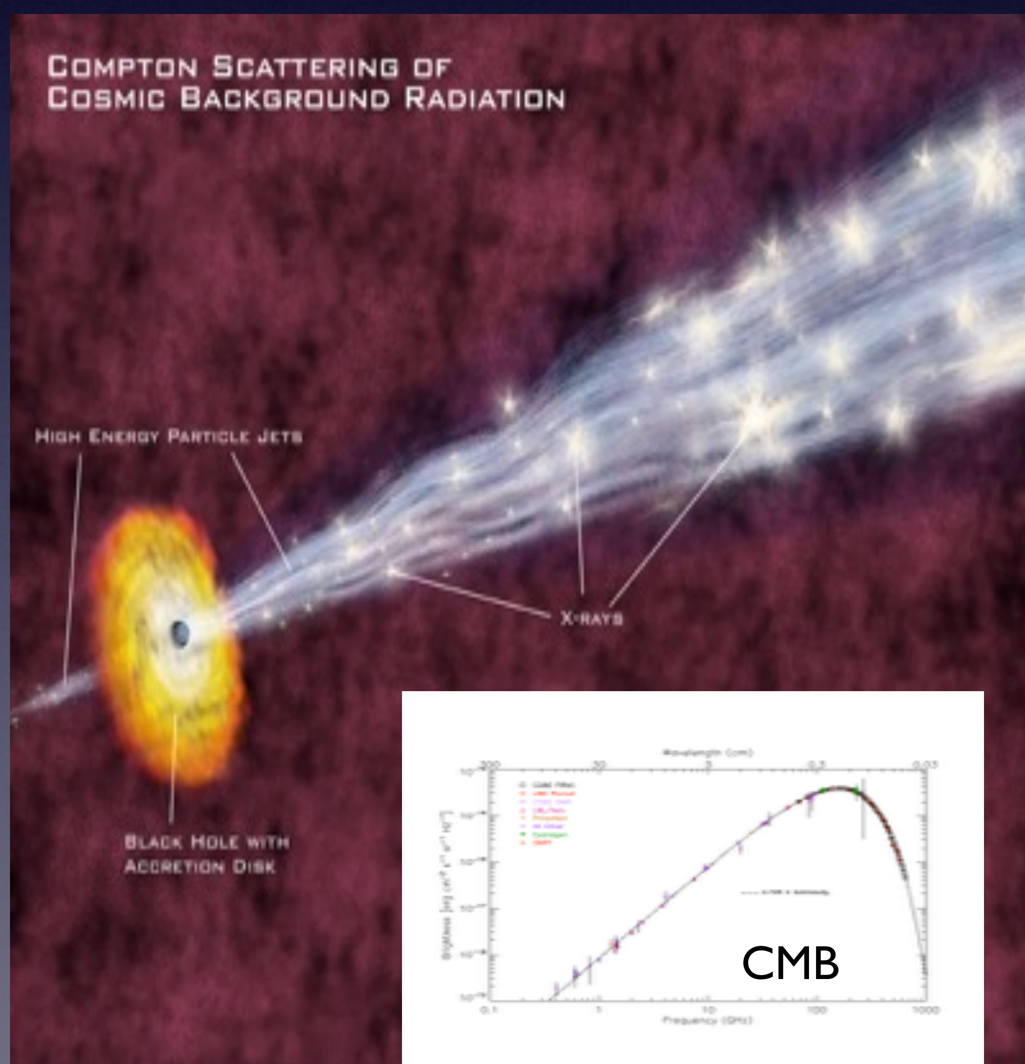

FRII-PKS0637-75

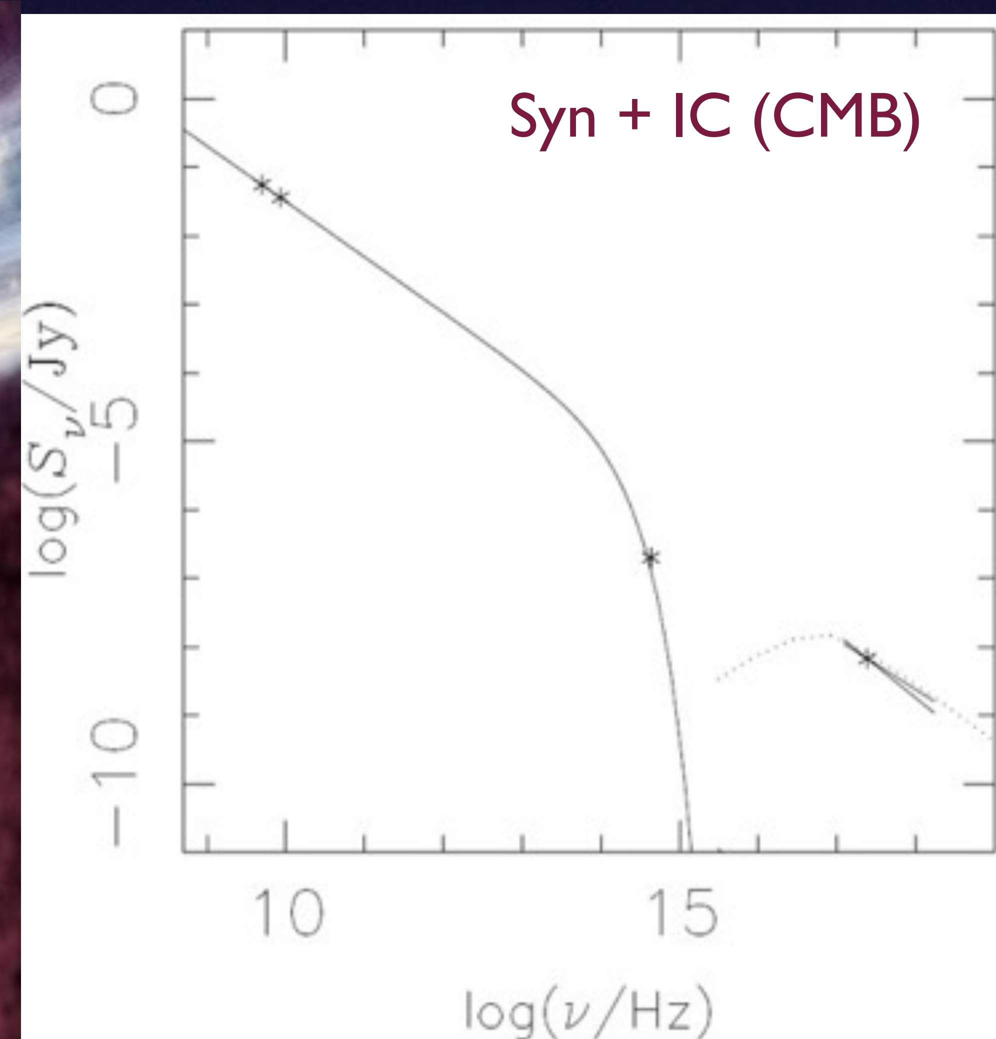

Lobes

relativistic electrons

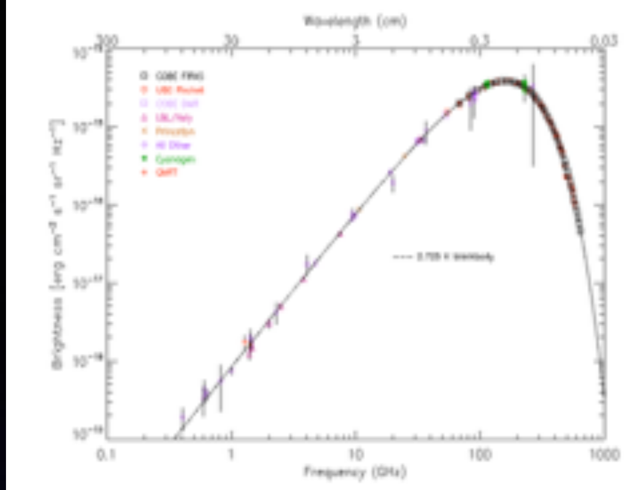

CMB

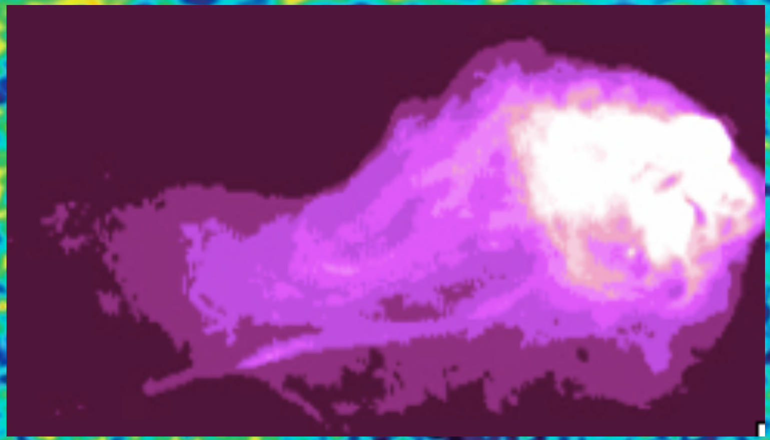

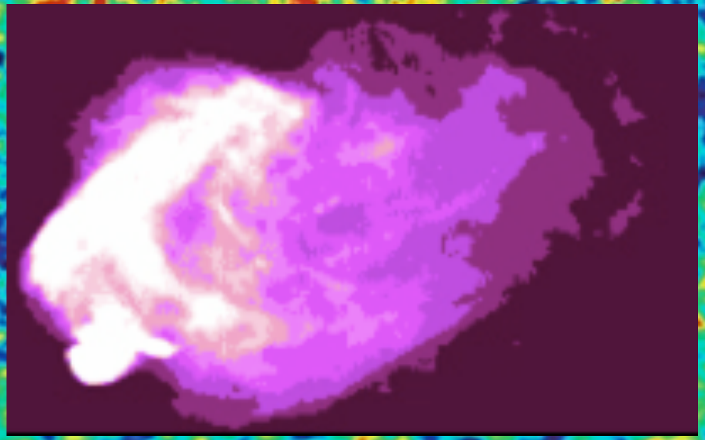

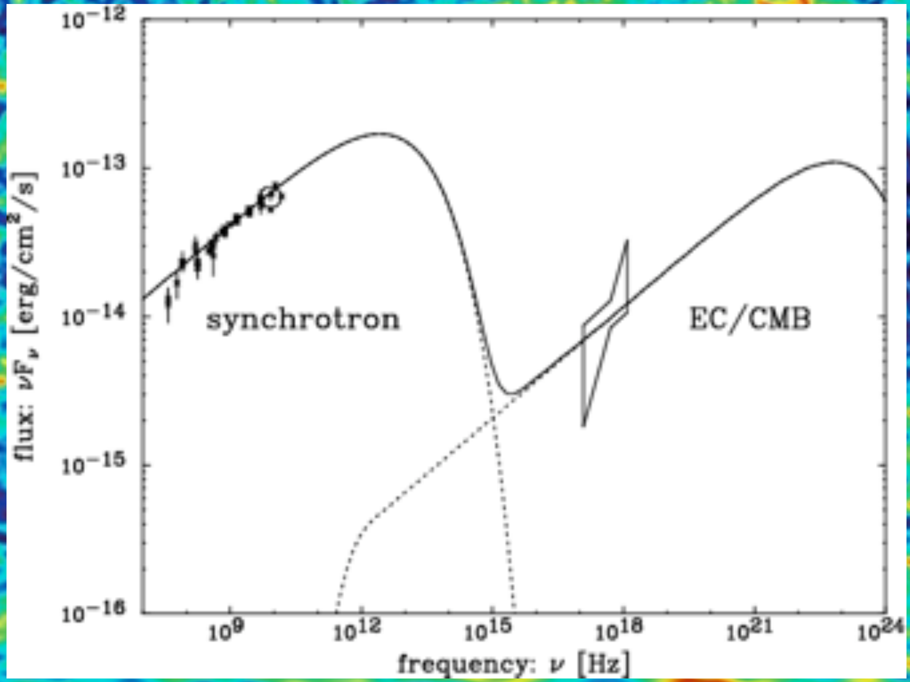


Questions?